UiT The Arctic University of Norway

Faculty of Science and Technology, Department of Geosciences

Planktonic foraminifers and shelled pteropods in the Barents Sea:

Seasonal distribution and contribution to the carbon pump of the living fauna, and foraminiferal development during the last three millennia

Griselda Anglada-Ortiz

A dissertation for the degree of Philosophiae Doctor

August 2023

Planktonic foraminifers and shelled pteropods in the Barents Sea:

Seasonal distribution and contribution to the carbon pump of the living fauna, and foraminiferal development during the last three millennia

Griselda Anglada-Ortiz

A dissertation for the degree of Philosophiae Doctor

UiT The Arctic University of Norway

Faculty of Science and Technology

Department of Geosciences

August 2023

Supervisor:

Prof. Dr. Tine L. Rasmussen

Department of Geosciences
UiT The Arctic University of Norway, Tromsø, Norway.

Co-supervisors:

Dr. Melissa Chierici

IMR – Institute of Marine Research
Fram Centre, Tromsø, Norway.

Dr. Agneta Fransson

NPI – Norwegian Polar Institute
Fram Centre, Tromsø, Norway.

Dr. Katarzyna Zamelczyk

Department of Geosciences
UiT The Arctic University of Norway, Tromsø, Norway

Prof. Dr. Patrizia Ziveri

ICTA – Institut de Ciència i Tecnologia Ambiental (Institute of Environmental Science and Technology)
UAB Autonomous University of Barcelona, Catalonia, Spain.

ICREA – Institut Català de Recerca i Estudis Avançats (Catalan Institution for Research and Advanced Studies), Catalonia, Spain.

ISBN: 978-82-8236-555-0

Front page image: Sea ice at 79.66°N in May 2021.

I el tèrbol atzur de ser tres voltes rebel.

Maria-Mercè Marçal, 1977.

ACKNOWLEDGEMENTS

First, I would like to thank my supervisor and co-supervisors Tine L., Rasmussen, Melissa Chierici, Agneta Fransson, Katarzyna Zamelczyk and Patrizia Ziveri for all that I have learned from you. Specially, thanks to Tine for her support and trust during this journey and for all the opportunities to participate on cruises and conferences. To Melissa and Agneta, thanks for your constructive feedback and contagious positivity, I never thought chemistry was that fun! Finally, thanks Patrizia for your guidance. Who would have thought that the internship at ICTA would end up here? I would also like to thank Julie Meilland for sharing her knowledge and positive discussions.

Special thanks to Marit Reigstad for managing the Nansen Legacy project, your knowledge and humanity are such an inspiration. Also, thanks to all the project administration dream team: Elisabeth Halvorsen, Mona Isaksen, Erin Kunisch, Lena Seuthe and Ingrid Wiedmann, you have made this journey way easier.

The samples of this thesis would not exist without the help from the captain and crew of RV Helmer Hansen and Kronprins Haakon, and all the engineers. Thanks to Trine, Karina, Ingvild and Matteus for your help in the lab. Thanks to Simon and Fabio for always helping with the logistic pre- and post- cruise, and to André, Cecilie, Mariana and Zeynep for their admin support.

Spending time at sea is always nice, and there are people who make it even better. I would like to thank all the cruise leaders who accommodate our needs and requirements. Thank you very much Libby, for your contagious energy and taking care of our small chemistry team. Thanks Miriam, for your managing skills and the patience you had with us, and Anette for all your help onboard. Thanks to all cruise participants and Early Career Researchers (ECR) from the project, especially Amanda, Arunima, Julia, Maria, Nadjejda, Natalie, Robynne, Stephen, Snorre and Thaise for sharing their laughs no matter what time of day it is. To Chrissie and Yasemin, thank you very much for the time spent on and offboard. I cannot imagine how this Ph.D. journey and the life in Tromsø would have been without your friendship. Al petit Èric i al Martinet (a.k.a. “Gaudí gang”) per fer-me sentir com a casa al mig de l´Àrtic. Els bailoteos, risis i el temps amb vosaltres m´omplen l´ànima. I have learned tones with all of you! :)

Getting bored in the office is not that easy with all the corridor mates. Thanks to the ECR from the Department, and members of the JEDI group and *Strikk og Drikk* (Ani, Carly, Carmen,

Christine, Colin, Cornelia, Fatih, Frances, Frank, Julian, Knut Ola, Kaya, Lina, Leo, Maria, Marie, Max, Orlando, Siri, Sofia, Stine, Stephan, Tristan and Vårin) for the lunch breaks but most importantly for the cakes, drinks, and laughs. Thanks to the current foram-office members Adele, Christine, and Freya for your energy. To Kasia and Marie for all the breaks, brunches, and memes. Thanks to my personal IT problem solver and fellow procrastinator Przemek. Special and deep thanks to Marina and Naima, por ser y por estar. Este camino hubiera sido más difícil y aburrido sin vosotras, gràcies/eskerrik asko!

Thanks to ARCTOS members for their feedback and all the get-together, and specially to Eva and Tiziana for sharing their joy and giggles.

Thanks to all MERS members from the Autonomous University of Barcelona for all the meetings and gatherings. Al Jordi qui, sense saber-ho, va encaminar-me al món de l´oceanografia. La teva curiositat i personalitat seran sempre una font d´inspiració. To Graham for sharing his scientific and personal knowledge, I always learn something new talking with you. Thank you, Mika, for your honesty, help and advice. Thank you to all Ph.D. and postdocs that I met there (Anaid, Arturo, Barbara, Eloise, Miki, Roberta, Sonia, Stephanie, and Sven). To my favourite lab partner Laura. Por todas las risas, las lágrimas, los nervios e inseguridades compartidas. Mudarme a Tromsø fue un poco más difícil sabiendo que no tendría en el lab a mi umpalumpi preferida. No estaría aquí sin tu amistad y críticas crueles pero constructivas.

A l´Àurea, la Clàudia, la Laura B., i la Mireia que fan que el temps siguin relatius. Especialment a la Juvi, que malgrat la distància, seguim caminant juntes. Tornar-vos a veure sempre m´omple el cor de riure fins la propera visita.

Last but not least, a la meva familia. A les àvies i avis, als tiets i tietes, a la Clara i al Pau. A la mama, el papís i el Roger per la seva incansable ajuda i motivació, i per animar-me a fer el que em fa feliç a 3292.72 quilòmetres de distància (depèn de a qui preguntis). Això hagués sigut impensable i impossible sense vosaltres, moltes gràcies juguetons.

PREFACE

This thesis is the result of four years of research and education at the Department of Geosciences UiT The Arctic University of Norway, in Tromsø, from May 2019 to August 2023. It has been supervised by Professor Tine L. Rasmussen (CAGE/IG–UiT) and co-supervised by Dr. Melissa Chierici (IMR), Dr. Agneta Fransson (NPI), Dr. Katarzyna Zamelczyk (CAGE/IG now HF– UiT) and Prof. Dr. Patrizia Ziveri (ICTA–UAB). The funding was provided through The Nansen Legacy Project (Research Council of Norway, #276730) and Centre for Arctic Gas Hydrate, Environment and Climate (CAGE) (through the Centers of Excellence scheme from the Research Council of Norway, #223259, and until February 2023).

The educational component from the Ph.D. program was carried out by conducting the following courses: *Artic Ocean functioning: Interdisciplinary perspectives from geology to ecosystems* (BIO-8026 at UiT), *ARCTOS colloquium* (BIO-8504 at UiT), *Marine Geology and Geophysics Cruise* (GEO-8144 at UiT), *Workshop in Arctic Marine Geology and Geophysics* (GEO-8145 at UiT), *Philosophy of science and ethics* (SVF-8600 at UiT), *Leadership skills-preparing Ph.D. students for taking on leadership tasks* (FSK-8003 at UiT), *How to communicate your research* (GEN-8007 at UiT), *Geochronological methods in marine sediments* (GEO-8801 at UiT), and *Arctic marine biogeochemistry: an introduction to the cycling and impact of elements in the physical and biological environment of the Arctic Ocean* (Norwegian University of Science and Technology, Trondheim, Norway). As a Ph.D. candidate, I was part of the research schools: Geoscience Research Academy of Tromsø (GReAT), the Norwegian Research School on Changing Climates in the coupled Earth Systems (CHESS) and The Arctic Marine Ecosystem Research Network (ARCTOS).

The duty work assigned (25%) was fulfilled by teaching the laboratory exercises of GEO-3111 (Reconstructing Quaternary Environments and Climate) and GEO-3122 (Micropaleontology), assisting on research cruises and teaching cruises from the department, the research stays abroad and other activities including laboratory work and participating and organizing the *Geologiens dag* in 2020. During the period of the Ph.D., I have repeatedly visited my co-supervisor Dr. Patrizia Ziveri at ICTA–UAB with a total of 6 months.

The research conducted during the Ph.D. have been disseminated, both in poster (9) and oral (7) presentations, in national and international conferences and symposiums, in person and/or as virtual meetings: Geoscience Research Academy of Tromsø (GReAT) annual meetings 2020

and 2022; CAGE winter meeting 2019; The Nansen Legacy project meetings in 2019, 2020, 2021, 2022 and 2023; Arctic Frontiers in 2019 (Tromsø, Norway); Arctic Change 2020 Conference (virtual); Association for the Sciences of Limnology and Oceanography (ASLO) meeting 2021 (virtual) and 2023 (Mallorca, Spain); Ocean Science Meeting 2022 (virtual); International Conference of Paleoceanography 2022 (Bergen, Norway); and International symposium on the Ocean in a high CO2 world in 2022 (Lima, Perú).

During this period, I had the opportunity to participate in several cruises, spending over 150 days at sea (see Table I). Most of those cruises were part of *The Nansen Legacy* project collecting seasonal data for this thesis onboard of the research vessel *Kronprins Haakon* to the northern Barents Sea and the Arctic Basin. I have also participated on cruises on board of RV *Helmer Hanssen* as part of the duty work and assisting in a teaching cruise.

Table I. List of cruises during the Ph.D. period.

Cruise name	Dates	Research vessel	Main activities and study area
Hunting gas flares and launching a seafloor observatory (CAGE/IG)	09/07–23/07/2019	Helmer Hansen	Various tasks as part of duty work. Kong Karls Land Platform and Prins Karls Forland
Seasonal cruise Q3 (*The Nansen Legacy* project)	05/08–27/08/2019	Kronprins Haakon	Collecting seasonal data for the PhD project. Latitudinal transect in the Barents Sea (Figure 3).
Calypso coring in the Fram Strait (CAGE/IG)	19/10–09/11/2019	Kronprins Haakon	Various tasks as part of duty work. Fram Strait and Yermak Plateau.
Seasonal cruise Q1 (*The Nansen Legacy* project)	02/03–24/03/2021	Kronprins Haakon	Collecting seasonal data for the PhD project. Latitudinal transect in the Barents Sea (Figure 3).
Seasonal cruise Q2 (*The Nansen Legacy* project)	27/04–20/05/2021	Kronprins Haakon	Collecting seasonal data for the PhD project. Latitudinal transect in the Barents Sea (Figure 3).
AKMA/CAGE 2021 (CAGE/IG)	22/05–30/05/2021	Kronprins Haakon	Various tasks as part of the educational component
Arctic Basin Joint Cruise 2-2	24/08–24/09/2021	Kronprins Haakon	Collecting data. Northwestern Barents Sea, Nansen Basin, Gakkel Ridge and Amundsen Basin.
Educational cruise in GEO–3111 and –3122	13/10–15/10/2022	Helmer Hansen	Teaching. Southwestern Barents Sea (Mefjorden and Håkjerringdjupet).

Also, in collaboration with the faculty of Biosciences, Fisheries and Economics (BFE, UiT) I had the opportunity to co-supervise, together with Prof. Marit Reigstad (PI) and Yasemin Bodur (Ph.D. candidate), a master thesis investigating the seasonal patterns on the vertical flux of carbon, both inorganic and organic, in the northern Barents Sea (expected submission date: November 2023).

During the Ph.D. period, I have collaborated with several researchers that will or have resulted in the co-authorship of research papers:

- Pallacks, S., Ziveri, P., Martrat, B., Mortyn, P. G., Grelaud, M., Schiebel, R., Incarbona, A., Garcia-Orellana, J., **Anglada-Ortiz, G.**, 2021. Planktic foraminiferal changes in the western Mediterranean Anthropocene. Global Planetary Change. https://doi.org/10.1016/j.gloplacha.2021.103549.

- Zamelczyk, K., Fransson, A., Chierici, M., Jones, E., Meilland, J., **Anglada-Ortiz, G.**, Lødemel, H. H., 2021. Distribution and abundances of planktic foraminifera and shelled pteropods during the polar night in the sea-ice covered northern Barents Sea. Frontiers in Marine Science, 1516. https://doi.org/10.3389/fmars.2021.644094.

- Ziveri, P., Gray, W.R., **Anglada-Ortiz, G.**, Manno, C., Grelaud, M., Incarbona, A., Rae, J.W.B., Subhas, A.V., Pallacks, S., White, A., Adkins, J.F., Berelson, W., 2023. Pelagic calcium carbonate production and shallow dissolution in the North Pacific Ocean. Nature Communications 14(1):805. https://doi.org/10.1038/s41467-023-36177-w.

This thesis consists of three research articles:

- **Paper I.** Anglada-Ortiz, G., Zamelczyk, K., Meilland, J., Ziveri, P., Chierici, M., Fransson, A., Rasmussen, T. L., 2021. **Planktic Foraminiferal and Pteropod Contributions to Carbon Dynamics in the Arctic Ocean (North Svalbard Margin).** Frontiers in Marine Science. doi:10.3389/fmars.2021.661158.

- **Paper II.** Anglada-Ortiz, G., Meilland, J., Ziveri, P., Chierici, M., Fransson, A., Jones, E., Rasmussen, T. L. **Seasonality of marine calcifiers in the northern Barents Sea: Spatiotemporal distribution of planktonic foraminifers and shelled pteropods and their contribution to carbon dynamics.** Progress in Oceanography. doi.org/10.1016/j.pocean.2023.103121.

- **Paper III.** Anglada-Ortiz, G., Rasmussen, T. L., Chierici, M., Fransson, A., Ziveri, P., Zamelczyk, K., Meilland, J., Garcia-Orellana, J. **Reconstruction of changes in environments and productivity based on planktonic foraminiferal faunas in the northern and southern Barents Sea during the last three millennia.** Submitted to Continental Shelf Research.

I. Synthesis

II. Research papers

I. Synthesis

1 Introduction

This Ph.D. project is part of *The Nansen Legacy (NL)* (Norwegian: *Arven etter Nansen, AeN*), an interdisciplinary project which aims to provide knowledge on the present and past state of the Barents Sea and the Arctic Ocean to better predict how this region will develop in the future. Specifically, the current work mainly focused on the "ocean acidification effects on planktonic calcifiers and biological pump efficiency" (subtask 2.1.4 under Research Focus RF2: Human Impacts) and contributed to the "high-resolution time series of sea-ice and ocean climate properties on long time scales" (subtask 1.3.1 under RF1: Physical Drivers).

1.1 Background and rationale

The Arctic Ocean is the smallest ocean on Earth and is divided almost half-half, by shelf and basin and by seasonal and permanent sea-ice cover, respectively (Bluhm et al., 2015, 2021). The Barents Sea is a shelf sea that is seasonally ice covered (annual mean Area = 1.47 10^6 km^2, annual mean Sea Surface Temperature = 0.9°C, annual mean Sea Surface Salinity = 34.2 (Sakshaug and Slagstad 1992; Smedsrud et al., 2022)). It is bordered by the Nansen Basin (Arctic Ocean) to the north, the Norwegian Sea to the south-west, and the Greenland Sea to the west. The Arctic Ocean and the Barents Sea are affected by different physical processes such as polar amplification and "Atlantification". Polar amplification is a term that refers to the larger effect of for instance climate change in polar areas. The term "Atlantification" refers to an increased inflow of Atlantic water, bringing not only warmer and more saline water but also nutrients and new marine species of southern affinity. Atlantification has already been observed by increasing temperatures and intrusion of Atlantic species in the northern Svalbard margin and the Barents Sea (Bjørklund et al., 2012; Polyakov et al. 2020; **Paper I;** Ingvaldsen et al., 2021). An increased inflow of Atlantic water in the Barents Sea is also a driver for sea ice loss (Asbjørnsen et al., 2020). During the last decades, the sea ice has retreated 61×10^3 km^2/decade and 218×10^3 km^2/decade between 1980–2010 and 1998–2008, respectively (Årthun et al., 2012). These facts, together with the already low calcium saturation states make the Barents Sea highly susceptible to ocean acidification (Chierici and Fransson, 2018).

The goal of this thesis is to study (1) the distribution of planktonic foraminifers and shelled pteropods and their contribution to carbon standing stocks and export production on the northern Svalbard margin in the Arctic Ocean (**Paper I**), (2) their spatiotemporal variability

and contribution to carbon dynamics on a seasonal basis in a transect from the northern Barents Sea into the Nansen Basin in the Arctic Ocean (**Paper II**), and (3) to reconstruct the changes of planktonic foraminiferal faunas and their preservation states in sediment cores comparing the northern and the southern Barents Sea focusing on the last three millennia (**Paper III**).

1.1.1 Ocean acidification

Ocean acidification is a process that turns the ocean more acidic by decreasing pH, the calcium carbonate saturation state ($\Omega CaCO_3$), and the carbonate ion concentration (CO_3^{-2}). It is due to an increase of carbon dioxide (CO_2) uptake from the atmosphere to the ocean. Since the early 1900s, the CO_2 emissions from anthropogenic activities (e.g., burning of fossil fuel, deforestation, and intense agriculture) have been increasing. The observatory from Mauna Loa in Hawaii has been recording an increase of atmospheric CO_2 from c. 320 parts per million (ppm) in the 1960´s to 421.7 ppm on August 1, 2023 (Tans and Keeling, 2023). When the CO_2 dissolves in the ocean it reacts with water molecules resulting in the formation of carbonic acid (H_2CO_3) (Figure 1):

$$\boldsymbol{CO_2 + H_2O \rightarrow H_2CO_3}$$

The more CO_2 that dissolves in the ocean, the more H_2CO_3 is formed. However, H_2CO_3 dissociates easily to bicarbonate (HCO_3^-) and protons (H^+):

$$\boldsymbol{H_2CO_3 \rightleftarrows HCO_3^- + H^+}$$

$$\boldsymbol{HCO_3^- \rightleftarrows CO_3^{-2} + H^+}$$

The increasing H_2CO_3, therefore, increases the concentration of H^+ in seawater, and results in a decrease of the pH ($pH = -\log [H^+]$) acidifying the seawater. This increasing concentration of H^+ together with its reaction with carbonate (CO_3^{-2}) hampers the process of calcification performed by calcifying organisms (see **1.1.3 Marine calcifiers**).

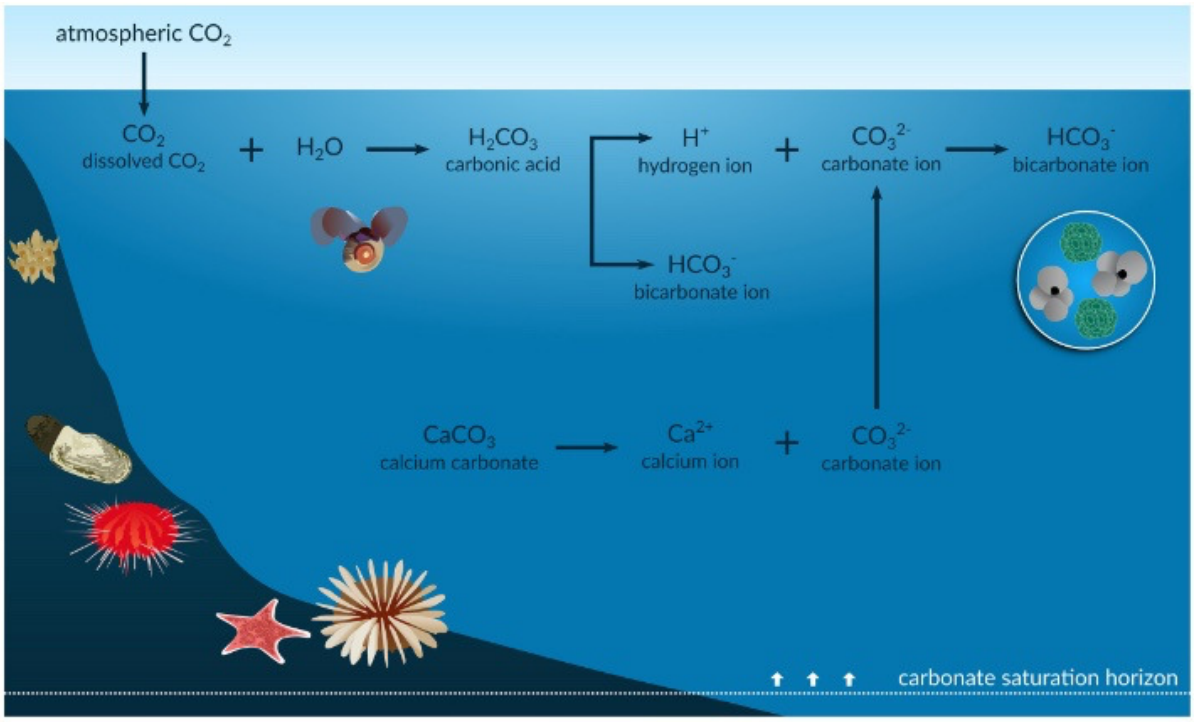

Figure 1. Reaction of CO_2 dissolving in the sea water. From Figuerola et al. (2021).

1.1.2 Oceanic carbon pump

There is a constant gas exchange between the atmosphere and the ocean. Specifically, CO_2 is dissolved in the ocean, consumed through photosynthesis by phytoplankton and transferred to secondary producers. The remaining organic material will sink to the sea floor where it can be preserved in the sediment and/or consumed by the benthic community. This process is known as the **organic carbon or soft-tissue pump** (De la Rocha and Passow, 2014). At the same time, CO_2 is released from the ocean to the atmosphere by processes of respiration and decay of organic matter, as well as calcification performed by marine calcifiers (known as **carbonate counter pump**; Salter et al., 2014; Manno et al., 2018). The calcium carbonate ($CaCO_3$, both in calcitic and aragonitic forms) in planktonic calcifiers is exported to the sea floor when these organisms die and sink.

1.1.3 Marine calcifiers

Marine calcifiers are those making a shell of calcium carbonate ($CaCO_3$) through calcification processes. They use the existence of calcium (Ca^{+2}) and carbonate (CO_3^{-2}) ions naturally present in the water, as follows:

$$\boldsymbol{Ca^{+2} + CO_3^{-2} \rightarrow CaCO_3}$$

Marine calcifiers are divided into benthic (living in or on the sediment) and planktonic (living in the water column). Planktonic foraminifers and shelled pteropods are ubiquitous marine calcifiers, found from equatorial to polar waters. Together with coccolithophores, they contribute significantly to the carbon cycle. They export organic (soft tissue), but mainly inorganic carbon from their calcareous shells to the seabed when they die and sink. Moreover, marine calcifiers in general, but pteropods specifically, have been extensively used as bioindicators for ocean acidification studies showing damages on their aragonitic shells when exposed to acidified water conditions (Fabry, 2008; Fabry et al., 2008; Comeau et al., 2009, 2010, 2012; Bednaršek et al., 2012b, 2012d, 2014a, 2014b, 2019; Manno et al., 2012, 2017; Schiebel et al., 2017).

Several studies, conducted from low to high latitudes have investigated the role of planktonic foraminifers (Schiebel and Movellan 2012; Salter et al., 2014; Meilland et al., 2016a, 2016b, 2018; Rembauville et al., 2016) and pteropods (Hunt et al., 2008; Bednaršek et al., 2012a; Roberts et al. 2014) in the carbon cycle. When studied together results show that pteropods usually contribute equally or higher than foraminifers to the export of $CaCO_3$ (i.e., Hunt et al., 2008; Buitenhuis et al., 2019; **Paper I**; Knecht et al., 2023; Ziveri et al., 2023)). Due to the major role that planktonic calcifiers play in the carbon pump, some studies have suggested that the carbon cycle from different regions might be affected under conditions of ocean acidification (i.e., Feely et al., 2004; Davis et al., 2017; **Paper I**).

When their shells sink to the sea floor, and if it is located above the carbon compensation depth (CCD), they accumulate in the sediment and the fossil record and can be used (mainly foraminifers) to reconstruct the environmental conditions and even the carbon cycle (i.e., John et al., 2013) from when they were alive. The CCD is the limit from which the carbon gets dissolved in the water column and is located below the lysocline, that represents the depth where the dissolution rate increases the most. This depth in the Arctic Ocean is, at present, located at around 3500-meter water depth (Jutterström and Anderson, 2005) and has been, at least, as deep as at 4000-m water depth for the last 1.5 million years (Morris and Clark, 1985). Hence, all the samples studied in this thesis are unlikely to be dissolved in the water column. Specifically in the shelf areas of the Barents Sea (see **1.3 Oceanographic settings from the northern Svalbard margin and Barents Sea**) no dissolution on the water column has been observed, which agrees with the findings from **Paper II**. However, dissolution in the sediment is a process that has been described in the past and discussed in detail in **Paper III**.

1.2 Objectives and research questions

The main objective of this thesis is to investigate planktonic foraminifers and shelled pteropods in the Barents Sea and the adjacent Arctic Basin to shed new light on the knowledge of:

- The distribution patterns of these living marine calcifiers and contribution to the carbon standing stocks ($\mu g/m^3$) and export production (mg/m^2d) in different oceanic regimes at the north Svalbard margin (**Paper I**) and the northern Barents Sea (**Paper II**).
- Which environmental parameters, including carbonate chemistry, affect the distribution of these marine calcifiers (**Paper I, II and III**).
- Their seasonal variability in a seasonally sea-ice covered area of the northern Barents Sea (**Paper II**).
- The reconstructed foraminiferal production for the last few thousand years from the fossil record at two locations in the Barents Sea (north and south of the Arctic Polar Front) (**Paper III**).

The associated research questions of this thesis are:

- Which are the factors controlling the abundance and size distribution of the planktonic calcifiers and their contribution to the carbon standing stocks and export production in the Atlantic influenced Svalbard margin (Arctic Ocean)? (**Paper I**).
- How do seasonality, sea-ice cover, and physico-chemical parameters (e.g., temperature, salinity, chlorophyll-a, and carbonate chemistry) affect the distribution patterns of these planktonic calcifiers in a latitudinal transect along the (northern) Barents Sea? How do their contribution to the carbon standing stocks and export production change through the seasons? (**Paper II**).
- How are the assemblages and biomass changing from the pre-industrial Revolution until the present in the Barents Sea? Are those changes potentially related to the increasing temperatures and CO_2 emissions? Are there any differences between the northern and the southern Barents Sea? (**Paper III**).

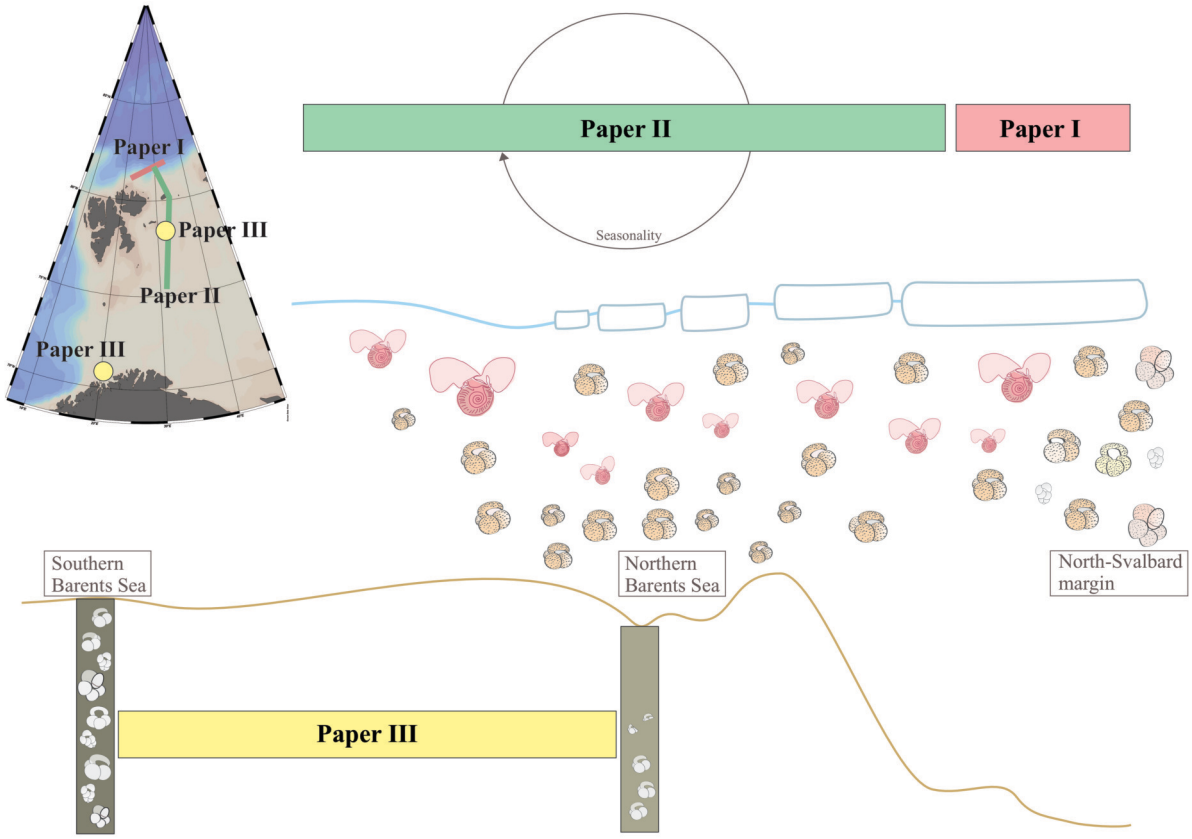

Figure 2. Schematic of the objectives of the thesis and the three papers.

1.3 Oceanographic settings from the northern Svalbard margin and Barents Sea

This thesis is focusing on different areas in the Arctic Ocean and the Barents Sea: the north Svalbard margin (**Paper I**), the northern Barents Sea (**Paper II and III**) and the southern Barents Sea (**Paper III**) (Figure 2).

The northern Svalbard margin is mainly influenced by the Atlantic surface Water through the Svalbard branch from the West Spitsbergen Current (Meyer et al., 2017) and Atlantic Intermediate Water (Figure 3 and **Paper I**). Both water masses are characterized by being warmer and more saline compared to the Arctic Water (Sundfjord et al., 2020). Moreover, Atlantic Water transports nutrients to the Arctic Ocean and Barents Sea (Torres-Valdés et al., 2013; Duarte et al., 2021). Recent studies have described an increasing inflow of Atlantic Water since the 1970´s (Onarheim et al., 2014), an important control of variations in sea-ice cover, and nutrients (Tuerena et al., 2022). Due to this increasing inflow of Atlantic Water this area

is prone to "Atlantification" causing a decrease in seasonal sea ice, an increase in nutrients, and the introduction of new marine species from the south (Bjørklund et al., 2012, **Paper I**).

The Barents Sea is divided into the northern and the southern Barents Sea by the Polar Front (black dashed line, Figure 3). The Polar Front is an area that separates the seasonally sea-ice covered Barents Sea in the north with the permanently sea-ice free Barents Sea in the south. The location of this front has been relatively stable located at 74–76 °N during the last few millennia (**Paper II** and references therein). In the early Holocene, it was located at c. 70°N and retreated northwards during the mid-Holocene (Risebrobakken and Berben, 2018). The front represents a gradient in temperature, salinity, and nutrient availability from the southern to the northern Barents Sea. Atlantic waters flow along the Norwegian continental slope and enter the northern Barents Sea through the Fram Strait Branch of the West Spitsbergen Current, and the southern Barents Sea through the Barents Sea Branch (Lundesgaard et al., 2022 and references therein; red arrows Figure 3). Arctic waters are formed through different cooling processes and interactions with Atlantic Water, sea-ice, and meltwater (Lundesgaard et al., 2022; blue arrows, Figure 3). They flow from the Arctic Ocean to the northern Barents Sea via the East Spitsbergen Current and Persey Current (Harris et al., 1998). Sundfjord et al. (2020) updated the water mass definitions from the Barents Sea based on the conservative temperature (CT), absolute salinity (SA), and density (σ_0). In the northern Barents Sea, we found *Polar Water* ($CT \leq 0.0°C$, $\sigma_0 \leq 27.97$ kg m^{-3}), *warm Polar Water* ($0.0 < CT < 4.0°C$, $S_A < 35.06$ g kg^{-1}), *Atlantic Water* ($CT > 2.0°C$, $S_A \geq 35.06$ g kg^{-1}), and *modified Atlantic Water* ($0.0 < CT \leq 2.0°C$, $S_A \geq 35.06$ g kg^{-1}) (Sundfjord et al., 2020; **Paper II**). The water masses in the southern Barents Sea are the *Norwegian Coastal Current* ($CT > 4°C$, $S_A < 35.06$) and *Atlantic Water* (Sundfjord et al., 2020; **Paper III**).

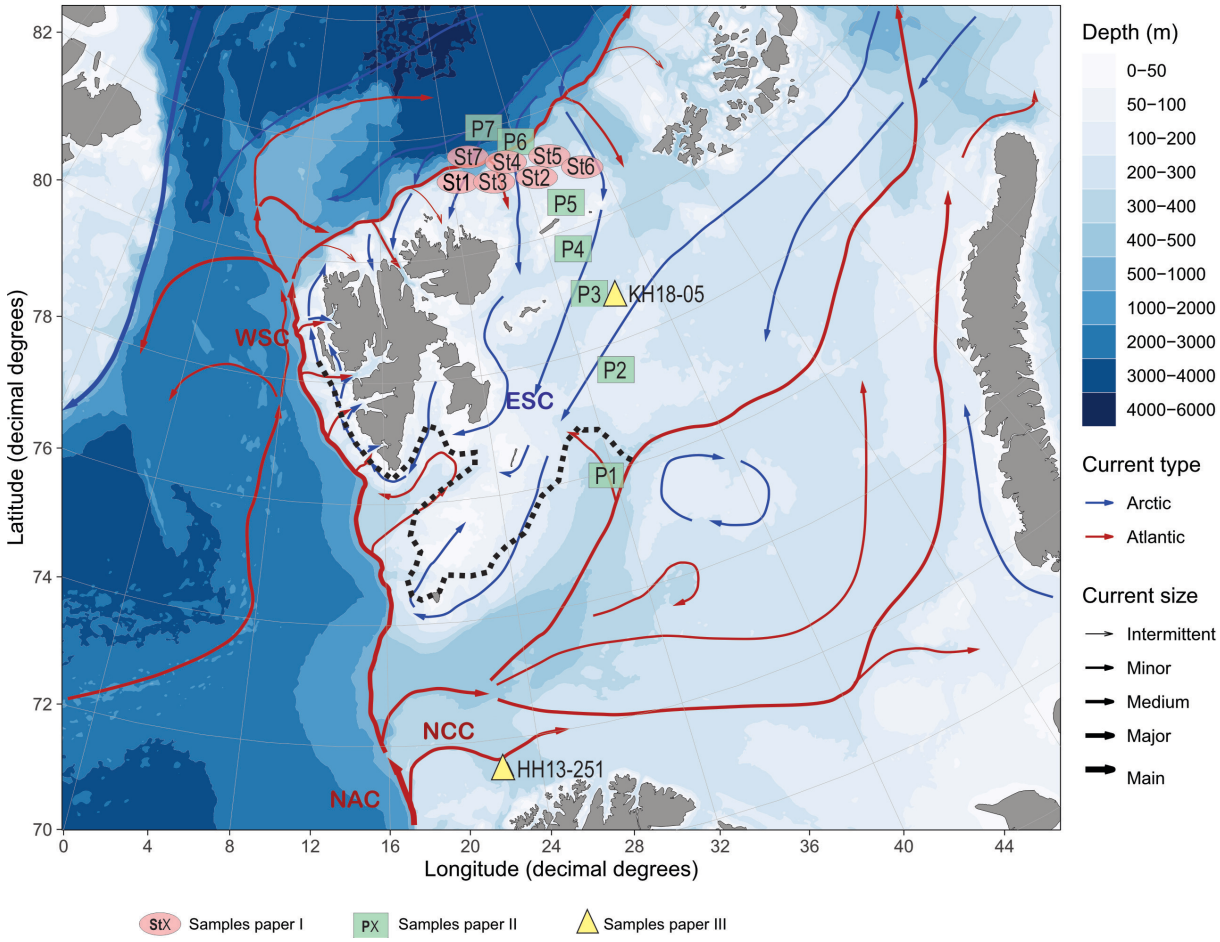

Figure 3. Map of the study area including the path of Atlantic (red arrows) and Arctic (blue arrows) waters from Vihtakari (2020), as well as the Polar Front (black dashed line, from Loeng (1991)). Sampling locations are color coded: pink circles for Paper I, green squares for Paper II and yellow triangles for Paper III.

Table 1. Sample positions (station name, latitude, longitude, and water depth) and type of sample (PT = plankton tow, Ws = water sample for carbonate chemistry, and MC = multicore).

	Name	Latitude (°N)	Longitude (°E)	Water depth (m)	Type of sample
Paper I	St 1	81.32	22.14	378	PT, Ws
	St2	81.49	28.95	368	PT, Ws
	St3	81.30	25.93	510	PT, Ws
	St4	81.45	26.68	1019	PT, Ws
	St5	81.64	28.76	2166	PT, Ws
	St6	81.55	31.29	853	PT, Ws
	St7	81.77	25.31	3094	PT, Ws
Paper II	P1	76.00	31.22	322	PT
	P2	77.50	34.00	190	PT
	P3	78.70	34.00	307	PT
	P4	79.70	34.23	332	PT
	P5	80.50	33.96	158	PT
	P6	81.50	31.50	840	PT
	P7	82.00	28.8	3120	PT
Paper III	HH13-251	71.67	22.99	428	MC
	KH18-05	78.77	33.99	301	MC, PT, Ws

2 Scientific approach

The results presented in this thesis are based on two different sampling strategies, including plankton tows (see **2.2 Planktonic calcifiers in the water column**) and sediment (see **2.3 Planktonic calcifiers in the fossil record**) (Table 1 and Figure 4). The samples from **Paper I** and **Paper III** were collected before the start of this Ph.D. project, between 2013 and 2018, and under the careful attention of N. El bani Altuna, S. Ofstad, K. Zamelczyk and T. L. Rasmussen onboard the RV *Helmer Hansen* and *Kronprinss Haakon*. The samples from **Paper II** were collected on a seasonal basis, between 2019 and 2021, onboard the RV *Kronprins Haakon* as part of *The Nansen Legacy* project. The description of the methodology is illustrated on Figure 4 and detailed in this section.

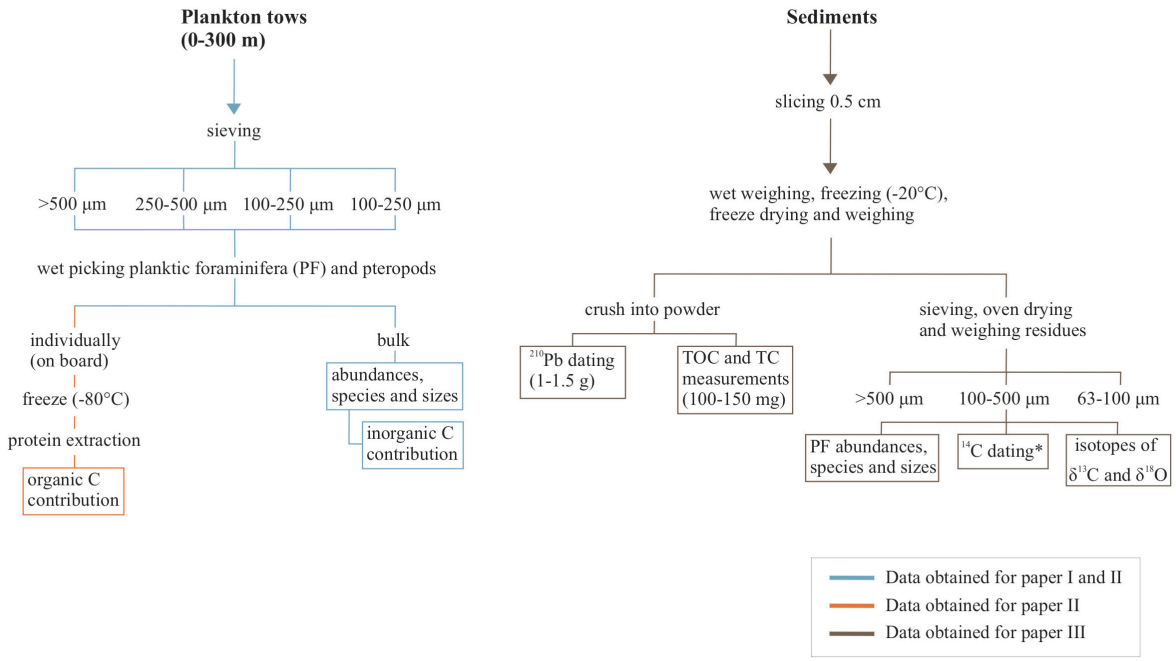

Figure 4. Outline of the methods used in this thesis. Blue lines represent the data used for **Paper I** and **II**, orange for exclusively **Paper II**, and grey for **Paper III**.

2.1 Ecology of marine calcifiers

Planktonic foraminifers and shelled pteropods are two distinct groups of marine calcifiers found in all oceans. Both are heterotrophic, feeding both from phytoplankton and zooplankton.

2.1.1 Planktonic foraminifers

Planktonic foraminifers are protists with a shell (or "test") made of calcite (the less soluble form of $CaCO_3$). Olsson et al. (1999) pointed their first occurrence during the early Paleocene, almost 65 million years (Ma) ago, but recent studies indicate they were diversified from the benthic foraminifers already in the Jurassic, around 200 Ma ago (K BouDagher-Fadel, 2015). Planktonic foraminifers apparently move through the water column by performing diel vertical migration as other zooplankton (i.e., copepods). However, Meilland et al. (2019) in the subtropical North Atlantic showed that migration did not occur and has also not been observed in Arctic and sub-Arctic studies (Manno and Pavlov, 2014; **Paper I**). They are considered omnivorous. Most of the spinose species mainly prey on other zooplankton, while many of the non-spinose species are mainly herbivorous (Schiebel and Hemleben, 2017). Planktonic foraminifers, mainly spinose, are usually found in symbiosis with dinoflagellates and chrysophytes (Schiebel and Hemleben, 2017). Their life cycle is not fully understood. Sediment trap studies have indicated a life of approximately six months (Nigam et al., 2003; Nigam, 2005). They mostly reproduce sexually even though asexual reproduction has been observed from cultured specimens of *Neogloboquadrina incompta* (Schiebel and Hemleben, 2017) and *Neogloboquadrina pachyderma* (Meilland et al., 2022; Westgård et al., 2023). They are found in all oceans and from the equator to the poles (Schiebel and Hemleben, 2017). The diversity of species is the highest in the equatorial and warmer waters and low in the polar areas (Schiebel and Hemleben, 2017). In Arctic and polar areas, the fauna is entirely dominated by *N. pachyderma* which is considered the only polar species of planktonic foraminifers. In sub-Arctic areas the species is accompanied by sub-polar or Atlantic species, mainly *Turborotalita quinqueloba, Globigerinita uvula* and *N. incompta* (Figure 5).

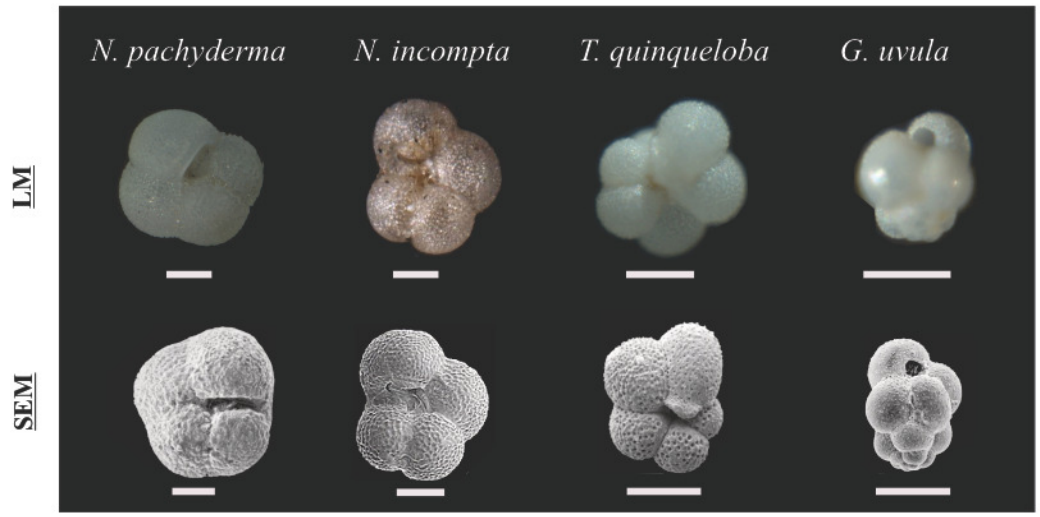

Figure 5. Specimens of planktonic foraminifers from light microscope (LM, upper panels) and scanning electron microscope (SEM, lower panels). LM pictures from G. Anglada-Ortiz (*Neogloboquadrina pachyderma*, *Turborotalita quinqueloba* and *Globigerinita uvula*) and Young et al., 2017 (*Neogloboquadrina incompta*). SEM pictures from Schiebel and Hemleben (2017) (*N. pachyderma*, *T. quinqueloba* and *G.uvula*) and Darling et al. (2006) (*N. incompta*). The white bars represent 100 µm length.

Studies from the Arctic and sub-Arctic show dominance of these species both in the living assemblages from plankton tows (Pados and Spielhagen, 2014; Schiebel et al., 2017; Meilland et al., 2020; **Paper I**; Zamelczyk et al., 2021; **Paper II**; **Paper III**) and surface sediments and fossil records (Husum and Hald, 2012; Pados and Spielhagen, 2014; Schiebel et al., 2017; Risebrobakken and Berben, 2018; Sahoo et al., 2022; **Paper III**). The species composition of faunas found in the sediment reflects well the population living in the water column and, especially in the Fram Strait, they are best correlated with the assemblages found at subsurface depth in the water column (50–100 m depth) (Pados and Spielhagen, 2014).

- The species ***N. pachyderma*** (see Figure 5) finds its highest abundances at the sea-ice margin (i.e., Pados and Spielhagen, 2014; Schiebel and Hemleben, 2017). In summer, it represents 56–85% of the living foraminiferal fauna in the Arctic (i.e., in the Fram Strait, northern Barents Sea, and north Svalbard margin; Manno and Pavlov, 2014; Pados and Spielhagen, 2014; **Paper I** and **II**). In the sub-Arctic it constitutes less than 25% (i.e., Meilland et al., 2020; Ofstad et al., 2020).
- The subpolar species ***T. quinqueloba*** (see Figure 5) has been associated with high primary productivity found in mixing zones of water masses (i.e., frontal areas) and areas of influence of Atlantic Water. The species has therefore been used as a proxy for paleoproductivity and Atlantic Water inflow (Volkmann 2000, Husum and Hald 2012,

Schiebel and Hemleben 2017, Sahoo et al. 2022). They dominate the foraminiferal fauna, c. 85%, in areas influenced by Atlantic inflow such as in the West Spitsbergen Current (Volkmann 2000, Schiebel et al. 2017). They are present in the living polar assemblage together with *N. pachyderma* in the Fram Strait and the northern Barents Sea (i.e., Pados and Spielhagen, 2014; Zamelczyk et al., 2021; **Paper II**).

- The species ***G. uvula*** (see Figure 5) is most abundant in Coastal Water and therefore has been used as a proxy for surface water freshening (Husum and Hald, 2012). It is rare in polar and subpolar areas (<2%). It can be present in the water column but can be absent in the sediment below, probably due to its low preservation potential (Schiebel and Hemleben, 2017; Meilland et al., 2020; Sahoo et al., 2022).
- The subpolar species ***N. incompta*** (see Figure 5) is a surface-dwelling species with a low abundance at high latitudes. It dominates the foraminiferal fauna in areas of low productivity and in stratified water (Schiebel and Hemleben, 2000, 2017).

2.1.2 Shelled pteropods

Shelled (or thecosome) pteropods are gastropods with a shell made of aragonite (the more soluble form of $CaCO_3$). Because of the sensitivity of their shells towards changes in the environment (i.e., temperature or pH) they are commonly referred to as "the canary of the coalmine" for ocean acidification (i.e., Oakes and Sessa, 2020). Recent studies pointed that they developed during the early Cretaceous period, 139.1 Ma ago (Peijnenburg et al., 2020). Opposite to planktonic foraminifers, they are active swimmers. Like other gastropods, they are hermaphroditic and reproduce sexually (Lalli and Wells, 1978). Their feeding strategy is based on the secretion of a mucus web where organisms and particles get trapped (Peijnenburg et al., 2020). They are found in all oceans (Bednaršek et al., 2012a). The pteropod biomass is the highest at the surface between 0–10 m and between 40–50°N (Bednaršek et al., 2012a). Polar areas are dominated mainly by *Limacina helicina*, while *Limacina retroversa* is found in Atlantic-influenced areas in the Arctic (i.e., Fram Strait) and their presence have been associated with an increase of Atlantic inflow (or "Atlantification") (Meinecke and Wefer, 1990; Bauerfeind et al., 2014; Busch et al., 2015) (Figure 5). In the central Arctic Ocean (Canada Basin) *L. helicina* has a 1.5-to-2-year life cycle reaching their maximum size of c. 2.8 cm during late autumn (Kobayashi, 1974).

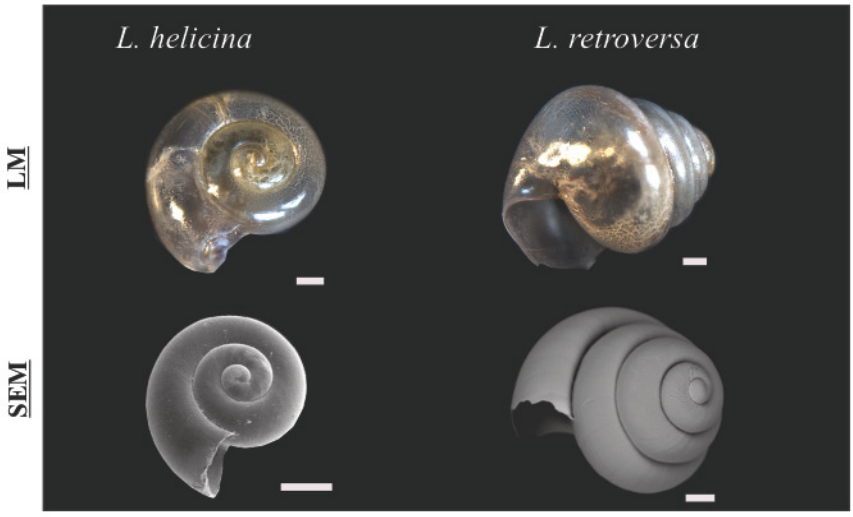

Figure 6. Specimens of pteropods from light microscope (LM, upper panels) and scanning electron microscope (SEM, lower panels). Pictures from LM from G. Anglada-Ortiz (*Limacina helicina* and *Limacina retroversa*). Pictures from SEM from Sato-Okoshi et al. (2010) (*L. helicina*) and León et al. (2019) (*L. retroversa*). The white bars represent 100 µm length.

2.2 Planktonic calcifiers in the water column

2.2.1 Sampling methods

For this thesis, living planktonic foraminifers and shelled pteropods were collected by vertical tows of plankton nets (WP2 mesh-size 90 µm **Paper I** and 63 µm **Paper III**; and Hydrobios Multinet mesh size 64 µm **Paper II**). We sampled the upper 300 meters of the water column or 10 m above bottom in case of shallower waters (i.e., P2 and P5 from **Paper II**). Seven stations from the north Svalbard margin were sampled as follows: 0–50, 50–100, 100–200 and 200–300 m (Table 1; **Paper I**). After the collection, the nets were rinsed with seawater and the samples were transferred to plastic bags and frozen at -20°C. Seven stations from the northern Barents Sea in the Nansen Legacy transect were seasonally sampled as follows: 0–50, 50–100, 100–150, 150–200, 200–300 m (August 2019), and 0–20, 20–50, 50–100, 100–200, 200–300 m (March, May and July 2021) (Table 1; **Paper II**). After the collection, the nets were rinsed with seawater and the samples were washed through a cascade of sieves (500, 250, 100 and 64 µm). Each subsample was rinsed with filtered seawater and transferred into a Petridish. Specimens were picked individually and collected in 1.5 ml Eppendorf tubes and frozen at -80°C for further analyses (see **2.2.2.2. Organic carbon**). The subsamples were then transferred into 250 ml Whirl-Pak® *Nasco* plastic bags and frozen at -20°C. Planktonic foraminifers and pteropods were counted, picked, and classified to species level on land or processed onboard.

Even though some studies have been sampling planktonic marine calcifiers through the whole water column from surface to the seabed, recent studies performed in the Arctic Ocean (Greco et al., 2019) and southern Barents Sea (Ofstad et al., 2020) focused on the upper 300 m of the water column, as was the case for the sampling of **Paper I** and **II**. Several studies have described that the different choices of mesh size influence the results on size and abundance of the planktonic organisms collected (i.e., Berger, 1969; Bednaršek et al., 2012a; **Paper I**; Feuilloley et al., 2022; Chaabane et al., 2023). Finer mesh sizes usually result in smaller organisms and higher abundances (Berger, 1969; Feuilloley et al., 2022). Due to the small sizes of planktonic organisms in Arctic and sub-Arctic waters, the most common mesh sizes are 63 µm (Manno and Pavlov, 2014; Pados and Spielhagen, 2014; Ofstad et al., 2020; Zamelczyk et al., 2021; **Paper II** and **III**), 90 µm (Manno et al., 2012; **Paper I**), or 100 µm (Greco et al., 2019; Meilland et al., 2020).

2.2.2 Estimating the contribution of planktonic calcifiers to carbon dynamics

To study carbon dynamics, carbon standing stocks (µg m^{-3}) and export production (mg $m^{-2}d^{-1}$) were estimated. The standing stocks represent how much carbon is contained in the water column per cubic meter. The standing stocks from **Paper I, II and III** were estimated in the productive zone (0–100 m water depth). The standing stock results presented in this thesis were obtained by dividing the total carbon as the sum of $CaCO_3$ and organic carbon from foraminifers and pteropods by the volume of water collected with the nets (see **Paper I** and **Paper II**). The export production represents how much carbon is reaching a specific depth. In this thesis 100 m depth was chosen as it aims to measure the initial flux of calcitic shells following Schiebel and Hemleben (2000). The results of export production were obtained by multiplying the standing stocks by the test sink velocity (and dividing by a factor of 1000 to convert from µg to mg). In the case of planktonic foraminifers, the test sink velocity was calculated by each size fraction (Takahashi and Bé, 1984; Schiebel, 2002; Meilland et al., 2018). For pteropods, we used a constant of 842 m d^{-1} calculated for a 500 µm specimen from Chang and Yen (2012). This velocity was considered more suitable than previously published by Lalli and Gilmer (1989) (864–1210 m d^{-1}). The contribution from foraminifers and pteropods of inorganic $CaCO_3$ from their shells and organic carbon from their soft tissue have been estimated separately.

2.2.2.1 Inorganic carbon

The shell size and weight have been used as a proxy for inorganic carbon content in planktonic foraminifers and pteropds. The shell weight of planktonic foraminifers has been used to estimate their content of $CaCO_3$ assuming that 1 µg of shell equals 1µg of $CaCO_3$. For this thesis, the individual mass of planktonic foraminifers larger than 100 µm has been measured with a microbalance (Mettler Toledo XP2U, 0.1 µg precision; **Paper I**). Their mass was also estimated from the minimum diameter of their shells using the following equations from Meilland et al. (2018) in **Paper I**, **II** and **III**, where the foraminiferal weight (y_m) is proportional to the diameter (x):

$$\boldsymbol{y_w = 2.04 \times 10^{-05} x^{2.2}} \text{ (all species)}$$

$$\boldsymbol{y_w = 8.46 \text{ x } 10^{-05} x^{1.9}} \ (N. pachyderma)$$

$$\boldsymbol{y_w = 7.92 \text{ x } 10^{-08} x^{3.3}} \ (G. uvula)$$

The weight (dry weight, *DW*, or wet weight, *WW*) of pteropods were estimated by measuring their diameter (*D,* for *L. helicina*) and length (*L,* for *L. retroversa*) using the equations from Bednaršek et al. (2012c) as follows:

$$\boldsymbol{DW = 0.137\ D^{1.5005}} \ (L. helicina)$$

$$\boldsymbol{WW = 0.000194 \times L^{2.5473}} \ (Limacina\ spp)$$

The wet weight was multiplied by 0.28 to convert it into dry weight (Davis and Wiebe 1985). The DW_{total} was obtained by multiplying the *DW* by the number of organisms. Then, the DW_{total} was transformed into biomass before converting into $CaCO_3$ as published in Larson (1986) and Bednaršek et al. (2012a).

2.2.2.2 Organic carbon

The protein content has been used as a proxy for organic carbon content assuming that 1 µg of protein equals 1 µg of organic carbon. The protocol for planktonic foraminifers was published by Movellan et al. (2012). However, this protocol was, to our knowledge, never applied to pteropods until published in **Paper II**. This protocol consists of measuring the protein content of preferably single individuals of different sizes to create a calibration curve as shown in Figure 7.

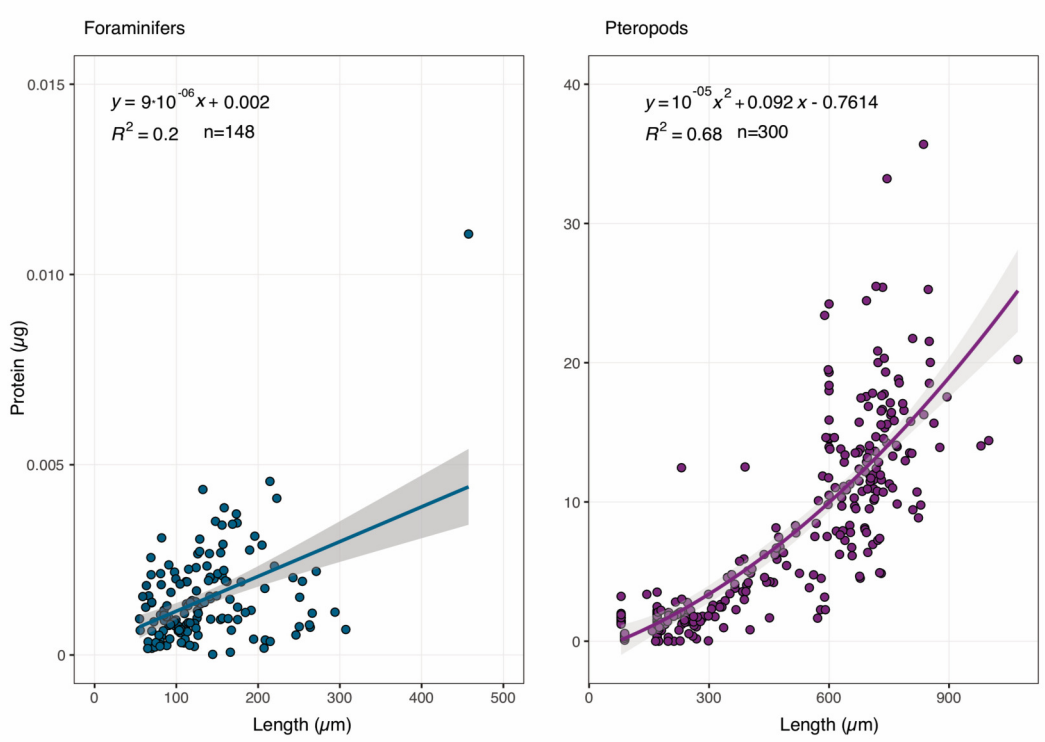

Figure 7. Calibration curve of protein content (µg) versus the shell length (µm) of foraminifers (left, blue) and pteropods (right, purple) from **Paper II**.

Several chemicals were used to perform this protocol: Bicinchoninic Acid (Sigma-Aldrich ref: B9943-1L), Copper (II) sulfate solution (Sigma-Aldrich ref: C2284-25ML) and Protein standard liquid (Sigma-Aldrich ref: PO914-10 AMP). Several different types of equipment were used: vortex shaker, NanoDrop™, micro- and pipette tips, and a binocular microscope with camera and software (Figure 8). The results from this thesis were obtained using a NanoDrop 2000® from the Department of Arctic Biology, UiT Arctic University of Norway, and measuring the minimum diameter of the individual organism to create a curve of the protein content (µg) and size of the organism (µm) (Figure 8). Prior to the protein measurements, the equipment was calibrated by analyzing six standardized samples with known concentrations of protein and *milliQ* (purified) water (X0–X10, Figure 8) and reagent. Three replicates of each were performed (A–C, Figure 8). The reagent solution was made by mixing 1 ml of Copper (II) sulfate with 49 ml of Bicinchoninic acid. The sizes of the organisms were estimated after the protein measurements, by taking pictures with a DMC4500 camera attached to a Leica Z16 APO binocular and using the imageJ software (Schneider et al. 2012).

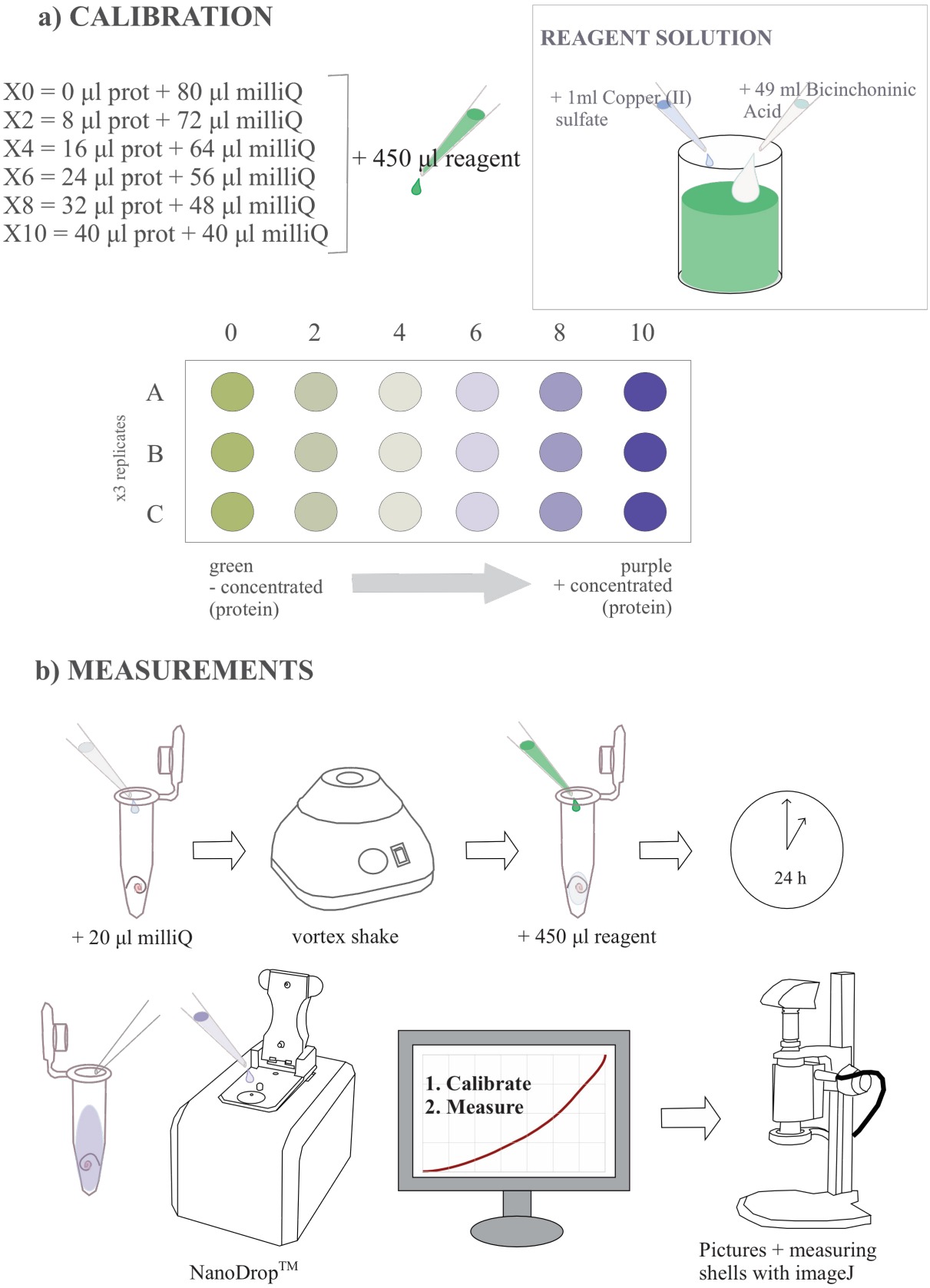

Figure 8. Illustrated protein extraction protocol based on the methods from Movellan et al. (2012), including the calibration (with protein (=prot) and milliQ water (a)), the reagent preparation, and the steps for the measurements (b).

2.3 Planktonic calcifiers in the fossil record (sediment samples)

2.3.1 Sampling methods

The fossils of planktonic foraminifers were collected from the sediments using multicorers (50-cm long, 10 cm inner diameter; **Paper III**). Two multicores were collected, from the northern and southern Barents Sea, respectively.

Immediately after the recovery of the sediment cores, they were sliced in high resolution (every 0.5 cm) or kept in the fridge (4°C) and sliced in the laboratory in the same high resolution. Next, the sediments were weighed, freeze dried, and weighed again to calculate the water content. Between 1–1.5 gram of dry sediment was taken from the upper 30 cm of both cores to measure the activity of Lead-210 (^{210}Pb, see **2.3.3. Age model**). The measurements were performed at the Environmental Radioactivity Lab at the Autonomous University of Barcelona, Catalonia, Spain. Between 100–150 milligrams were subtracted, from every second sample from both cores and homogenized to determine the Total Carbon (TC, %) and Total Organic Carbon (TOC, %). This was performed at the School of Geography and Sustainable Development from the University of Saint Andrews, Scotland, United Kingdom. A minimum of 10–15 gram of bulk sediment was wet sieved through a series of sieves (500, 100 and 63 μm), and each size fraction (>500, 100–500 and 63–100 μm) was oven dried at 40°C. Planktonic foraminifers (and broken shells) from the size fraction 100–500 μm were picked and counted and, only the intact organisms, were classified into species level.

The counting of broken shells and fragments and the calculation of the degree of fragmentation (or fragmentation index, *F(%)*) have been extensively used as a proxy to estimate the preservation of planktonic foraminifers in the north Atlantic and the Arctic (Crowley, 1981; Chapman et al., 2000, Zamelczyk et al., 2012, 2013; Aagaard-Sørensen et al., 2014; **Paper III**). This is calculated by the number of complete shells (*C*) and fragments (*F*), as follows:

$$\boldsymbol{F}(\%) = \mathbf{100} \times \boldsymbol{F}/(\boldsymbol{C} + \boldsymbol{F})$$

The fragmentation index is considered more subjective than other methods such as the shell weight (Berger, 1970; Kucera, 2007). Other methods such as the ratio between benthic and planktonic foraminifers have been used, as well as the absence of planktonic foraminifers in the sediment when they were observed in plankton tows (Aksu, 1983; **Paper III**). In Baffin Bay, located between Greenland and the Canadian Arctic Archipielago, Aksu (1983) found

that below 400 m water depth the sediment was mainly dominated by arenaceous specimens (=agglutinated benthic foraminifers), which are also taken as a sign of dissolution of calcareous specimens.

2.3.2 Stable isotopes

The ratio of carbon ($\delta^{13}C$) and oxygen ($\delta^{18}O$) isotopes have been extensively used in fossil (planktonic) foraminifers as a tool to reconstruct the conditions of the water column from when they were alive. In this thesis, we report the stable isotopes from 50 samples from the southern Barents Sea multicore analyzed at The Stable Isotope Lab at the Department of Geosciences UiT The Arctic University of Norway. The samples consist of at least 10 specimens of *N. pachyderma* shells (**Paper III**). Due to the almost zero abundances of foraminifers in the upper 20 cm of the core, isotopes were not measured in the core from the northern Barents Sea (**Paper III**).

In the Barents Sea, most studies have been focusing on the isotope signal in living (Ofstad et al., 2020) or fossilized specimens covering the Holocene period in low resolution (i.e., Lubinski et al., 2001; Berben et al., 2014). However, little is known about the variability in high-resolution stable isotope records for the late Holocene and under natural and anthropogenic conditions.

2.3.3 Age model

The construction of a robust age model for the late Holocene, and on a high-resolution basis is challenging. Most studies construct the age model by either using ^{210}Pb or Carbon-14 (^{14}C) dating (i.e., Figure 9), but it is uncommon to find the two methods combined (Zamelczyk et al., 2013, 2020; **Paper III**). The age model here combines both ^{210}Pb and ^{14}C through Bayesian statistics and using the *´rbacon´* package of the software Rstudio (Blaaw et al., December 22, 2022) with the calibration curve of Marine20.

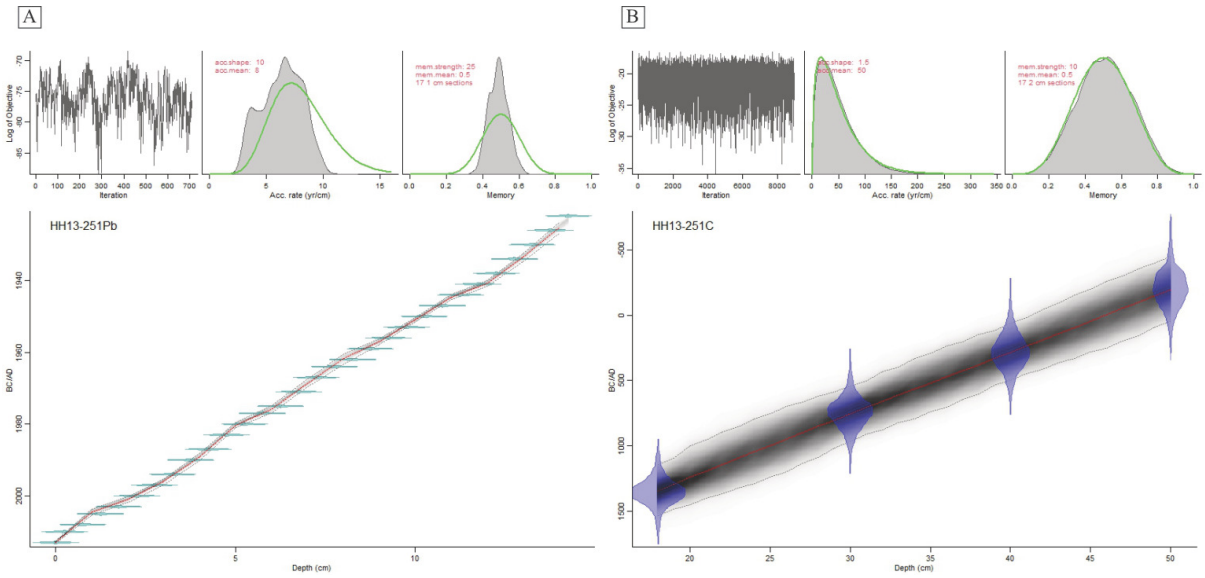

Figure 9. Example of two age models from the southern Barents Sea (HH13-251 MC) using the two dating methods separately. (A) ^{210}Pb to date the upper 13 cm, and (B) ^{14}C to date four points at 18, 30, 40 and 50 cm. Both age models are built with "rbacon" package from Blaaw et al. (December 22, 2022).

With the first use of ^{210}Pb to date recent marine and lacustrine sediments by Appleby and Oldfield (1978), more and more studies have relied on this method. This radionuclide (half-life $T_{1/2}$=22.23 years) is naturally present in the environment and allows dating of the last century (100–150 years) in very high resolution. There are two main sources of ^{210}Pb: (1) in the sediments by the decay of a radium radionuclide (^{226}Ra) referred as *supported*, and (2) in the atmosphere by the decay of a radon radionuclide (^{222}Rn), referred as *excess* (Sternbeck et al., 2006).

There are several models in order to calculate mass accumulation rates from excess ^{210}Pb data. The three most common are the Constant Initial Concentration (CIC), Constant Rate of Supply (CRS), and Constant Flux:Constant Sedimentation (CF:CS) (Krishnaswamy et al., 1971; Sternbeck et al., 2006; Appleby, 2008; Arias-Ortiz et al., 2018). All are based on different assumptions and have different analytical solutions, but they have three fundamental considerations in common: (1) the deposition of *excess* ^{210}Pb is at a steady state, (2) there is no mobility of ^{210}Pb after it is deposited, and (3) the deposition of *excess* ^{210}Pb follows the law of superposition, which is considered ideal (Arias-Ortiz et al., 2018). The ideal profile of ^{210}Pb activity is an exponential decrease with respect to depth in the sediment until it becomes stable, however, this is not always the case (i.e., Figure 10).

Based on the ^{210}Pb activity profile from the multicore from the southern Barents Sea, the model selected CRS model allowed us to date the upper 13 cm. However, the bimodal distribution

found in the northern Barents Sea (Figure 10A), complicated the use of any of the models and resulted in the assumption of a constant sedimentation rate in the upper 7 cm of the core (**Paper III)**.

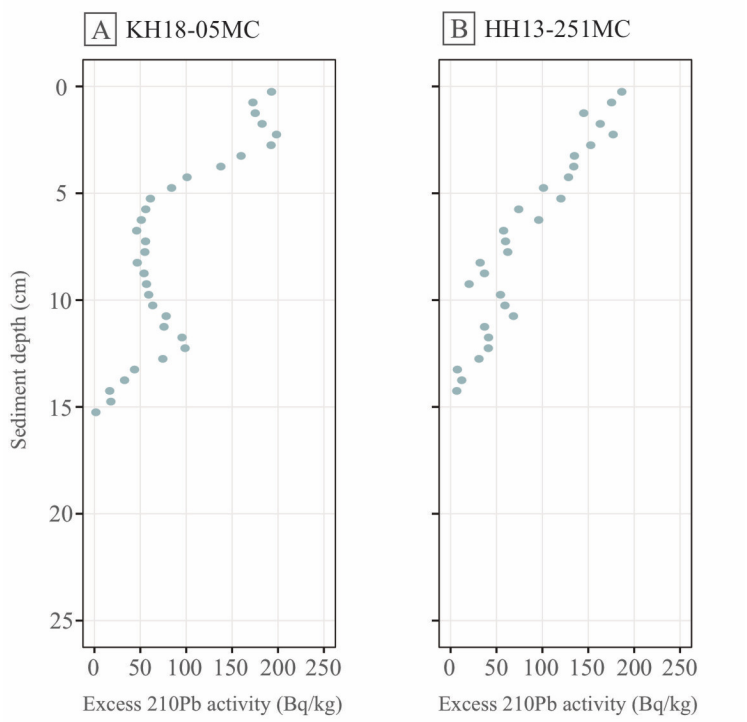

Figure 10. Excess of ^{210}Pb from the northern (A) and southern (B) Barents Sea

Due to the short half-life, we need to combine this method with radiocarbon (^{14}C) dating to extend the age-depth model. Carbon-14 dating has been widely used in paleontological studies since it was first described by Libby et al. (1949). It is based on both organic or inorganic carbon residues present in sediments from terrestrial and aquatic environments. The radionuclide ($T_{1/2}$=5730 years) allows to date carbon older than 1950 C.E. until 55,000 years ago (Li et al., 2021).

However, due to the slower radiocarbon exchange between the ocean surface water and the atmosphere driven by the slow marine circulation (known as the marine reservoir effect), there is a need to make age calibrations when dating marine samples with ^{14}C (i.e., Stuiver and Reimer, 1993; Chiu et al., 2017; Heaton et al., 2020, 2023a; Pieńkowski et al., 2022). On a global average, the marine reservoir age (R) is considered to be between 400 and 600 years (Heaton et al., 2020). Besides the reservoir age, there is a need to correct it with a regional or local ΔR, which considers in the case of Arctic and polar sediments the sea-ice cover, upwelling processes, and freshwater inflow (Mangerud et al., 2006; Pieńkowski et al., 2022). Specifically, the presence of sea-ice, which alters the sea-air exchange, has hindered the establishment of a

ΔR (Chiu et al. (2017) and references therein). Recently Pieńkowski et al. (2022) suggested a revised ΔR for the Barents Sea which is key to strengthen the ^{14}C age models in the Arctic. Unfortunately, this has not been resolved yet by the most updated calibration curves (e.g., Marine20 and Marine13) (Heaton et al., 2020) which difficult the creation of age models in these remote and understudied areas. However, due to the climatic stability during the Holocene Heaton et al. (2023b) suggested that polar Holocene samples can be calibrated directly against the Marine20 curve.

In marine sediments, mainly shells of planktonic foraminifers are used for ^{14}C dating, along with various molluscs or other calcareous organisms. The development of the Accelerator Mass Spectrometry (AMS) called MICADAS (MIni CArbon DAting System), has become more and more popular in polar research since the lower abundances and preservation in the Arctic Ocean were colliding with the amounts of material that were originally needed to use this method (6–10 mg, Gottschalk et al., 2018).

3 Summary of research papers

3.1 Paper I

Anglada-Ortiz, G., Zamelczyk, K., Meilland, J., Ziveri, P., Chierici, M., Fransson, A., Rasmussen, T. L. **Planktic Foraminiferal and Pteropod Contributions to Carbon Dynamics in the Arctic Ocean (North Svalbard Margin).** *Frontiers in Marine Sciences:* Section of Marine Geochemistry. doi: 10.3389/fmars.2021.661158.

Planktonic foraminifers and shelled pteropods are ubiquitous marine calcifiers. Due to their calcitic (foraminifers) and aragonitic shells (pteropods) these organisms contribute significantly to the carbon cycle, mainly exporting carbon, both organic and inorganic, from the surface to the seabed when they die and sink. Despite their role in the carbon cycle and their use as proxies for ocean warming and acidification, these organisms are rarely studied together at high latitudes. In this study, we investigated the distribution patterns of planktonic foraminifers and shelled pteropods in the upper 300 m of the water column, and their contribution to calcium carbonate ($CaCO_3$) standing stocks (μg m^{-3}) and export production (mg m^{-2} d^{-1}) at 100 m depth in the water column along a longitudinal transect on the northern Svalbard Margin (81.3–81.8°N) from 22.3 to 31.3°E.

The results show that shelled pteropods were almost exclusively living at the surface and subsurface in the upper 100 m, while foraminifers were mainly found deeper than 50 m. No difference between day or night conditions was observed among the samples. This suggested that their vertical distribution is not affected by diurnal vertical migration as previously observed in other high latitude areas (i.e., Fram Strait (Manno and Pavlov, 2014); Barents Sea (Ofstad et al., 2020); Arctic Ocean and North Atlantic (Greco et al., 2019; Meilland et al., 2020). Planktonic foraminifers dominated over pteropods, representing 68–95% of the population of calcifiers in the upper 300 m. The foraminiferal fauna was dominated by the polar species *Neogloboquadrina pachyderma* (average (av.) 55.9%) followed by the subpolar species *Turborotalita quinqueloba* (av. 21.7%), *N. incompta* (av. 13.5%) and *Globigerina bulloides* (av. 5.2%). The pteropod fauna was dominated by the polar species *Limacina helicina* (av. 99.6%, 94.2–100%). The relatively high abundance of subpolar species compared to other studies in the Arctic was explained by the fact that the year 2018 was warmer than usual with a very reduced cover of sea ice in late summer and autumn and characterized by an increased Atlantic inflow probably a sign of "Atlantification" (**Paper I**; Pieńkowski et al. 2021).

Despite the lower abundances of pteropods compared to foraminifers also in the upper 100 m of the water column, we calculated that their contribution to $CaCO_3$ standing stocks (66–96%) and export production (56.7–98.4%) was higher than from planktonic foraminifers (4–34% and 1.6–43.4%, respectively). Pteropods are significantly larger than foraminifers, thus the size of the organisms plays an important role when estimating the $CaCO_3$ content and the associated standing stocks and export production.

3.2 Paper II

Anglada-Ortiz, G., Meilland, J., Ziveri, P., Chierici, M., Fransson, A., Jones, E., Rasmussen, T. L. **Seasonality of marine calcifiers in the northern Barents Sea: Spatiotemporal distribution of planktonic foraminifers and shelled pteropods and their contribution to cabon dynamics.** In review in *Progress of oceanography* (since June 2023).

The seasonal distribution of planktonic foraminifers and shelled pteropods in the Arctic has rarely been studied. In the northern Barents Sea, the abundance of these organisms has mainly been investigated during the summer season due to the limited accessibility during winter. In this study, we have analyzed the seasonal distribution patterns of planktonic foraminifers and pteropods in relation to environmental conditions, and their contribution to the organic and inorganic carbon pump. That was done by estimating their organic and inorganic carbon standing stocks and export production in a latitudinal transect in the Barents Sea from 76˚ to 82˚ N. The study area encompasses the Polar Front, influenced by both Arctic and Atlantic Waters, and covers the shelf, the northern Barents Sea slope, and the Nansen Basin in the Arctic Ocean.

We found a clear seasonal signal in the abundances, sizes, and organic and inorganic carbon standing stocks (µg m^{-3}) and export production (mg m^{-2} d^{-1}) of planktonic foraminifers and pteropods. The abundance of foraminifers increased from winter (March) until summer (August) and was associated with higher temperatures and nutrient availability, being significantly higher in the Atlantic dominated stations compared to the Arctic stations. The foraminifers were almost absent in March, and the increasing abundances found in May was suggested to be related to a combination of Atlantic Water inflow carrying foraminifers, and a potential nursery role of the sea ice, as for other organisms in the Arctic (i.e., copepods, Søreide et al. (2010)). Their distribution patterns in the water column also changed with the season. In spring (May) they were mainly found in the upper 100 m of the water column and were well

spread throughout the upper 300 m in summer (July and August). The abundance and size of pteropods increased from winter (March) until autumn (December) and were associated with lower temperatures and salinity and the availability of nitrate. The pteropods were most abundant in the Arctic stations and along the seasonal and marginal ice zone. Generally, they were found at the surface and subsurface during all studied seasons except in March, when veliger larvae occupied the entire water column. The combined standing stocks and export production of foraminifers and pteropods increased from winter until autumn, dominated by the abundance of pteropods. The organic carbon contribution was almost negligible, representing up to c. 13% in summer of their total carbon contribution. Despite the abundances of foraminifers and pteropods in the upper 100 m of the water column being similar in numbers, the pteropods contributed 66% to the carbon export production compared to 34% from the foraminifers.

3.3 Paper III

Anglada-Ortiz, G., Rasmussen, T. L., Chierici, M., Fransson, A., Ziveri, P., Zamelczyk, K., Meilland, J., Garcia-Orellana, J. **Reconstruction of changes in environments and productivity based on planktonic foraminiferal faunas in the northern and southern Barents Sea during the last three millennia.** Submitted to Continental Shelf Research.

Planktonic foraminifers have been extensively used to reconstruct past ocean circulation and climate. In the Barents Sea, the paleo-studies focus on reconstructing the Holocene (last 12,000 years), mainly in low resolution. Here, we have investigated two sediment cores, from the northern and southern Barents Sea to reconstruct paleoceanographic and -climatic changes during the last three millennia. The foraminiferal abundances and fluxes, species distribution patterns, and size changes have been studied together with Total Organic Carbon (TOC, %), Total Carbon (TC, %), calcium carbonate content ($CaCO_3$, %), and carbon and oxygen isotopes ($\delta^{13}C$ and $\delta^{18}O$).

In general, high abundance and flux of foraminifers were found in the transition from warm to cold periods and vice versa. The highest productivity in the northern and southern Barents Sea occurred between c. 500 and 1000 C.E. during the Dark Ages Cold Period and the Medieval Warm Period. Nevertheless, there was a clear difference between the northern and southern Barents Sea in terms of total foraminiferal abundance and species distribution. The total abundances in the northern Barents Sea were 10–15 times lower than in the south. In the

northern Barents Sea *N. pachyderma* dominated the assemblages during the last three millennia. In the southern Barents Sea, the species *T. quinqueloba*, *G. uvula* and *N. incompta* dominated the assemblage together with *N. pachyderma* during the last two millennia. In both the northern and southern Barents Sea, we observed a general decreasing trend of foraminiferal abundances and fluxes in the upper part of the cores since the Industrial Revolution, from 1850 C.E.

Almost zero abundances and high fragmentation index were observed in the upper half of the northern Barents Sea core. These results combined with the high %TOC, low %$CaCO_3$, and the presence of solely agglutinated foraminifers suggest dissolution of $CaCO_3$ in the sediment.

4 Concluding remarks and future perspectives

This thesis focused on the distribution pattern of living planktonic foraminifers and shelled pteropods in the north Svalbard margin (**Paper I**) and on a seasonal basis in the northern Barents Sea (**Paper II**), in combination of physicochemical and biological parameters of the water column. It also studied the distribution of fossil planktonic foraminifers in the northern and southern Barents Sea to reconstruct their productivity in relation to climatic and environmental changes during the last few millennia (**Paper III**).

High abundances, carbon standing stocks, and export productions were found in the northern Svalbard margin (**Paper I**). The high temperatures and low sea ice concentration in 2018 were the results of an increased Atlantic Water inflow. This water was a source of nutrients and increased influx and abundances of the subpolar species *L. retroversa* carried by the West Spitsbergen Current. In the northern Barents Sea, the seasonal pattern of planktonic foraminifers and pteropods shows increasing productivity from winter until late summer and early autumn (**Paper II**). The highest productivity was observed along the Arctic shelf stations and in the seasonal and marginal ice zone (**Paper II**). However, the results from the sediment core from the northern Barents Sea do not concur with the seasonal observations. Almost no planktonic foraminiferal shells were found in the upper half part of the core which was attributed to dissolution of $CaCO_3$ in the sediment (**Paper III**). There was no apparent effect of dissolution of the living faunas and the upper 300 m of the water column was saturated in terms of Ωcalcite and Ωaragonite at all sites and seasons (**Paper II**; Jones et al., 2023, in review).

The results of this thesis can benefit society by increasing the knowledge of the present and past characteristics of the Barents Sea. The Barents Sea, which plays an important role in the climate system in the Arctic, is very relevant for the Norwegian fishing industry. These results will improve the capacity to predict how the Barents Sea might respond under ocean acidification conditions and climate change, both ecologically and in terms of carbon dynamics. The seasonal data on productivity from pteropods and planktonic foraminifers and the faunal composition can form a basis for future monitoring of the state of changes in the Barents Sea.

For the monitoring the effects of warming and acidification the measurement of shell density would be an important tool for early observations and warmings of eventual dissolution effects.

Decreased density due to carbonate loss and/or slight deformations to the shells can be found by XMCT scanning. The purpose would be to get a better understanding of the effects of ocean acidification on marine calcifiers. Moreover, the use of long-term sediment traps will provide a more detailed overview of their life cycles and eventual changes in their seasonality in the northern Barents Sea over time.

4.1 State of the shell

Recently, Ofstad et al. (2021) studied the shell density of living planktonic foraminifers (*N. pachyderma* and *T. quinqueloba*) and pteropods (*L. helicina*) from an area of intense seepage of methane in the central Barents Sea. Through X-ray microcomputed tomography (XMCT) scanning, the study concluded that denser organisms were living deep in the water column associated with continuous calcification and a more mature state of the specimens (Ofstad et al., 2021). The XMCT scans in the foraminiferal specimens from surface sediments showed no dissolution of the shells. However, in the water column, they showed species-specific differences, where *T. quinqueloba* was thinner and less dense than *N. pachyderma*. Hence, they suggested that the fossil composition found in the sediment might be potentially biased towards *N. pachyderma* (Ofstad et al., 2021). In the multicore from the southern Barents Sea (**Paper III**) shells of *T. quinqueloba* were larger and heavier than the shells of *N. pachyderma*. This could be a cause of the different environmental conditions in the two study areas and/or life cycles of the species. It is possible that the effects of methane seepage were stronger in *T. quinqueloba* and/or the specimens were less developed representing earlier stages compared to *N. pachyderma.* Therefore, their shells could be more susceptible to the chemistry of the ambient water.

In the ongoing collaboration with the Research and Development Center for Global Change–JAMSTEC with Dr. Katsunori Kimoto, specimens of *L. helicina* from the northern Barents Sea and from the different seasons studied here are currently analyzed. This study will shed light on the seasonal variability of the state of the shell in the northern Barents Sea. Moreover, the CT number (results from XMCT scans) on foraminifers collected in the Arctic Basin and exposed to different pH conditions suggest that their shell density and the pH of the treatment are well correlated (**unpublished data**, ongoing work).

4.2 Better constrain of their live cycle and seasonality: the sampling strategy matters

In polar and subpolar areas living planktonic foraminifers and pteropods are usually collected with small (<100 μm) mesh size nets (see **2.2.2 Sampling methods**). Stratified nets, as well as multiple casts at different depths, provide a screenshot of the vertical distribution of organisms throughout the water column at the moment of sampling. However, other methods such as long-term sediment traps, could be used to better understand their life cycle.

Long-term sediment traps (Figure 11) are mooring devices composed usually of 20 bottles that are programmed to collect sinking material (including planktonic foraminifers and pteropods) during a specific time of year. The samples collected are very relevant to understand the seasonality and are particularly interesting in areas with difficult accessibility, as is the Arctic. Since the 1970s, sediment traps around the world have been used to study changes in the assemblages and isotopic composition, and the carbon fluxes of foraminifers (Avnaim-Katav et al., 2020; Chernihovsky et al., 2020) and pteropods (Grossman et al., 1986; Almogi-Labin et al., 1988; Bathmann et al., 1991).

In the Barents Sea and the north Svalbard margin within the Nansen Legacy collaboration sediment traps have been used to investigate the vertical flux of total particulate matter, particulate organic and inorganic matter, and particulate organic carbon (POC) and nitrogen, together with chlorophyll a (chl-a), planktonic protists and fecal pellets from zooplankton (Dybwad et al. 2022). Moorings from the northern Barents Sea were also equipped to record physical parameters of the water and ocean currents at different depths (Lundesgaard et al. 2022). However, these studies have ignored the planktonic marine calcifiers. The results from the ongoing collaboration with BFE (Faculty of Biology, Fisheries and Economy) will focus on a study of their life cycles and seasonality (2019–2021) in the gateway of Atlantic Water through the West Spitsbergen Current in the northern Barents Sea.

In contrast, sediment traps from other Arctic areas such as the Fram Strait, have been examined for planktonic foraminifers (v. Gyldenfeldt et al., 2000) and pteropods (Bauerfeind et al., 2014, Busch et al., 2015). These studies observed a seasonal pattern based on the abundances and sizes, with abundance peaks in August–November and in September–January for foraminifers and pteropods, respectively. Also, the increased abundances of *L. retroversa* were associated with events of increasing Atlantic inflow. The long-term ecological research observatory

HAUSGARTEN (Fram Strait; 79°N, 4°E) provides a seasonal and interannual overview of plankton since 2000. From these sediment traps, several papers have studied the variability in plankton assemblages, POC and chl-a, as well as community changes of zooplankton due to "Atlantification" processes and sea-ice dynamics (Nöthig et al., 2015 and 2020; Lampe et al., 2021; Ramondenc et al., 2022). Usually in the Arctic they are deployed in the upper 300 m of the water column (Hargrave et al., 1994; Bauerfeind et al., 2009, 2014; Lalande et al., 2013; Metfies et al., 2017; Weydmann-Zwolicka et al., 2021). However, their deployment above the surface sediment (as in Bauerfeind et al. (2014)) in the Barents Sea would help understanding the dissolution of $CaCO_3$ in the water column. Specifically in the northern Barents Sea, we have observed a clear seasonal variability of foraminifers and pteropods (**Paper II**). In the upper half of the sediment record from the northern Barents Sea almost no shells of planktonic foraminifers were found (**Paper III**). The absence of shells was attributed to $CaCO_3$ dissolution in the sediment. However, the presence or absence of shells in deep sediment traps would either prove this theory or give an insight if the dissolution occurs right above the sediment surface. A better understanding of their life cycle and $CaCO_3$ preservation is needed for an improved usage of planktonic foraminifers as proxies for water mass properties in the past.

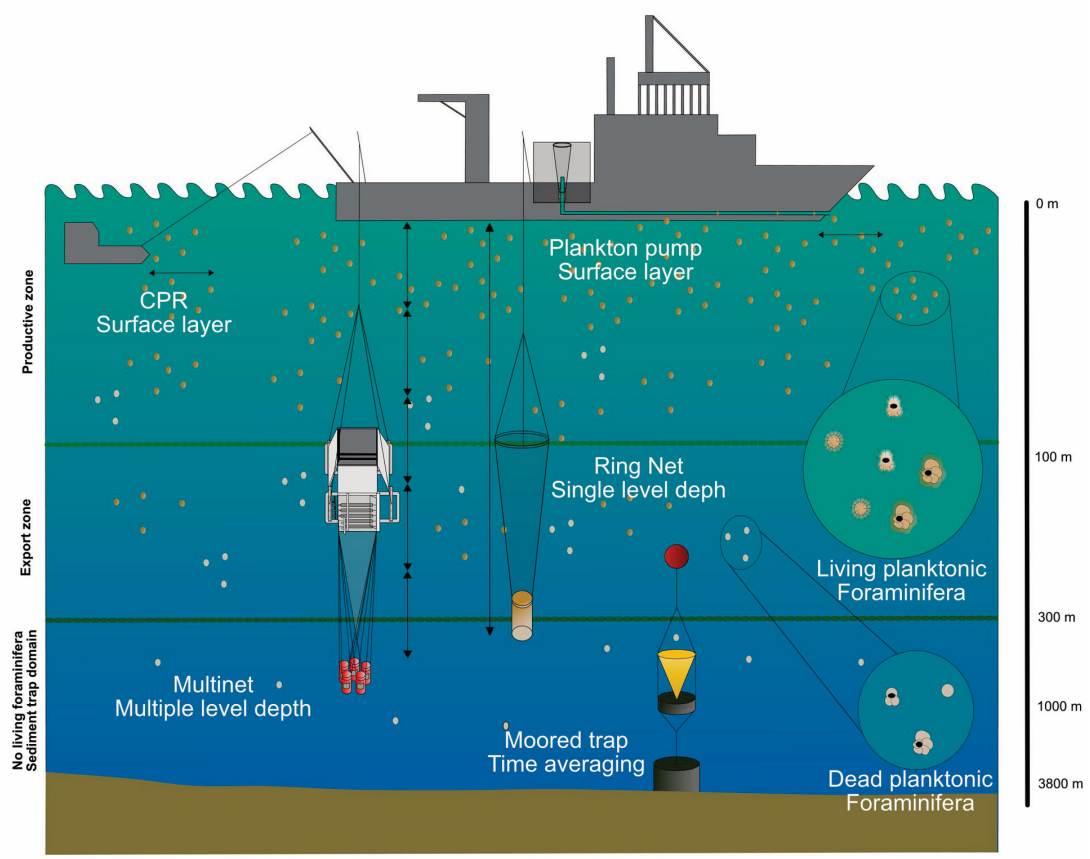

Figure 11. Different sampling strategies used to collect living planktonic calcifiers, mainly foraminifers, from Chaabane et al. (2023).

Specifically for the Arctic, little is known about the role that sea-ice has on the life cycle of planktonic foraminifers. The study of cores taken in sea-ice together with plankton tows, water samples, and sediment traps are key to understanding the increasing abundances from zero specimens in winter to high abundances in spring in the northern Barents Sea. In **Paper II** the increase is explained by a combination of the nursery role of sea ice and the Atlantic inflow carrying the foraminifers into the Barents Sea.

However, no matter how marine calcifiers are sampled, either with plankton nets or sediment traps, there is a need for interdisciplinary studies such as in the Nansen Legacy project. To better understand the system, both in the Arctic and elsewhere, different parameters must be studied simultaneously. During the Nansen Legacy cruises the parameters included, among others, temperature, salinity, and carbonate chemistry from the water column and the sea-ice, as well as chl-a, the phytoplankton and larger zooplankton communities from the water column and the benthos. Taking part in workshops and accessing carbonate chemistry and physical oceanography data was key to interpreting the data from this thesis. New data collected during the interdisciplinary cruises will also improve our knowledge of the distribution patterns of

planktonic calcifiers. Understanding their life cycle and abundance regarding the physical and chemical environmental parameters, and biological parameters such as e.g., primary productivity, food availability and type of food, and preservation states of their shells, will improve the interpretations for future paleoceanography studies in the northern Barents Sea. Overall, the creation of the seven task forces within the Nansen Legacy to collect all the obtained interdisciplinary knowledge of the Barents Sea in the form of synthesis papers, book chapters, and fact sheets about *Atlantic Water inflow*, *Sea-ice*, *Food webs*, *Seasonality*, *Human impacts* (and a specific one about *Ocean acidification*), *The Barents Sea: regional implications and global context*, and *Barents Sea 2050*.

5 References

Aagaard-Sørensen, S., Husum, K., Werner, K., Spielhagen, R.F., Hald, M., and Marchitto, T.M. (2014). "A late glacial–early holocene multiproxy record from the eastern fram strait, polar north atlantic." Marine Geology **355**: 15-26.

Aksu, A. E. (1983). "Holocene and Pleistocene dissolution cycles in deep-sea cores of Baffin Bay and Davis Strait: Palaeoceano-graphic implications." Marine Geology **53**(4): 331-348.

Almogi-Labin, A., Hemleben, C., and Deuser, W. (1988). "Seasonal variation in the flux of euthecosomatous pteropods collected in a deep sediment trap in the Sargasso Sea." Deep Sea Research Part A. Oceanographic Research Papers **35**(3): 441-464.

Anglada-Ortiz, G., Zamelczyk, K., Meilland, K., Ziveri, P., Chierici, M., Fransson, A., and Rasmussen, T.L. (2021). "Planktic Foraminiferal and Pteropod Contributions to Carbon Dynamics in the Arctic Ocean (North Svalbard Margin)." Frontiers in Marine Science **8**(636).

Anglada-Ortiz, G., Meilland, J., Ziveri, P., Chierici, M., Fransson, A., Jones, E., and Rasmussen, T.L. (2023). "Seasonality of marine calcifiers in the northern Barents Sea: Spatiotemporal distribution of planktonic foraminifers and shelled pteropods and their contribution to carbon dynamics." Progress in Oceanography: 103121.

Appleby, P. (2008). "Three decades of dating recent sediments by fallout radionuclides: a review." The Holocene **18**(1): 83-93.

Appleby, P. G. and Oldfield, F. (1978). "The calculation of lead-210 dates assuming a constant rate of supply of unsupported 210Pb to the sediment." Catena **5**(1): 1-8.

Arias-Ortiz, A., Masqué, P., Garcia-Orellana, J., Serrano, O., Mazarrasa, I., Marbà, N., Lovelock, C.E., Lavery, P.S., and Duarte, C.M. (2018). "Reviews and syntheses: 210 Pb-derived sediment and carbon accumulation rates in vegetated coastal ecosystems–setting the record straight." Biogeosciences **15**(22): 6791-6818.

Asbjørnsen, H., Årthun, M., Skagseth, Ø., and Eldevik, T. (2020). "Mechanisms Underlying Recent Arctic Atlantification." Geophysical Research Letters **47**(15): e2020GL088036.

Avnaim-Katav, S., Herut, B., Rahav, E., Katz, T., Weinstein, Y., Alkalay, R., Berman-Frank, I., Zlatkin, O., and Almogi-Labin, A. (2020). "Sediment trap and deep sea coretop sediments as tracers of recent changes in planktonic foraminifera assemblages in the southeastern ultra-oligotrophic Levantine Basin." Deep Sea Research Part II: Topical Studies in Oceanography **171**: 104669.

Bathmann, U.V., Noji, T.T., and von Bodungen, B. (1991). "Sedimentation of pteropods in the Norwegian Sea in autumn." Deep Sea Research Part A. Oceanographic Research Papers **38**(10): 1341-1360.

Bauerfeind, E., Nöthig, E.-M., Beszczynska, A., Fahl, K., Kaleschke, L., Kreker, K., Klages, M., Soltwedel, T., Lorenzen, C., and Wegner, J. (2009). "Particle sedimentation patterns in the eastern Fram Strait during 2000–2005: Results from the Arctic long-term observatory HAUSGARTEN." Deep Sea Research Part I: Oceanographic Research Papers **56**(9): 1471-1487.

Bauerfeind, E., Nöthig, E.M, Pauls, B., Kraft, A., and Beszczynska-Möller, A. (2014). "Variability in pteropod sedimentation and corresponding aragonite flux at the Arctic deep-sea long-term observatory HAUSGARTEN in the eastern Fram Strait from 2000 to 2009." Journal of Marine Systems **132**: 95-105.

Bednaršek, N., Možina, J., Vogt, M., O'brien, C., and Tarling, G. (2012a). "The global distribution of pteropods and their contribution to carbonate and carbon biomass in the modern ocean." Earth System Science Data **4**: 167-186.

Bednaršek, N., Tarling, G., Bakker, D., Fielding, S., Jones, E., Venables, H., Ward, P., Kuzirian, A., Lézé, B. and Feely, R. (2012b). "Extensive dissolution of live pteropods in the Southern Ocean." Nature Geoscience **5**(12): 881-885.

Bednaršek, N., Tarling, G., Fielding, S. and Bakker, D. (2012c). "Population dynamics and biogeochemical significance of Limacina helicina antarctica in the Scotia Sea (Southern Ocean)." Deep Sea Research Part II: Topical Studies in Oceanography **59**: 105-116.

Bednaršek, N., Tarling, G.A., Bakker, D.C., Fielding, S., Cohen, A., Kuzirian, A., McCorkle, D., Lézé, B., and Montagna, R. (2012d). "Description and quantification of pteropod shell dissolution: a sensitive bioindicator of ocean acidification." Global Change Biology **18**(7): 2378-2388.

Bednaršek, N., Feely, R., Reum, J., Peterson, B., Menkel, J., Alin, S., and Hales, B. (2014a). "Limacina helicina shell dissolution as an indicator of declining habitat suitability owing to ocean acidification in the California Current Ecosystem." Proceedings of the Royal Society B: Biological Sciences **281**(1785): 20140123.

Bednaršek, N., Tarling, G.A., Bakker, D.C., Fielding, S., and Feely, R.A. (2014b). "Dissolution dominating calcification process in polar pteropods close to the point of aragonite undersaturation." PloS one **9**(10): e109183.

Bednaršek, N., Feely, R.A., Howes, E.L., Hunt, B.P., Kessouri, F., León, P., Lischka, S., Maas, A.E., McLaughlin, K., and Nezlin, N.P. (2019). "Systematic Review and Meta-Analysis Toward Synthesis of Thresholds of Ocean Acidification Impacts on Calcifying Pteropods and Interactions With Warming." Frontiers in Marine Science **6**: 227.

Berben, S., Husum, K., Cabedo-Sanz, P., and Belt, S.T. (2014). "Holocene sub-centennial evolution of Atlantic water inflow and sea ice distribution in the western Barents Sea." Climate of the Past **10**(1): 181-198.

Berger, W.H. (1969). Ecologic patterns of living planktonic foraminifera. Deep Sea Research and Oceanographic Abstracts, Elsevier.

Berger, W.H. (1970). "Planktonic foraminifera: selective solution and the lysocline." Marine Geology **8**(2): 111-138.

Bjørklund, K.R., Kruglikova, S.B., and Anderson, O.R. (2012). "Modern incursions of tropical Radiolaria into the Arctic Ocean." Journal of Micropalaeontology **31**(2): 139-158.

Blaaw, M., Christen, J.A., Aquino Lopez, M.A., Esquivel Vázquez, J., Gonzalez, O.M., Belding,T., Theiler, J., Gough, B., and Karney, C. (December 22, 2022). Package ´rbacon´. Age-Depth Modelling using Bayesian Statistics**:** An approach to age-depth modelling that uses Bayesian statistics to reconstruct accumulation histories for deposits, through combining radiocarbon and other dates with prior information.

Bluhm, B., Kosobokova, K. and Carmack, E. (2015). "A tale of two basins: An integrated physical and biological perspective of the deep Arctic Ocean." Progress in Oceanography **139**: 89-121.

Buitenhuis, E.T., Le Quere, C., Bednaršek, N., and Schiebel, R. (2019). "Large contribution of pteropods to shallow CaCO3 export." Global Biogeochemical Cycles **33**(3): 458-468.

Busch, K., Bauerfeind, E., and Nöthig, E.-M. (2015). "Pteropod sedimentation patterns in different water depths observed with moored sediment traps over a 4-year period at the LTER station HAUSGARTEN in eastern Fram Strait." Polar Biology **38**: 845-859.

Chaabane, S., de Garidel-Thoron, T., Giraud, X., Schiebel, R., Beaugrand, G., Brummer, G.-J., Casajus, N., Greco, M., Grigoratou, M., Howa, H., Jonkers, L., Kucera, M., Kuroyanagi, A., Meilland, J., Monteiro, F., Mortyn, G., Almogi-Labin, A., Asahi, H., Avnaim-Katav, S., Bassinot, F., Davis, C.V., Field, D.B., Hernández-Almeida, I., Herut, B., Hosie, G., Howard, W., Jentzen, W., Johns, D.G., Keigwin, L., Kitchener, J., Kohfeld, K.E., Lessa, D.V.O., Manno, C., Marchant, M., Ofstad, S., Ortiz, J.D., Post, A,. Rigual-Hernandez, A., Rillo, M.C., Robinson, K., Sagawa, T., Sierro, F., Takahashi, K.T., Torfstein, A., Venancio, I., Yamasaki, M., and Ziveri, P. (2023). "The FORCIS database: A global census of planktonic Foraminifera from ocean waters." Scientific Data **10**(1): 354.

Chang, Y. and Yen, J. (2012). "Swimming in the Intermediate Reynolds Range: Kinematics of the Pteropod Limacina helicina." Integrative and Comparative Biology **52**(5): 597-615.

Chapman, M.R., Shackleton, N.J., and Duplessy, J.-C. (2000). "Sea surface temperature variability during the last glacial–interglacial cycle: assessing the magnitude and pattern of climate change in the North Atlantic." Palaeogeography, Palaeoclimatology, Palaeoecology **157**(1-2): 1-25.

Chernihovsky, N., Almogi-Labin, A., Kienast S.S., and Torfstein, A. (2020). "The daily resolved temperature dependence and structure of planktonic foraminifera blooms." Scientific reports **10**(1): 17456.

Chierici, M. and Fransson, A. (2018). Arctic chemical oceanography at the edge: focus on carbonate chemistry (chapter 13). At the edge. P. Wassmann.

Chiu, P.-Y., Chao, W.-S., Gyllencreutz, R., Jakobsson, M., Li, H.-C., Löwemark, L., and O'Regan, M. (2017). "New constraints on Arctic Ocean Mn stratigraphy from radiocarbon dating on planktonic foraminifera." Quaternary International **447**: 13-26.

Comeau, S., Alliouane, S., and Gattuso, J.-P. (2012). "Effects of ocean acidification on overwintering juvenile Arctic pteropods Limacina helicina." Marine Ecology Progress Series **456**: 279-284.

Comeau, S., Gorsky, G., Jeffree, R., Teyssié, J.-L., and Gattuso, J.-P. (2009). "Impact of ocean acidification on a key Arctic pelagic mollusc (Limacina helicina)." Biogeosciences **6**(9): 1877-1882.

Comeau, S., Jeffree, R., Teyssie, J.-L., and Gattuso, J.-P. (2010). "Response of the Arctic pteropod Limacina helicina to projected future environmental conditions." PloS one **5**(6).

Crowley, T. J. (1981). "Temperature and circulation changes in the eastern North Atlantic during the last 150,000 years: evidence from the planktonic foraminiferal record." Marine Micropaleontology **6**(2): 97-129.

De La Rocha, C. L. and Passow, U. (2014). 8.4 - The Biological Pump. Treatise on Geochemistry (Second Edition). H. D. Holland and K. K. Turekian. Oxford, Elsevier**:** 93-122.

Darling, K.F., Kucera, M., Kroon, D., and Wade, C. M. (2006). "A resolution for the coiling direction paradox in Neogloboquadrina pachyderma." Paleoceanography **21**(2).

Davis, C.S. and Wiebe, P.H. (1985). "Macrozooplankton biomass in a warm‐core Gulf Stream ring: Time series changes in size structure, taxonomic composition, and vertical distribution." Journal of Geophysical Research: Oceans **90**(C5): 8871-8884.

Davis, C.V., Rivest, E.B., Hill, T.M., Gaylord, B., Russell, A.D., and Sanford, E. (2017). "Ocean acidification compromises a planktic calcifier with implications for global carbon cycling." Scientific reports **7**(1): 1-8.

Duarte, P., Meyer, A., and Moreau, S. (2021). "Nutrients in water masses in the Atlantic sector of the Arctic Ocean: Temporal trends, mixing and links with primary production." Journal of Geophysical Research: Oceans **126**(8): e2021JC017413.

Dybwad, C., Lalande, C., Bodur, Y.V., Henley, S.F., Cottier, F., Ershova, E., Hobbs, L., Last, K.S., Dąbrowska, A., and Reigstad, M. (2022). "The influence of sea ice cover and Atlantic water advection on annual particle export north of Svalbard." Journal of Geophysical Research: Oceans **127**(10): e2022JC018897.

Fabry, V.J. (2008). "Marine calcifiers in a high-CO2 ocean." Science **320**(5879): 1020-1022.

Fabry, V.J., Seibel, B.A., Feely, R.A., and Orr, J.C. (2008). "Impacts of ocean acidification on marine fauna and ecosystem processes." ICES Journal of Marine Science **65**(3): 414-432.

Feely, R. A., Sabine, C.L., Lee, K., Berelson, W., Kleypas, J., Fabry, V.J., and Millero, F.J. (2004). "Impact of anthropogenic CO2 on the CaCO3 system in the oceans." Science **305**(5682): 362-366.

Feuilloley, G., Fromentin, J.-M., Saraux, C,, Irisson, J.-O., Jalabert, L., and Stemmann, L. (2022). "Temporal fluctuations in zooplankton size, abundance, and taxonomic composition since 1995 in the North Western Mediterranean Sea." ICES Journal of Marine Science **79**(3): 882-900.

Figuerola, B., Hancock, A.M., Bax, N., Cummings, V.J., Downey, R., Griffiths, H.J., Smith, J., and Stark, J.S. (2021). "A Review and Meta-Analysis of Potential Impacts of Ocean Acidification on Marine Calcifiers From the Southern Ocean." Frontiers in Marine Science **8**(24).

Gottschalk, J., Szidat, S., Michel, E., Mazaud, A., Salazar, G., Battaglia, M., Lippold, J., and Jaccard, S.L. (2018). "Radiocarbon measurements of small-size foraminiferal samples with the mini carbon dating system (MICADAS) at the University of Bern: Implications for paleoclimate reconstructions." Radiocarbon **60**(2): 469-491.

Greco, M., Jonkers, L., Kretschmer, K., Bijma, J., and Kucera, M. (2019). "Depth habitat of the planktonic foraminifera Neogloboquadrina pachyderma in the northern high latitudes explained by sea-ice and chlorophyll concentrations." Biogeosciences **16**(17): 3425-3437.

Grossman, E.L., Betzer, P.R., Dudley, W.R., and Dunbar, R.B. (1986). "Stable isotopic variation in pteropods and atlantids from North Pacific sediment traps." Marine Micropaleontology **10**(1): 9-22.

Hargrave, B.T., von Bodungen, B., Stoffyn-Egli, P., and Mudie, P.J. (1994). "Seasonal variability in particle sedimentation under permanent ice cover in the Arctic Ocean." Continental Shelf Research **14**(2): 279-293.

Harris, C., Plueddemann, A., and Gawarkiewicz, G. (1998). "Water mass distribution and polar front structure in the western Barents Sea." Journal of Geophysical Research: Oceans **103**(C2): 2905-2917.

Heaton, T.J., Köhler, P., Butzin, M., Bard, E., Reimer, R.W., Austin, W.E., Ramsey, C.B., Grootes, P.M., Hughen, K.A., and Kromer, B. (2020). "Marine20—the marine radiocarbon age calibration curve (0–55,000 cal BP)." Radiocarbon **62**(4): 779-820.

Heaton, T.J., Bard, E., Bronk Ramsey, C., Butzin, M., Hatté, C., Hughen, K.A., Köhler, P., and Reimer, P.J. (2023a). "A response to community questions on the Marine20 radiocarbon age calibration curve:

marine reservoir ages and the calibration of 14C samples from the oceans." Radiocarbon **65**(1): 247-273.

Heaton, T.J., Butzin, M., Bard, E., Bronk Ramsey, C., Hughen, K.A., Köhler, P., and Reimer, P.J. (2023b). "Marine radiocarbon calibration in Polar regions: A simple approximate approach using Marine20." Radiocarbon: 1-28.

Hunt, B.P.V., Pakhomov, E.A., Hosie, G.W., Siegel, V., Ward, P., and Bernard, K. (2008). "Pteropods in Southern Ocean ecosystems." Progress in Oceanography **78**(3): 193-221.

Husum, K. and Hald, M. (2012). "Arctic planktic foraminiferal assemblages: Implications for subsurface temperature reconstructions." Marine Micropaleontology **96**: 38-47.

Ingvaldsen, R.B., Assmann, K.M., Primicerio, R., Fossheim, M., Polyakov I.V., and Dolgov, A.V. (2021). "Physical manifestations and ecological implications of Arctic Atlantification." Nature Reviews Earth & Environment **2**(12): 874-889.

John, E.H., Pearson, P.N., Coxall, H.K., Birch, H., Wade, B.S., and Foster, G.L. (2013). "Warm ocean processes and carbon cycling in the Eocene." Philosophical Transactions of the Royal Society A: Mathematical, Physical and Engineering Sciences **371**(2001): 20130099.

Jones, E., Chierici, M., Fransson, A., Assman, K., Renner, A.H.H., and Lødemel, H.H. (2023 in review). "Inorganic carbon and nutrient dynamics in the marginal ice zone of the Barents Sea: seasonality and implications for ocean acidification." Progress in Oceanography.

Jutterström, S. and Anderson, L.G. (2005). "The saturation of calcite and aragonite in the Arctic Ocean." Marine Chemistry **94**(1): 101-110.

K BouDagher-Fadel, M. (2015). Biostratigraphic and geological significance of planktonic foraminifera, UCL Press.

Knecht, N.S., Benedetti, F., Elizondo, U.H., Bednaršek, N., Chaabane, S., de Weerd, C., Peijnenburg, K.T., Schiebel, R., and Vogt, M. (2023). "The impact of zooplankton calcifiers on the marine carbon cycle." Global Biogeochemical Cycles: e2022GB007685.

Kobayashi, H. (1974). "Growth cycle and related vertical distribution of the thecosomatous pteropod Spiratella ("Limacina") helicina in the central Arctic Ocean." Marine Biology **26**(4): 295-301.

Krishnaswamy, S., Lal, D., Martin, J., and Meybeck, M. (1971). "Geochronology of lake sediments." Earth and Planetary Science Letters **11**(1-5): 407-414.

Kucera, M. (2007). "Chapter six planktonic foraminifera as tracers of past oceanic environments." Developments in marine geology **1**: 213-262.

Lalande, C., Bauerfeind, E., Nöthig, E.-M., and Beszczynska-Möller, A. (2013). "Impact of a warm anomaly on export fluxes of biogenic matter in the eastern Fram Strait." Progress in Oceanography **109**: 70-77.

Lalli, C.M. and Gilmer, R.W. (1989). Pelagic snails: the biology of holoplanktonic gastropod mollusks, Stanford University Press.

Lalli, C.M. and Wells, F.E. (1978). "Reproduction in the genus Limacina (Opisthobranchia: Thecosomata)." Journal of Zoology **186**(1): 95-108.

Lampe, V., Nöthig, E.-M., and Schartau, M. (2021). "Spatio-temporal variations in community size structure of Arctic protist plankton in the Fram Strait." Frontiers in Marine Science **7**: 579880.

Larson, R. (1986). "Water content, organic content, and carbon and nitrogen composition of medusae from the northeast Pacific." Journal of Experimental Marine Biology and Ecology **99**(2): 107-120.

León, P., Bednaršek, N., Walsham, P., Cook, K., Hartman, S.E., Wall-Palmer, D., Hindson, J., Mackenzie, K., Webster, L., and Bresnan, E. (2019). "Relationship between shell integrity of pelagic gastropods and carbonate chemistry parameters at a Scottish Coastal Observatory monitoring site." ICES Journal of Marine Science **77**(1): 436-450.

Li, W., Li, X., Mei, X., Zhang, F., Xu, J., Liu, C., Wei, C., and Liu, Q. (2021). "A review of current and emerging approaches for Quaternary marine sediment dating." Science of The Total Environment **780**: 146522.

Libby, W.F., Anderson E.C., and Arnold, J.R. (1949). "Age determination by radiocarbon content: world-wide assay of natural radiocarbon." Science **109**(2827): 227-228.

Loeng, H. (1991). "Features of the physical oceanographic conditions of the Barents Sea." Polar Research **10**(1): 5-18.

Lubinski, D.J., Polyak, L., and Forman, S.L. (2001). "Freshwater and Atlantic water inflows to the deep northern Barents and Kara seas since ca 13 14Cka:: foraminifera and stable isotopes." Quaternary Science Reviews **20**(18): 1851-1879.

Lundesgaard, Ø., Sundfjord, A., Lind, S., Nilsen, F., and Renner, A.H.H. (2022). "Import of Atlantic Water and sea ice controls the ocean environment in the northern Barents Sea." Ocean Sci. **18**(5): 1389-1418.

Mangerud, J., Bondevik, S., Gulliksen, S., Hufthammer, A.K., and Høisæter, T. (2006). "Marine 14C reservoir ages for 19th century whales and molluscs from the North Atlantic." Quaternary Science Reviews **25**(23-24): 3228-3245.

Manno, C., Morata, N., and Primicerio, R. (2012). "Limacina retroversa's response to combined effects of ocean acidification and sea water freshening." Estuarine, Coastal and Shelf Science **113**: 163-171.

Manno, C. and Pavlov, A. (2014). "Living planktonic foraminifera in the Fram Strait (Arctic): absence of diel vertical migration during the midnight sun." Hydrobiologia **721**(1): 285-295.

Manno, C., Bednaršek, N., Tarling, G.A., Peck, V.L., Comeau, S., Adhikari, D., Bakker, D.C., Bauerfeind, E., Bergan, A.J., and Berning, M.I. (2017). "Shelled pteropods in peril: assessing vulnerability in a high CO2 ocean." Earth-Science Reviews **169**: 132-145.

Manno, C., Giglio, F., Stowasser, G., Fielding, S., Enderlein, P., and Tarling, G. (2018). Threatened species drive the strength of the carbonate pump in the northern Scotia Sea. Nature Communications **9**:4592.

Meilland, J., Fabri-Ruiz, S., Koubbi, P., Monaco, C. L., Cotte, C., Hosie, G.W., Sanchez, S., and Howa, H. (2016a). "Planktonic foraminiferal biogeography in the Indian sector of the Southern Ocean: Contribution from CPR data." Deep Sea Research Part I: Oceanographic Research Papers **110**: 75-89.

Meilland, J., Howa, H., Monaco, C.L., and Schiebel, R. (2016b). "Individual planktic foraminifer protein-biomass affected by trophic conditions in the Southwest Indian Ocean, 30° S–60° S." Marine Micropaleontology **124**: 63-74.

Meilland, J., Schiebel, R., Monaco, C.L., Sanchez, S., and Howa, H. (2018). "Abundances and test weights of living planktic foraminifers across the Southwest Indian Ocean: Implications for carbon fluxes." Deep Sea Research Part I: Oceanographic Research Papers **131**: 27-40.

Meilland, J., Siccha, M., Weinkauf, M.F., Jonkers, L., Morard, R., Baranowski, U., Baumeister, A., Bertlich, J., Brummer, G.-J., and Debray, P. (2019). "Highly replicated sampling reveals no diurnal vertical migration but stable species-specific vertical habitats in planktonic foraminifera." Journal of Plankton Research **41**(2): 127-141.

Meilland, J., Howa, H., Hulot, V., Demangel, I., Salaun, J., and Garlan, T. (2020). "Population dynamics of modern planktonic foraminifera in the western Barents Sea." Biogeosciences **17**(6): 1437-1450.

Meilland, J., Ezat, M. M., Westgård, A., Manno, C., Morard, R., Siccha, M., and Kucera, M. (2022). "Rare but persistent asexual reproduction explains the success of planktonic foraminifera in polar oceans." Journal of Plankton Research: 1-18.

Meinecke, G. and Wefer, G. (1990). "Seasonal pteropod sedimentation in the Norwegian Sea." Palaeogeography, Palaeoclimatology, Palaeoecology **79**(1): 129-147.

Metfies, K., Bauerfeind, E., Wolf, C., Sprong, P., Frickenhaus, S., Kaleschke, L., Nicolaus, A., and Nöthig, E.-M. (2017). "Protist Communities in Moored Long-Term Sediment Traps (Fram Strait, Arctic)–Preservation with Mercury Chloride Allows for PCR-Based Molecular Genetic Analyses." Frontiers in Marine Science **4**.

Meyer, A., Sundfjord, A., Fer, I., Provost, C., Villacieros Robineau, N., Koenig, Z., Onarheim, I.H., Smedsrud, L.H., Duarte, P., and Dodd, P.A. (2017). "Winter to summer oceanographic observations in the Arctic Ocean north of Svalbard." Journal of Geophysical Research: Oceans **122**(8): 6218-6237.

Morris, T. H. and Clark, D.L. (1985). Calcite lysocline of the central Arctic Ocean and its paleoclimatic significance. Geological Society of America, 17, Conference: 98. annual meeting of the Geological Society of America, Orlando, FL, USA, 28 Oct 1985. United States. **17:** Medium: X; Size: Pages: 669.

Movellan, A., Schiebel, R., Zubkov, M., Smyth, A., and Howa, H. (2012). "Quantification of protein biomass of individual foraminifers using nano-spectrophotometry." Biogeosciences Discussions **9**(6).

Nigam, R. (2005). "Sediment traps as a new tool for estimation of longevity of planktonic foraminifera."

Nigam, R., Saraswat, R., and Mazumder, A. (2003). "Life spans of planktonic foraminifers: New insight through sediment traps." Journal of The Palaeontological Society of India **48**: 129-133.

Nöthig, E.-M., Bracher, A., Engel, A., Metfies, K., Niehoff, B., Peeken, I., Bauerfeind, E., Cherkasheva, A., Gäbler-Schwarz, S., and Hardge, K. (2015). "Summertime plankton ecology in Fram Strait—a compilation of long-and short-term observations." Polar Research **34**(1): 23349.

Nöthig, E.-M., Ramondenc, S., Haas, A., Hehemann, L., Walter, A., Bracher, A., Lalande, C., Metfies, K., Peeken, I., and Bauerfeind, E. (2020). "Summertime chlorophyll a and particulate organic carbon standing stocks in surface waters of the Fram Strait and the Arctic Ocean (1991–2015)." Frontiers in Marine Science **7**: 350.

Oakes, R.L. and Sessa, J.A. (2020). "Determining how biotic and abiotic variables affect the shell condition and parameters of Heliconoides inflatus pteropods from a sediment trap in the Cariaco Basin." Biogeosciences **17**(7): 1975-1990.

Ofstad, S., Meilland, J., Zamelczyk, K., Chierici, M., Fransson, A., Gründger, F., and Rasmussen, T.L. (2020). "Development, productivity, and seasonality of living planktonic foraminiferal faunas and

Limacina helicina in an Area of intense methane seepage in the Barents Sea." Journal of Geophysical Research: Biogeosciences **125**(2): e2019JG005387.

Ofstad, S., Zamelczyk, K., Kimoto, K., Chierici, M., Fransson, A., and Rasmussen, T.L. (2021). "Shell density of planktonic foraminifera and pteropod species Limacina helicina in the Barents Sea: Relation to ontogeny and water chemistry." PloS one **16**(4): e0249178.

Olsson, R.K., Berggren, W.A., Hemleben, C., and Huber, B.T. (1999). "Atlas of Paleocene planktonic foraminifera."

Onarheim, I.H., Smedsrud, L.H., Ingvaldsen, R.B., and Nilsen, F. (2014). "Loss of sea ice during winter north of Svalbard." Tellus A: Dynamic Meteorology and Oceanography **66**(1): 23933.

Pados, T. and Spielhagen, R.F. (2014). "Species distribution and depth habitat of recent planktic foraminifera in Fram Strait, Arctic Ocean." Polar Research **33**(1): 22483.

Peijnenburg, K.T.C.A., Janssen, A.W., Wall-Palmer, D., Goetze, E., Maas, A.E., Todd, J.A., and Marlétaz, F. (2020). "The origin and diversification of pteropods precede past perturbations in the Earth's carbon cycle." Proceedings of the national academy of sciences **117**(41): 25609-25617.

Pieńkowski, A.J., Husum, K., Belt, S.T., Ninnemann, U., Köseoğlu, D., Divine, D.V., Smik, L., Knies, J., Hogan, K., and Noormets, R. (2021). "Seasonal sea ice persisted through the Holocene Thermal Maximum at 80°N." Communications Earth & Environment **2**(1): 124.

Pieńkowski, A.J., Husum, K., Furze, M.F., Missana, A.F., Irvalı, N., Divine, D.V., and Eilertsen, V.T. (2022). "Revised ΔR values for the Barents Sea and its archipelagos as a pre-requisite for accurate and robust marine-based 14C chronologies." Quaternary Geochronology **68**: 101244.

Polyakov, I.V., Alkire, M.B., Bluhm, B.A., Brown, K.A., Carmack, E.C., Chierici, M., Danielson, S.L., Ellingsen, I., Ershova, E.A., and Gårdfeldt, K. (2020). "Borealization of the Arctic Ocean in response to anomalous advection from sub-Arctic seas." Frontiers in Marine Science **7**: 491.

Ramondenc, S., Nöthig, E.M., Hufnagel, L., Bauerfeind, E., Busch, K., Knüppel, N., Kraft, A., Schröter, F., Seifert, M., and Iversen, M.H. (2022). "Effects of Atlantification and changing sea‐ice dynamics on zooplankton community structure and carbon flux between 2000 and 2016 in the eastern Fram Strait." Limnology and Oceanography.

Rembauville, M., Meilland, J., Ziveri, P., Schiebel, R., Blain, S., and Salter, I. (2016). "Planktic foraminifer and coccolith contribution to carbonate export fluxes over the central Kerguelen Plateau."

Risebrobakken, B. and Berben, S.M. (2018). "Early holocene establishment of the Barents Sea Arctic front." Frontiers in Earth Science **6**: 166.

Roberts, D., Hopcroft, R.R., and Hosie, G.W. (2014). "Southern Ocean Pteropods."

Sahoo, N., Saalim, S.M., Matul, A., Mohan, R., Tikhonova, A., and Kozina, N. (2022). "Planktic Foraminiferal Assemblages in Surface Sediments From the Subpolar North Atlantic Ocean." Frontiers in Marine Science **8**: 2045.

Sakshaug, E. and Slagstad, D. (1992). "Sea ice and wind: effects on primary productivity in the Barents Sea." Atmosphere-Ocean **30**(4): 579-591.

Salter, I., Schiebel, R., Ziveri, P., Movellan, A., Lampitt, R., and Wolff, G.A. (2014). "Carbonate counter pump stimulated by natural iron fertilization in the Polar Frontal Zone." Nature Geoscience **7**(12): 885-889.

Sato-Okoshi, W., Okoshi, K., Sasaki, H., and Akiha, F. (2010). "Shell structure of two polar pelagic molluscs, Arctic Limacina helicina and Antarctic Limacina helicina antarctica forma antarctica." Polar Biology **33**(11): 1577-1583.

Schiebel, R. (2002). "Planktic foraminiferal sedimentation and the marine calcite budget." Global Biogeochemical Cycles **16**(4): 3-1-3-21.

Schiebel, R. and Hemleben, C. (2000). "Interannual variability of planktic foraminiferal populations and test flux in the eastern North Atlantic Ocean (JGOFS)." Deep Sea Research Part II: Topical Studies in Oceanography **47**(9-11): 1809-1852.

Schiebel, R. and Hemleben, C. (2017). Planktic foraminifers in the modern ocean, Springer.

Schiebel, R. and Movellan, A. (2012). "First-order estimate of the planktic foraminifer biomass in the modern ocean." Earth System Science Data **4**: 75-89.

Schiebel, R., Spielhagen, R.F., Garnier, J., Hagemann, J., Howa, H., Jentzen, A., Martínez-Garcia, A., Meilland, J., Michel, E., and Repschläger, J. (2017). "Modern planktic foraminifers in the high-latitude ocean." Marine Micropaleontology **136**: 1-13.

Schneider, C.A., Rasband, W.S., and Eliceiri, K.W. (2012). "NIH Image to ImageJ: 25 years of image analysis." Nature methods **9**(7): 671-675.

Smedsrud, L.H., Muilwijk, M., Brakstad, A., Madonna, E., Lauvset, S.K., Spensberger, C., Born, A., Eldevik, T., Drange, H., and Jeansson, E. (2022). "Nordic Seas heat loss, Atlantic inflow, and Arctic sea ice cover over the last century." Reviews of Geophysics **60**(1): e2020RG000725.

Søreide, J.E., Leu, E.V., Berge, J., Graeve, M., and Falk-Petersen, S. (2010). "Timing of blooms, algal food quality and Calanus glacialis reproduction and growth in a changing Arctic." Global Change Biology **16**(11): 3154-3163.

Sternbeck, J., Land, M., and Nilsson, Ö. (2006). Oskarshamn and Forsmark site investigation. 210Pb and 14C dating of sediments and peat: accumulation rates of carbon, nitrogen and phosphorus, Svensk kärnbränslehantering AB (SKB).

Stuiver, M. and Reimer, P.J. (1993). "Extended 14C Data Base and Revised CALIB 3.0 14C Age Calibration Program." Radiocarbon **35**(1): 215-230.

Sundfjord, A., Assmann, K.M., Lundesgaard, Ø., Renner, A.H.H., Lind, S., and Ingvaldsen, R.B. (2020). Suggested water mass definitions for the central and northern Barents Sea, and the adjacent Nansen Basin: Workshop Report. The Nansen Legacy Report Series 8/2020. Tromsø, Norway.

Takahashi, K. and Bé, A. (1984). "Planktonic foraminifera: factors controlling sinking speed: Deep-Sea Research I, v. 12A."

Tans, P., and Keeling, R. (2023) "Trends in Atmospheric Carbon Dioxide." Global Monitoring Laboratory measurements from NOAA. https://gml.noaa.gov/ccgg/trends/data.html

Torres-Valdés, S., Tsubouchi, T., Bacon, S., Naveira-Garabato, A.C., Sanders, R., McLaughlin, F.A., Petrie, B., Kattner, G., Azetsu-Scott, K., and Whitledge, T.E. (2013). "Export of nutrients from the Arctic Ocean." Journal of Geophysical Research: Oceans **118**(4): 1625-1644.

Tuerena, R.E., Mahaffey, C., Henley, S.F., de la Vega, C., Norman, L., Brand, T., Sanders, T., Debyser, M., Dähnke, K., Braun, J., and März, C. (2022). "Nutrient pathways and their susceptibility to past and future change in the Eurasian Arctic Ocean." Ambio **51**(2): 355-369.

v. Gyldenfeldt, A.-B., Carstens, J., and Meincke, J. (2000). "Estimation of the catchment area of a sediment trap by means of current meters and foraminiferal tests." Deep Sea Research Part II: Topical Studies in Oceanography **47**(9): 1701-1717.

Vihtakari., M. (2020). PlotSvalbard: PlotSvalbard - Plot research data from Svalbard on maps.

Volkmann, R. (2000). "Planktic foraminifers in the outer Laptev Sea and the Fram Strait—Modern distribution and ecology." The Journal of Foraminiferal Research **30**(3): 157-176.

Westgård, A., Ezat, M.M., Chalk, T.B., Chierici, M., Foster, G.L., and Meilland, J. (2022) Large-scale culturing of *Neogloboquadrina pachyderma*, its growth in, and tolerance of, variable environmental conditions. Journal of Plankton Research. 1-14.

Weydmann-Zwolicka, A., Prątnicka, P., Łącka, M., Majaneva, S., Cottier F., and Berge, J. (2021). "Zooplankton and sediment fluxes in two contrasting fjords reveal Atlantification of the Arctic." Science of The Total Environment **773**: 145599.

Young, J.R., Wade, B.S., & Huber B.T. (eds) pforams@mikrotax website. 21 Apr. 2017. URL: http://www.mikrotax.org/pforams

Zamelczyk, K., Fransson, A., Chierici, M., Jones, E., Meilland, J., Anglada-Ortiz, G., and Hodal Lødemel, H. (2021). "Distribution and abundances of planktic foraminifera and shelled pteropods during the polar night in the sea-ice covered northern Barents Sea." Frontiers in Marine Science: 1516.

Zamelczyk, K., Rasmussen, T.L., Husum, K., Haflidason, H., de Vernal, A., Ravna, E.K., Hald, M., and Hillaire-Marcel, C. (2012). "Paleoceanographic changes and calcium carbonate dissolution in the central Fram Strait during the last 20 ka." Quaternary Research **78**(3): 405-416.

Zamelczyk, K., Rasmussen, T.L., Husum, K., and Hald, M. (2013). "Marine calcium carbonate preservation vs. climate change over the last two millennia in the Fram Strait: Implications for planktic foraminiferal paleostudies." Marine Micropaleontology **98**: 14-27.

Zamelczyk, K., Rasmussen, T.L., Raitzsch, M., and Chierici, M. (2020). "The last two millennia: climate, ocean circulation and paleoproductivity inferred from planktic foraminifera, south-western Svalbard margin." Polar Research. 2020, 39, 3715.

Ziveri, P., Gray, W.R., Anglada-Ortiz, G., Manno, C., Grelaud, M., Incarbona, A., Rae, J.W.B., Subhas, A.V., Pallacks, S., White, A., Adkins, J.F., and Berelson, W. (2023). "Pelagic calcium carbonate production and shallow dissolution in the North Pacific Ocean." Nature communications **14**(1): 805.

Årthun, M., Eldevik, T., Smedsrud, L., Skagseth, Ø., and Ingvaldsen, R. (2012). "Quantifying the influence of Atlantic heat on Barents Sea ice variability and retreat." Journal of Climate **25**(13): 4736-4743.

II. Research papers

Paper I

frontiers in Marine Science

ORIGINAL RESEARCH
published: 09 June 2021
doi: 10.3389/fmars.2021.661158

Planktic Foraminiferal and Pteropod Contributions to Carbon Dynamics in the Arctic Ocean (North Svalbard Margin)

Griselda Anglada-Ortiz[1], Katarzyna Zamelczyk[2], Julie Meilland[3], Patrizia Ziveri[4,5], Melissa Chierici[6], Agneta Fransson[2] and Tine L. Rasmussen[1]*

[1] Centre for Arctic Gas Hydrate, Environment and Climate (CAGE), Department of Geosciences, UiT The Arctic University of Norway, Tromsø, Norway, [2] Oceans and Sea Ice, Norwegian Polar Institute (NPI), Tromsø, Norway, [3] MARUM Center for Marine Environmental Sciences, University of Bremen, Bremen, Germany, [4] Institute of Environmental Science and Technology (ICTA), Autonomous University of Barcelona, Barcelona, Spain, [5] ICREA, Catalan Institution for Research and Advanced Studies, Barcelona, Spain, [6] Oceanography and Climate, Institute of Marine Research (IMR), Tromsø, Norway

Planktic foraminifera and shelled pteropods are some of the major producers of calcium carbonate ($CaCO_3$) in the ocean. Their calcitic (foraminifera) and aragonitic (pteropods) shells are particularly sensitive to changes in the carbonate chemistry and play an important role for the inorganic and organic carbon pump of the ocean. Here, we have studied the abundance distribution of planktic foraminifera and pteropods (individuals m^{-3}) and their contribution to the inorganic and organic carbon standing stocks (μg m^{-3}) and export production (mg m^{-2} day^{-1}) along a longitudinal transect north of Svalbard at 81° N, 22–32° E, in the Arctic Ocean. This transect, sampled in September 2018 consists of seven stations covering different oceanographic regimes, from the shelf to the slope and into the deep Nansen Basin. The sea surface temperature ranged between 1 and 5°C in the upper 300 m. Conditions were supersaturated with respect to $CaCO_3$ ($\Omega > 1$ for both calcite and aragonite). The abundance of planktic foraminifera ranged from 2.3 to 52.6 ind m^{-3} and pteropods from 0.1 to 21.3 ind m^{-3}. The planktic foraminiferal population was composed mainly of the polar species *Neogloboquadrina pachyderma* (55.9%) and the subpolar species *Turborotalita quinqueloba* (21.7%), *Neogloboquadrina incompta* (13.5%) and *Globigerina bulloides* (5.2%). The pteropod population was dominated by the polar species *Limacina helicina* (99.6%). The rather high abundance of subpolar foraminiferal species is likely connected to the West Spitsbergen Current bringing warm Atlantic water to the study area. Pteropods dominated at the surface and subsurface. Below 100 m water depth, foraminifera predominated. Pteropods contribute 66–96% to the inorganic carbon standing stocks compared to 4–34% by the planktic foraminifera. The inorganic export production of planktic foraminifera and pteropods together exceeds their organic contribution by a factor of 3. The overall predominance of pteropods over foraminifera in this high Arctic region during the sampling period suggest that inorganic standing stocks and export production of biogenic carbonate would be reduced under the effects of ocean acidification.

Keywords: inorganic and organic carbon pump, planktic calcifiers, standing stocks, export production, Atlantification

OPEN ACCESS

Edited by:
Sunil Kumar Singh,
Physical Research Laboratory, India

Reviewed by:
Arun Deo Singh,
Banaras Hindu University, India
Sushant Naik,
National Institute of Oceanography (CSIR), India

****Correspondence:***
Griselda Anglada-Ortiz
griselda.a.ortiz@uit.no

Specialty section:
This article was submitted to Marine Biogeochemistry, a section of the journal Frontiers in Marine Science

Received: *30 January 2021*
Accepted: *05 May 2021*
Published: *09 June 2021*

Citation:
Anglada-Ortiz G, Zamelczyk K, Meilland J, Ziveri P, Chierici M, Fransson A and Rasmussen TL (2021) Planktic Foraminiferal and Pteropod Contributions to Carbon Dynamics in the Arctic Ocean (North Svalbard Margin). Front. Mar. Sci. 8:661158. doi: 10.3389/fmars.2021.661158

INTRODUCTION

The increasing atmospheric uptake of CO_2 by the surface ocean is changing the seawater carbonate chemistry by reducing the pH, the carbonate ion concentration and the calcium carbonate ($CaCO_3$) saturation state (Ω). This process, referred to as ocean acidification, may have irreversible consequences for marine calcifiers, such as planktic foraminifera and shelled pteropods. Ocean acidification can cause reduced calcification rates (Fabry, 2008; Moy et al., 2009; Manno et al., 2017; Schiebel et al., 2017) or dissolution or damage of the shells in case of $CaCO_3$ undersaturation ($\Omega < 1$) (Peck et al., 2018) and references therein. Due to the sensitivity of their shells, planktic foraminifera and pteropods are used as biological indicators of ocean acidification [e.g., Orr et al. (2005), Fabry et al. (2008), Moy et al. (2009), Bednaršek et al. (2012c)]. Moreover, they are important for the carbonate budget and changes in their distribution patterns and productivity can alter the buffer capacity of the ocean (Schiebel, 2002; Ziveri et al., 2007; Langer, 2008; Bednaršek et al., 2012a; Salter et al., 2014; Buitenhuis et al., 2019).

Planktic foraminifera are unicellular protists with shells made of calcite. They mainly occur in the upper 300 m of the water column. Due to their sensitivity to environmental conditions and the excellent preservation patterns in sedimentary geological records, they are extensively used as proxies to reconstruct past physical and chemical parameters of the upper ocean (Katz et al., 2010). However, only few studies have investigated their sensitivity to present and past ocean acidification (Moy et al., 2009; Roy et al., 2015; Davis et al., 2017; Fox et al., 2020).

Shelled pteropods are holoplanktic gastropods with a shell made of aragonite. They live in the upper water column. Aragonite is the most soluble form of $CaCO_3$ and therefore more vulnerable to water carbonate chemistry changes than calcite (Bednaršek et al., 2012b; Manno et al., 2017). The pteropod species *Limacina helicina* has shown damage of the aragonite shell even in supersaturated waters with a Ω_{AR} of 1.5 (Bednaršek et al., 2014, 2019).

Planktic foraminifera and pteropods are the major zooplankton producers of $CaCO_3$ and a key component of the ocean carbon cycle (Guinotte and Fabry, 2008). Besides coccolithophores (unicellular phytoplankton), they have an important role in exporting carbon from the surface to the deep ocean. In particular, shelled pteropods contribute to the biological carbon pump exporting organic carbon (particulate organic carbon) through formation of aggregates and fecal pellets (Manno et al., 2018) and references therein. Planktic foraminifera and shelled pteropods also contribute to the opposite process known as the carbonate counter pump. Through the calcification of their inorganic shells, the carbonate counter pump results in producing CO_2 and exporting inorganic carbon (particulate inorganic carbon) to the ocean floor (Salter et al., 2014; Manno et al., 2018). In the Southern Ocean (Scotia Sea), both foraminifera and pteropods have been found to contribute significantly to the seasonal productivity, with pteropods being the major producer of $CaCO_3$ (Manno et al., 2018).

Productivity patterns in the Arctic are strongly dependent on the degree of sea-ice cover, availability of nutrients and light, and surface stratification (Bluhm et al., 2015). The primary production is characterized by a spring phytoplankton bloom occurring between April and July when the sea ice retreats (Sakshaug, 1997; Lee et al., 2015) and a second phytoplankton bloom in late summer (Wassmann et al., 2019). This production represents the major food source for the zooplankton (Sakshaug, 1997) and references therein.

The northern Barents Sea is located in an Arctic region where rising atmospheric and ocean surface temperatures as well as sea-ice loss are occurring at increasing rates (Descamps et al., 2017). The sea-ice loss may increase the direct gas uptake from the atmosphere, which will have unknown effects on the physical, biogeochemical and ecological conditions (Bates and Mathis, 2009). Because the solubility of CO_2 increases in cold water, and the already low saturation states, the polar oceans in general, and the Barents Sea in particular, are expected to be especially vulnerable to ocean acidification (Chierici and Fransson, 2018). Despite the importance of this region, little is known about the distribution of marine calcifiers, their present state of calcification and how they would respond to ocean acidification. This present study aims to estimate the inorganic and organic carbon standing stocks ($\mu g\ m^{-3}$) and export productivity (flux = $mg\ m^{-2}\ day^{-1}$) of planktic foraminifera and shelled pteropods on the northern margin of Barents Sea, north of Svalbard and into the Arctic Ocean deep Nansen Basin. The calcium carbonate reaching the sea floor derived from planktic foraminifera has been determined to be from 32 to 80% of the total global fluxes (Schiebel, 2002). The diversity of foraminifera in the polar regions is low with dominance of *Neogloboquadrina pachyderma, Turborotalita quinqueloba* and *Globigerina bulloides* (Schiebel et al., 2017). Their vertical distribution has recently been suggested to be delimited to the upper 100 m of the water column (Greco et al., 2019; Meilland et al., 2020). A recent study of the inorganic and organic carbon budgets and the organic-inorganic carbon ratio (C_{ORG}/C_{INORG}) along the southern polar zone in the Southwest Indian Ocean, estimated the C_{ORG}/C_{INORG} to be between 0.17 and 0.5 (Meilland et al., 2018). The inorganic contribution from the planktic foraminiferal faunas represented between 67 and 85% of the total carbon budget and indicates that foraminifera can be a major component in the carbon pump of the ocean. The present study represents the first quantification of carbonate contributions from pteropods and foraminifera from this remote and rarely studied northern Barents Sea area and Nansen basin in the Arctic Ocean.

MATERIALS AND METHODS

Study Area

The northern Svalbard margin is influenced by the flow of warm Atlantic Water, which represents the main supplier of heat to the Arctic Ocean (**Figure 1**). It is conveyed to the area and into the Nansen Basin through the Svalbard Branch of the West Spitsbergen Current (Meyer et al., 2017). The Atlantic water north of Svalbard has a major control of the extent

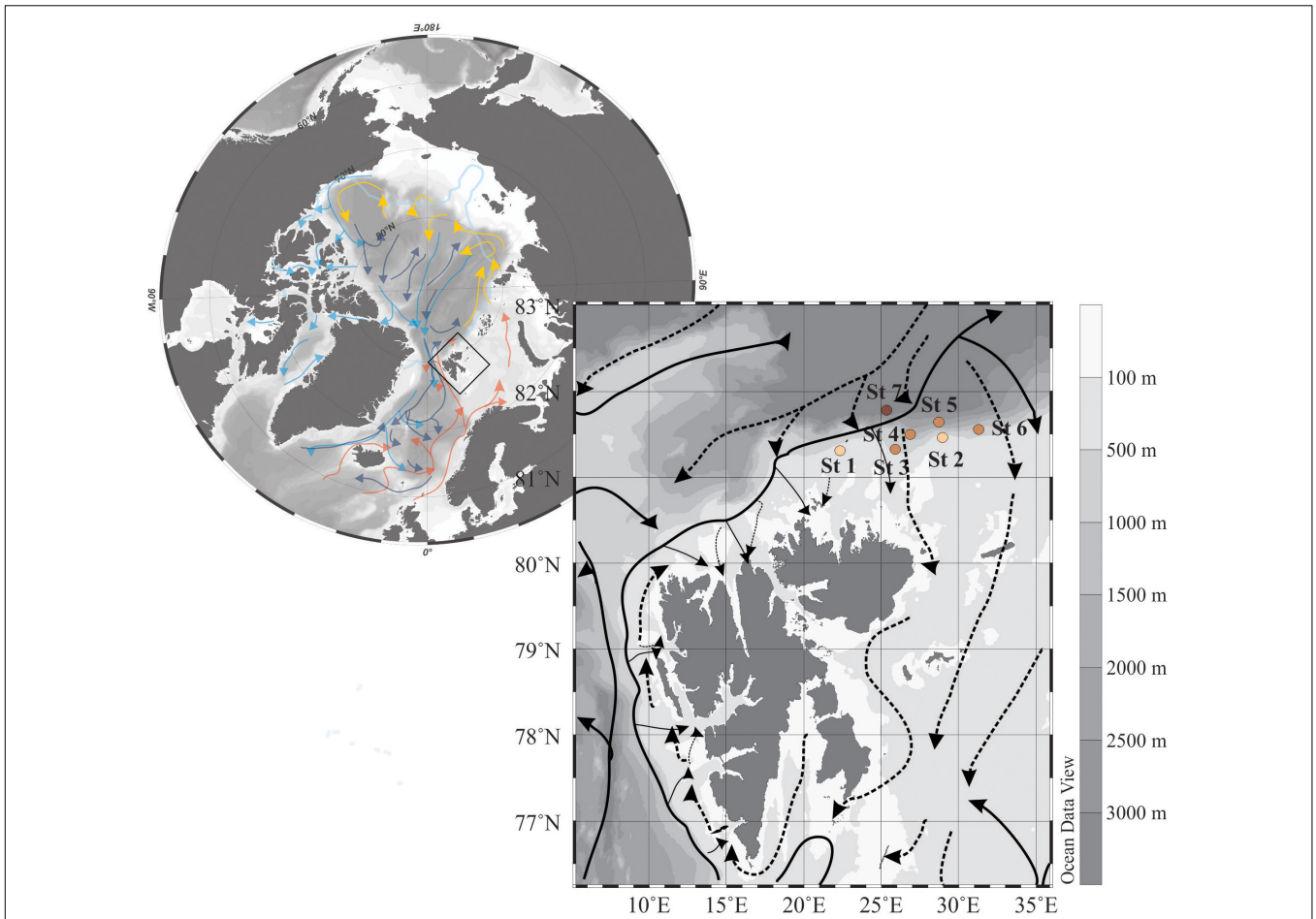

FIGURE 1 | Map of the Arctic Ocean with warm and cold surface, intermediate and deep waters in red, blue, yellow, and dark blue arrows [modified from Anderson and Macdonald (2015). Detailed surface Atlantic (solid line) and Arctic (dashed line) currents from Hop et al. (2019)].Sea ice extent on September 2018 in light blue, and study area framed in black. Zoom in the study area with the sampling stations.

of the sea-ice cover, and has been warming during the last decades (Meyer et al., 2017; Renner et al., 2018) since monitoring started in 1977 (Onarheim et al., 2014). In September 2018, the northern Svalbard margin was ice-free up to 82.40 °N, where the sea-ice edge occurred. This coincided with the fact that 2018 was an anomalously warm year. In September 2018 the Arctic sea-ice cover by area was 25.3% below the 1981–2010 average (NOAA NCFEI, 2018).

Sampling and Sample Analysis

Plankton and water samples were retrieved onboard RV *Helmer Hanssen*, during cruise HH18-6 to the northern Svalbard margin, between August 28 and September 12, 2018. Seven stations were sampled along a longitudinal transect along 81°N, from 22 to 32°E covering the shelf and slope, and the Nansen deep basin in different light conditions (**Figure 1** and **Table 1**). The sampling stations are numbered from west to east: shelf stations

TABLE 1 | Location, latitude (°N) and longitude (°E), water depth (m), sampling date and light conditions, sea surface temperature (°C) and sea surface salinity.

	Location	Latitude (°N)	Longitude (°E)	Water depth (m)	Sampling date	Sampling light conditions	SST (°C)	SSS
St 1	Shelf	81.3	22.3	376	05.09.2018	Night	4.6	34.5
St 2	Shelf	81.5	29.0	368	04.09.2018	Day	4.03	34.4
St 3	Slope	81.3	25.9	510	08.09.2018	Day	3.0	34.0
St 4	Slope	81.5	26.7	1019	04.09.2018	Day	2.8	33.8
St 5	Slope	81.6	28.7	2166	08.09.2018	Night	2.9	34.2
St 6	Slope	81.6	31.3	853	04.09.2018	Night	3.1	34.1
St 7	Basin	81.8	25.3	3094	07.09.2018	Day	1.2	32.9

TABLE 2 | Average size, SD, minimum and maximum value and number of individuals measured.

	Planktic foraminifera				Shelled pteropods			
	>500 μm	250–500 μm	100–250 μm	90–100 μm	>500 μm	250–500 μm	100–250 μm	90–100 μm
Average (μm)		323.3	162.2	95.4	693.1	394.1	226.8	101.7
SD		8.5	46.8	8.7	161.2	70.4	37.0	4.0
Minimum value		309.1	81.5	82.4	438.5	245.8	172.1	97.2
Maximum value		330.3	281. 1	106.6	1371.8	549.6	283.1	104.6
Number of individuals		5	239	13	153	210	14	3

1 and 2, slope stations 3–6, and Nansen Basin deep station 7 (**Figure 1**).

Water Samples

Prior to each plankton tow, the physicochemical parameters of the water column were measured with a CTD (Conductivity, Temperature, Depth) SeaBird 911 Plus equipped with a 12-Niskin bottle Rosette. Seawater for the variables of carbonate chemistry was collected from each Niskin bottle and transferred into 250 mL borosilicate bottles using a silicon tube. The samples were preserved with 50 μL saturated mercuric acid before the post-cruise analyses of dissolved inorganic carbon (DIC) and total alkalinity (AT) at the laboratory of the Institute of Marine Research (IMR), Tromsø, Norway, following standard procedures outlined in Dickson et al. (2007) at a temperature around 25°C. DIC was determined using a coulometric titration with a Versatile Instrument for the Determination of Titration Alkalinity (VINDTA 3D, Marianda, Germany). AT was determined from potentiometric titration with 0.1 N hydrochloric acid in a closed cell using a Versatile Instrument for the Determination of Titration Alkalinity (VINDTA 3S, Marianda, Germany). The accuracy and precision for DIC and AT were assured by repeated measurements of Certified Reference Material (CRM, provided by A. G. Dickson, Scripps Institution of Oceanography, United States), and were ±2 μmol kg^{-1} for both DIC and AT.

Partial pressure of CO_2 (pCO_2), pH and aragonite and calcite saturations (**Ω**) were calculated using DIC and AT in combination with the *in situ* water pressure, salinity, temperature, silicate and phosphate concentrations using the chemical speciation model CO2SYS (Pierrot et al., 2006). The carbonic acid dissociation constants of Mehrbach et al. (1973) as refitted by Dickson and Millero (1987) were used in combination with the bisulfate dissociation constant from Dickson (1990), and the total boron concentration of Lee et al. (2010). The aragonite and calcite stoichiometric solubility constants of Mucci (1983) were used with the pressure corrections of Millero (1979) and the calcium concentration and salinity ratio of Riley and Tongudai (1967).

Planktic Foraminifera and Pteropod Samples

Planktic foraminifera and pteropods were collected using a WP2 zooplankton net (Hydro-bios 90-μm mesh size, Ø = 0.57 m). The upper 300 meters of the water column were towed at regular depth intervals of 0–50 m, 50–100 m, 100–200 m and 200–300 m. The surface layer sample (0–50 m) from station 7 was lost. Immediately after recovery, the samples were frozen at −80°C. The samples were analyzed in the laboratory of the Department of Geosciences, UiT the Arctic University of Norway, Tromsø, Norway.

Each frozen plankton sample was melted and gently wet-sieved with cold water through a cascade of sieves with mesh sizes 500, 250, 100, and 63 μm. Each size fraction obtained (>500, 250–500, 100–250, and 90–100 μm) was wet-picked separately for absolute abundance and flux estimates (note 90 μm was the mesh size of the plankton net) (see below). Only living specimens (containing cytoplasm) of planktic foraminifera and pteropods were counted. Living specimens >100 μm were identified to species level and percentages of individual species calculated. In the following, pteropods >500 μm (most likely young adults) are referred to as large-sized, and size range 250–500 μm (most likely veligers and juveniles) are referred to as medium-sized and, 100–250, and 90–100 μm as small-sized. Planktic foraminifera from the size range 250–500 μm are referred as large-sized, 100–250 μm are referred as medium-sized, and 90–100 μm are referred to as small-sized. The absolute abundance (ind m^{-3}) was calculated dividing the number of individuals by the volume of water sampled with the WP2. The volume was calculated following the general cylinder formula ($V = \pi r^2 h$) where the radius (r) is 0.285 m and h is the height of the target water column depth profile.

In order to estimate the average maximum diameter (Lischka and Riebesell, 2012) of shells per size fraction, 153 (>500 μm), 210 (250–500 μm), 14 (100–250 μm), and 3 (<100 μm) pteropod shells were randomly selected and photographed (**Table 2**) with a DMC4500 camera attached to the binocular Leica Z16 APO (magnification ×0.57–9.2). Their diameter was measured using the software ImageJ (Schneider et al., 2012). We estimated the average dry weight of pteropods (DW) from the average diameter (D) with the equation reported in Bednaršek et al. (2012a) ($DW = 0.137\ D^{1.5005}$). The average individual shell weight was estimated using the calculations described in Bednaršek et al. (2012a). The carbon biomass (μg) of the pteropods was estimated as reported in Bednaršek et al. (2012a) from the dry weight (DW).

In order to estimate the average weight per size fraction, 17 (250–500 μm) and 111 (100–250 μm) foraminiferal shells were

randomly selected, picked and weighed using a Mettler Toledo XP2U (0.1 μg precision) balance.

No treatment to remove the remaining cytoplasm was applied to the shells; therefore the weight acquired also contain organic carbon from the dried cytoplasm, which we consider negligible compared to the shell weight. There is a large density difference between calcite and wet cytoplasm with negligible contribution of the organic carbon to the dry test mass (Schiebel et al., 2007; Beer et al., 2010). The average foraminiferal shell weight was thereafter calculated for each size fraction. In addition, the weight measurements were combined with estimated weights of 5 (250–500 μm), 239 (100–250 μm), and 13 (90–100 μm) foraminiferal shells using the equation reported by Meilland et al. (2018) ($y_m = 2.04 \times 10^{-05} x^{2.2}$) where the mass ($y_w$) is proportional to the minimum diameter (x) of an individual. The average individual weight of calcium carbonate from planktic foraminifera was assumed to be equal to the average individual shell weight. Similarly, the foraminiferal carbon biomass (μg of protein with an estimated 1:1 ratio between protein and organic carbon concentration) was estimated following the equation reported in Meilland et al. (2018) ($y_p = 5.10 \times 10^{-05} x^{1.77}$), where the protein content (y_w) is proportional to the minimum diameter (x) of an individual.

Carbon Standing Stocks and Export Production

The standing stocks (μg m^{-3}) from the upper ocean (0–100 m) were calculated based on the methods described in Meilland et al. (2018). The average weight of $CaCO_3$ (inorganic carbon) and the carbon biomass (organic carbon) of planktic foraminifera and pteropods (μg) were multiplied by integrating the absolute abundance (ind m^{-3}) of the various size fractions from the upper 100 m.

The inorganic carbon production (flux = mg m^{-2} day^{-1}) from foraminifera and pteropods at 100 m (depth of the productive zone) were calculated based on the methods described in Meilland et al. (2018). In this study, the potential inorganic export production at 100 m was derived from the foraminifera and pteropods collected between 50 and 100 m. The depth of 100 m is considered the initial flux level of tests (Schiebel and Hemleben, 2000). The average individual shell weight (μg) or the protein content (μg) (for inorganic and organic carbon, respectively) was multiplied by the absolute abundance of foraminifera and pteropods (ind m^{-3}) and by the test sinking velocity (m day^{-1}) (Schiebel, 2002; Meilland et al., 2018). In case of foraminifera, the test sinking velocity was calculated per size fraction using the formula described by Takahashi and Bé (1984): $Y = 10^a z^b$, where Y is the test sinking velocity (mm s^{-1}), z the shell weight and a and b constants of 2.06 and 0.64, respectively (Schiebel, 2002; Meilland et al., 2018). According to Chang and Yen (2012) the sinking velocity of pteropods is positively correlated with their size, and in this study we used 5 mm s^{-1}. We consider this velocity, even though estimated from a 500-μm shell size, more suitable to apply to all size fractions than other previously reported [e.g., 864–1210 m/day by Lalli and Gilmer (1989)].

RESULTS

Physical and Chemical Environment North of Svalbard

In the study area, the deeper stations (>500 m water depth: slope stations 3, 4, 5 and 6 and basin station 7) are characterized by the presence of Intermediate Water ($-1.1°C < \theta \leq 0°C$), in contrast to the shelf stations 1 and 2 (368–376 m water depth) that are influenced by the Atlantic Water ($\theta > 2.0°C$, $S \geq 34.9$) (Sundfjord et al., 2020; **Figure 2** and **Supplementary Figure 1**). All stations are defined by the presence of a shallow (0–50 m) warm late summer Polar water layer with temperatures of 1–5°C and salinities of 30.17–34.93 (**Figure 2** and **Supplementary Figure 1**). In general, sea surface temperatures from shelf stations not influenced by Arctic deep water are warmer (4–4.6°C) than the slope and basin stations (1.15–3.14°C) (**Table 1**). Moreover, shelf stations have a narrower range of surface salinities (33.68–34.93) compared to deeper stations (30.17–34.55). Specifically, slope station 6 and basin station 7 show a wider range of salinity and the most fresh surface water masses ($S < 30$) are recorded (**Figure 2** and **Supplementary Figure 1**). Beneath this layer, the Atlantic water reaches 500–700 m water depth, with temperature decreasing down to 2°C. The modified Atlantic Water ($0.0°C < \theta \leq 2°C$, $S \geq 34.9$) (Sundfjord et al., 2020) and Intermediate Water are found below the Atlantic water, with temperatures ranging between −0.9 and 1°C and salinity around 34.89 (**Supplementary Figure 1**).

The dissolved inorganic carbon (DIC), total alkalinity (AT) and pCO_2 gradually increase from west to east and from surface to bottom water (**Figure 2**). pH and saturation state α (both aragonite and calcite) generally decrease from surface to bottom (**Figure 2**). The greatest values of DIC (2200 μmol/kg), pH (8.00) and pCO_2 (425 μatm) are recorded below 50 m depth from 29 to 31°E corresponding to the shelf station 2 and slope stations 5 and 6 (**Figure 2**). In these same stations the lowest aragonite (<1.40) and calcite (<2.25) saturation states are recorded in Atlantic Water at 200 m and 150 m depth, respectively. No undersaturated conditions with respect to $CaCO_3$ occur along the transect.

Abundance and Vertical Distribution of Foraminifera and Pteropods

In general, planktic foraminifera dominate in the study area, representing between 68 and 95% of the total community of planktic foraminifera and pteropods together (**Figure 3** and **Table 3**). Planktic foraminifera (<250 μm) are the most abundant and mainly observed between 50 and 300 m (66–95%), whereas the upper 50 m is mainly dominated by pteropods > 250–μm (29–59%) (**Figure 4** and **Supplementary Tables 1,2**). Pteropods are rare or absent below 100 m in any of the stations (**Figures 3–5**).

The planktic foraminiferal fauna along the transect is dominated by *N. pachyderma* and *T. quinqueloba*, followed by *N. incompta* (**Figure 6**). In the entire study area, these three species together represent on average 91.1% of the total assemblage. The lowest occurrence of the three species is 75%

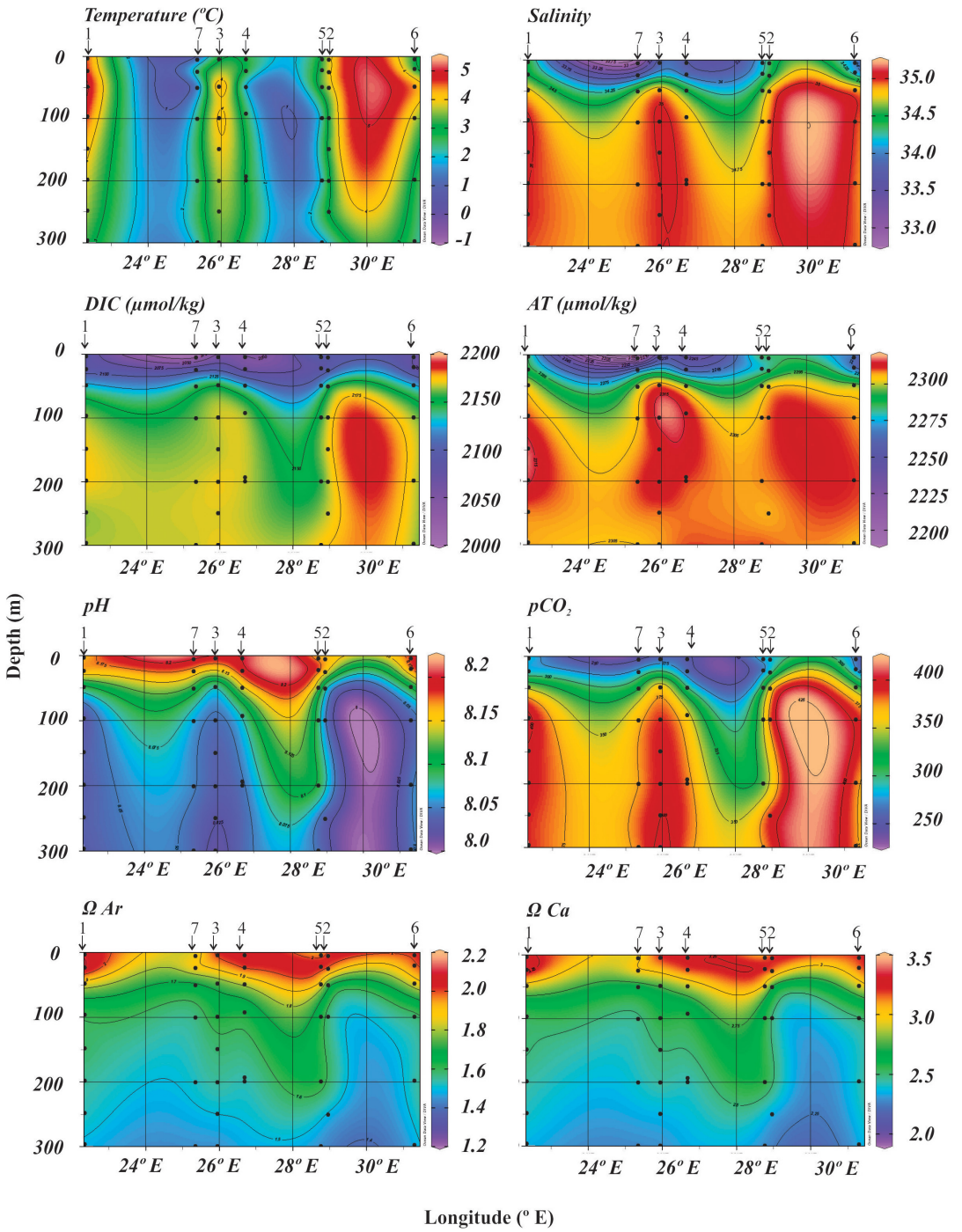

FIGURE 2 | Seawater chemistry sections along the transect. The position of each station represented with black arrows.

(at slope station 6 between 100 and 200 m) and the highest is 100%, in the shallower depth interval of the easternmost shelf station 2 and the north slope station 5 (**Table 4**). The subpolar species *G. bulloides* is part of the foraminiferal community although present in low percentages (**Table 4**). In general, the relative abundance of *N. pachyderma* remains constant in surface samples from all stations in contrast to deeper intervals (**Figure 6**). The highest (73.6% of the total planktic foraminifera community) and the lowest (33.3%) percentages are found at the same depth interval (100–200 m) at stations 4 and 6, respectively (**Table 3**).

The relative abundance of *N. incompta* is variable in the subsurface samples (**Figure 6**). The highest (33.9%) percentages of *N. incompta* is found at 50–100 m at shelf station 1 (**Table 4**).

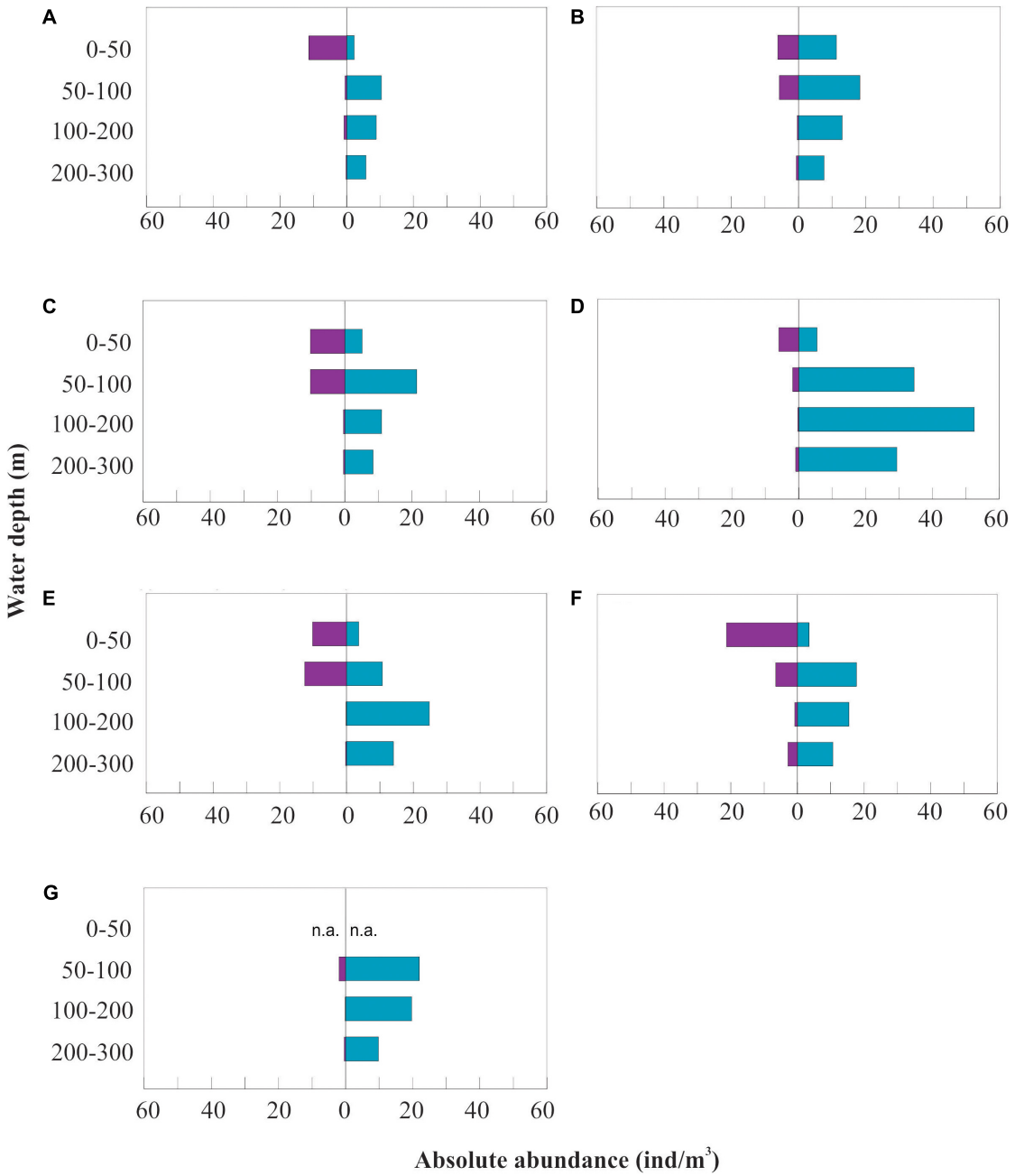

FIGURE 3 | Absolute abundance (ind m^{-3}) of planktic foraminifera (blue) and pteropods (purple) of stations 1–7 **(A–G)** along the water column (n.a., not available).

No specimens are found at the easternmost slope station 6 (**Table 4**).

In general, relatively high percentages of *T. quinqueloba* are found below 50 m water depth with highest relative abundance of 41.2% at slope station 3 and lowest of 8.1% at shelf station 1 and slope station 3 (**Table 3**). The relative abundance of this species below 100 m depth varies between stations (**Figure 6**).

The distribution of *G. bulloides* does not follow any particular pattern and it is generally of low relative abundance (**Table 4**). At slope stations 5 and 6, and basin station 7, the highest percentages of *G. bulloides* are found at 100–200 m depth, while at shelf stations 1 and 2 they occur at 50–100 m depth. At slope stations 3 and 4, the highest abundances are found in the upper 50 m of the water column. This species is most abundant at slope station 3 (12.9%). It is absent at some stations and depths (**Table 4**).

The polar species *Limacina helicina* dominates the pteropod fauna at all stations and depths (94.2–100%). The highest relative abundance of *L. helicina* (100%) was found at shelf station 1, slope stations 3, 4 and 5, and basin station 7 in all sampled intervals. At shelf station 2 and slope station 6 high percentages of *L. helicina*

TABLE 3 | Results of the two-way ANOVA test.

	Foraminifera	Pteropods
	p value	*p* value
Relative abundance/depth	3.2e-06***	2.06e-07***
Relative abundance/size	0.12	0.8
Size/depth	1	1

*Only two size fractions (90–100 and 100–250 μm) were taken into account for foraminifera. ***p < 0.01.*

(>97.2%) occurred in all sampled intervals. Low percentages of *Limacina retroversa* (0.7–5.8%) are found at shelf station 2 (50–100 m) and slope stations 3 (0–100 m) and 6 (0–50 m) (**Table 4**). At slope station 3, which is more influenced by Atlantic Water, is where *L. retroversa* is most abundant (up to 5.8%). No specimens of *L. retroversa* are found below 100 m.

Foraminiferal and Pteropod Carbonate Standing Stock and Export Production in the Upper 100 m of the Water Column

The inorganic standing stocks and export production of foraminifera ranged from 10.6 to 33.1 μg $CaCO_3$ m^{-3}, and from 2.3 to 7.9 mg $CaCO_3$ m^{-2} day^{-1}, respectively. The organic standing stocks and production ranged from 1.9 to 6.2 μg m^{-3}, and from 0.5 to 1.6 mg m^{-2} day^{-1}, respectively. Inorganic standing stocks and export production of pteropods ranged from 57.3 to 439.2 μg $CaCO_3$ m^{-3}, and from 6.1 to 227.6 mg $CaCO_3$ m^{-2} day^{-1}, respectively. The

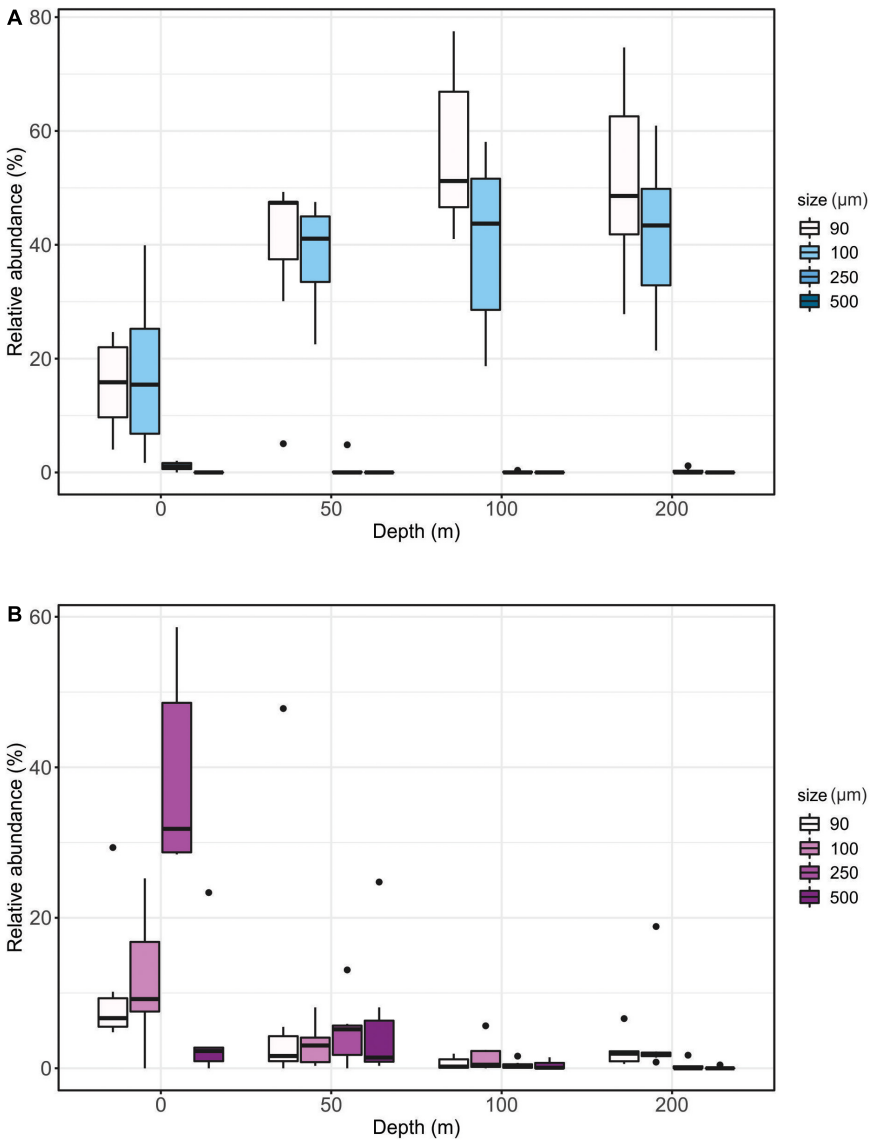

FIGURE 4 | Relative (%) size distribution of planktic foraminifera **(A)** and pteropods **(B)** relative to water depth.

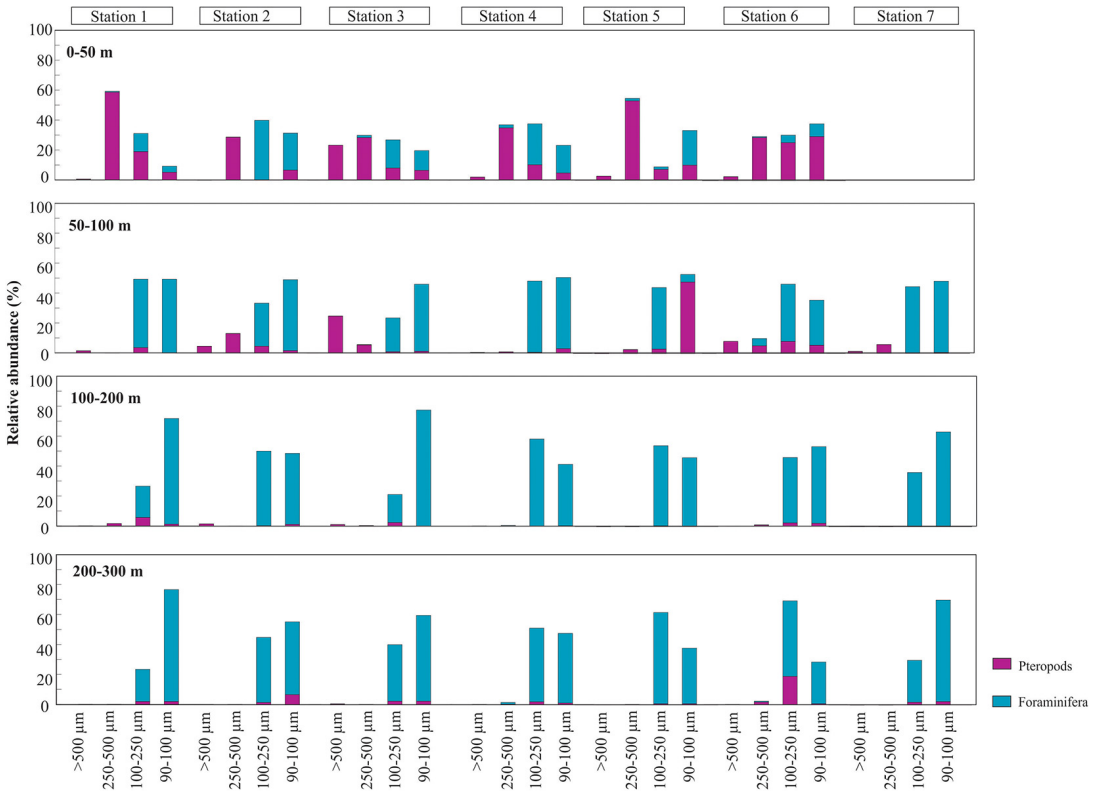

FIGURE 5 | Relative abundance (%) of planktic foraminifera (blue) and pteropods (purple) per size fraction and station. The panels represent from top to bottom: 0 to 50 m, 50 to 100 m, 100 to 200 m, and 200 to 300 m.

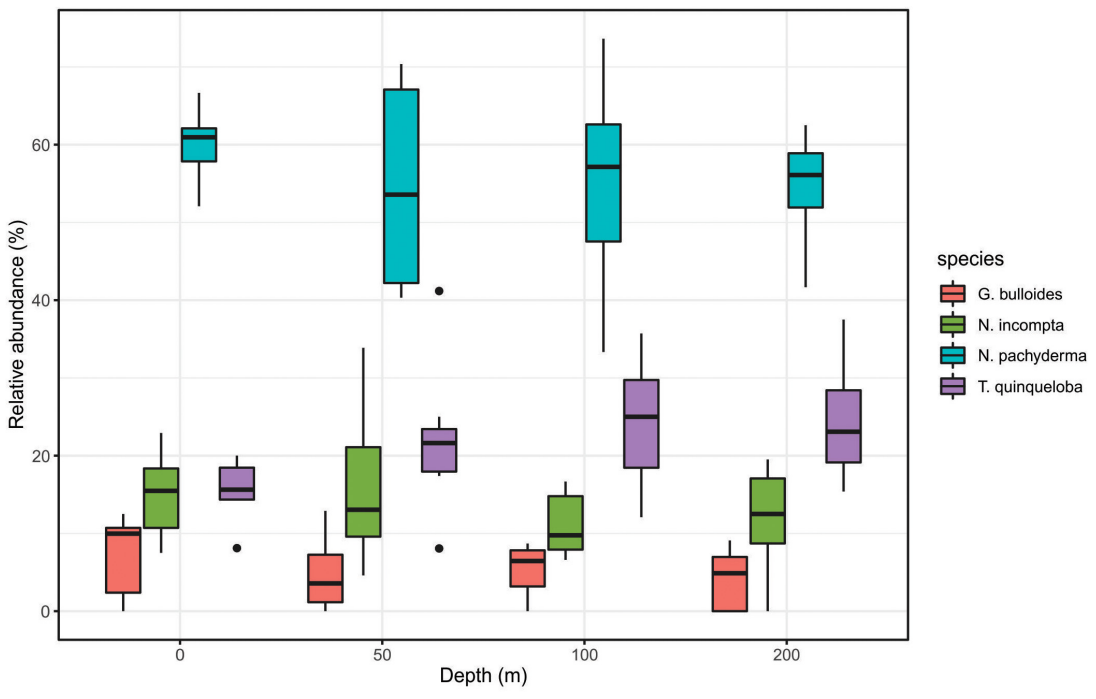

FIGURE 6 | Relative (%) species distribution of planktic foraminifera relative to water depth.

TABLE 4 | Cumulative and absolute abundance (ind m^{-3}) and relative abundance of the main species.

	Cumulative absolute abundance	water depth	Absolute abundance foraminifera	*N. pachyderma*	*T. quinqueloba*	*N. incompta*	*G bulloides*	unknown	Absolute abundance pteropods	*L. helicina*	*L. retroversa*
ST 1	10.09	0–50	**2.3**	61.9	19.0	9.5	9.5	0.0	**11.4**	100	0.00
		50–100	**10.4**	40.3	8.1	33.9	12.9	4.8	**0.6**	100	0.00
		100–200	**8.9**	43.5	30.4	8.7	8.7	8.7	**0.8**	100	0.00
		200–300	**5.8**	53.8	23.1	15.4	0.0	7.7	**0.2**	100	0.00
ST 2	15.79	0–50	**11.3**	57.1	14.3	14.3	0.0	14.3	**6.2**	100	0.00
		50–100	**18.3**	70.4	18.5	7.4	3.7	0.0	**5.7**	97.26	2.74
		100–200	**13.0**	57.1	35.7	7.1	0.0	0.0	**0.4**	100	0.00
		200–300	**7.6**	62.5	25.0	12.5	0.0	0.0	**0.7**	100	0.00
ST 3	16.81	0–50	**5.2**	62.2	8.1	18.9	10.8	0.0	**10.3**	94.17	5.83
		50–100	**21.4**	41.2	41.2	11.8	0.0	5.9	**10.3**	97.69	2.31
		100–200	**10.9**	66.7	12.5	16.7	4.2	0.0	**0.4**	100	0.00
		200–300	**8.4**	41.7	37.5	8.3	0.0	12.5	**0.4**	100	0.00
ST 4	32.72	0–50	**5.5**	52.1	14.6	22.9	10.4	0.0	**6.0**	100	0.00
		50–100	**34.5**	69.0	21.8	4.6	2.3	2.3	**1.8**	100	0.00
		100–200	**52.6**	73.6	12.1	6.6	2.2	5.5	**0.3**	100	0.00
		200–300	**29.4**	50.0	31.8	9.1	9.1	0.0	**0.9**	100	0.00
ST 5	19.11	0–50	**3.7**	66.7	16.7	16.7	0.0	0.0	**10.2**	100	0.00
		50–100	**10.7**	43.2	21.6	24.3	10.8	0.0	**12.5**	100	0.00
		100–200	**24.8**	51.6	29.0	12.9	6.5	0.0	**0.2**	100	0.00
		200–300	**14.1**	56.1	19.5	19.5	4.9	0.0	**0.3**	100	0.00
ST 6	19.70	0–50	**3.5**	60.0	20.0	7.5	12.5	0.0	**21.3**	99.29	0.71
		50–100	**17.7**	65.2	17.4	13.0	0.0	4.3	**6.5**	100	0.00
		100–200	**15.4**	33.3	25.0	16.7	8.3	16.7	**0.8**	100	0.00
		200–300	**10.7**	61.5	15.4	0.0	7.7	15.4	**2.9**	100	0.00
ST 7	17.99	0–50									
		50–100	**22.0**	53.6	25.0	17.9	3.6	0.0	**2.0**	100	0.00
		100–200	**19.7**	58.5	24.4	9.8	7.3	0.0	**0.1**	100	0.00
		200–300	**9.8**	56.3	18.8	18.8	6.3	0.0	**0.4**	100	0.00

The bold was used to differenciate the total absolute abundance to the species relative abundance.

organic standing stocks and production ranged from 18.6 to 142.5 μg m^{-3}, and from 2.0 to 73.9 mg m^{-2} day^{-1}.

Shelf

On the shelf, the absolute abundance of planktic foraminifera and pteropods increases from west (station 1, 12.3 ind m^{-3} from 0–100 m and 11 ind m^{-3} from 50–100 m) to east (station 2, 20.7 ind m^{-3} from 0–100 m and 24 ind m^{-3} from 50–100 m) (**Figure 3** and **Tables 5**, **6**).

The westernmost station 1 is where we find the lowest abundance of planktic foraminifera of all the stations in the transect (6.4 ind m^{-3} and 10.4 ind m^{-3}, from 0–100 m and 50–100 m, respectively) (**Figure 3** and **Tables 5**, **6**). Thus, we estimate the lowest foraminiferal inorganic (10.6 μg $CaCO_3$ m^{-3}) and organic (1.9 μg m^{-3}) carbon standing stocks and inorganic (2.3 mg m^{-2} day^{-1}) and organic (0.5 mg m^{-2} day^{-1}) export production (**Tables 5**, **6**). Moreover, the lowest pteropod production (6.1 mg $CaCO_3$ m^{-2} day^{-1} and 2.0 mg m^{-2} day^{-1} of organic carbon) is estimated at this westernmost shelf station causing the lowest inorganic carbon (8.4 mg m^{-2} day^{-1}) and carbon (2.4 mg m^{-2} day^{-1}) export production in our transect (**Table 6**).

Slope

Over the slope, the integrated abundances of planktic foraminifera and pteropods in the upper 100 m are highest at stations 3, 4 and 6 (23.6–24.5 ind m^{-3}) (**Figure 3** and **Table 5**). The vertically integrated abundance of planktic foraminifera is highest at the westernmost station 4 (20 ind m^{-3}) while pteropods, increase from west (station 4, 3.9 ind m^{-3}) to east (station 6, 13.9 ind m^{-3}) (**Figure 3** and **Table 5**).

At the same time, the abundances of planktic foraminifera and pteropods at the subsurface (50–100 m) decrease from west (stations 3 and 4, 31.7 ind m^{-3} and 36.3 ind m^{-3}) to east (stations 5 and 6, 23.3 ind m^{-3} and 24.2 ind m^{-3}) (**Figure 3** and **Table 6**). The highest inorganic (459.5 μg $CaCO_3$ m^{-3}) and organic (146.2 μg m^{-3}) standing stocks and inorganic (231.3 mg $CaCO_3$ m^{-2} day^{-1}) and organic (74.6 mg m^{-2} day^{-1}) export production are found at slope station 3 (**Tables 5**, **6**).

TABLE 5 | Integrated (upper 100 m) absolute abundance (m^{-3}) and derived $CaCO_3$ standing stocks ($\mu g\ m^{-3}$) and carbon biomass ($\mu g\ m^{-3}$) and the contribution from planktic foraminifera and pteropods.

	Integrated abundance (m^{-3})	$CaCO_3$ ($\mu g\ m^{-3}$)	Carbon biomass ($\mu g\ m^{-3}$)	Foraminifera abundance (m^{-3})	Foraminifera $CaCO_3$ ($\mu g\ m^{-3}$)	Foraminifera C biomass ($\mu g\ m^{-3}$)	Pteropod abundance (m^{-3})	Pteropod $CaCO_3$ ($\mu g\ m^{-3}$)	Pteropod C biomass ($\mu g\ m^{-3}$)
Station 1	12.3	140.1	44.0	6.4	10.6	1.9	6.0	129.5	42.0
Station 2	20.7	171.6	52.3	14.8	23.2	4.2	6.0	148.4	48.1
Station 3	23.6	459.5	146.2	13.3	20.3	3.6	10.3	439.2	142.5
Station 4	23.9	111.8	31.5	20.0	33.1	6.0	3.9	78.7	25.6
Station 5	18.6	161.6	50.5	7.2	13.8	2.6	11.4	147.8	48.0
Station 6	24.5	269.1	84.5	10.6	20.8	3.9	13.9	248.3	80.6
Station 7*	23.9	86.4	24.8	22.0	29.2	6.2	2.0	57.3	18.6

**The surface sample of the Nansen Basin station 7 was missing, therefore the values presented here are considering only the subsurface samples.*

TABLE 6 | Absolute abundance (m^{-3}) from 50 to 100 m and derived $CaCO_3$ export production ($mg\ m^{-2}\ d^{-1}$) and carbon biomass ($mg\ m^{-2}\ d^{-1}$) and the contribution from planktic foraminifera and pteropods.

	Abundance (m^{-3})	$CaCO_3$ ($mg\ m^{-2}\ d^{-1}$)	Carbon biomass ($mg\ m^{-2}d^{-1}$)	Foraminifera abundance (m^{-3})	Foraminifera $CaCO_3$ ($mg\ m^{-2}\ d^{-1}$)	Foraminifera C biomass ($mg\ m^{-2}d^{-1}$)	Pteropod abundance (m^{-3})	Pteropod $CaCO_3$ ($mg\ m^{-2}\ d^{-1}$)	Pteropod C biomass ($mg\ m^{-2}\ d^{-1}$)
Station 1	11.0	8.4	2.4	10.4	2.3	0.5	0.6	6.1	2.0
Station 2	24.0	73.4	23.4	18.3	3.3	0.7	5.7	70.1	22.8
Station 3	31.7	231.3	74.6	21.4	3.7	0.7	10.3	227.6	73.9
Station 4	36.3	18.1	4.9	34.5	7.9	1.6	1.8	10.3	3.3
Station 5	23.3	31.5	9.7	10.7	4.1	0.8	12.5	27.4	8.9
Station 6	24.2	84.3	26.1	17.7	7.2	1.1	6.5	77.1	25.0
Station 7	23.9	29.6	9.0	22.0	4.9	1.0	2.0	24.7	8.0

Basin

In the basin station the surface sample was missing, therefore we only have subsurface data (50–100 m) to estimate the standing stocks and production. This station shows high concentration of planktic foraminifera (22 ind m^{-3}) and a negligible concentration of pteropods (2 ind m^{-3}) (**Figure 3** and **Table 4**). We estimate here the lowest total inorganic (86 $\mu g\ m^{-3}$) and organic (24.8 $\mu g\ m^{-3}$) carbon standing stock in our transect and a relatively low inorganic (29.6 $mg\ m^{-2}\ day^{-1}$) and organic (9 $mg\ m^{-2}\ day^{-1}$) carbon export production (**Tables 5**, **6**).

DISCUSSION

Vertical Distribution

In this particular area and time of the year, the absolute abundance of planktic foraminifera is higher below 50 m depth correlating in high salinity water ($\approx$ 35), while pteropods are more abundant at the surface, when salinity is lower than 34.5 (**Table 3**, **Figures 3–5**, and **Supplementary Tables 1**, **2**). There is no clear correlation between the distribution of planktic foraminiferal abundance and depth in the water column ($R = 0.11$), while it correlates well with the carbonate chemistry in the water column of total alkalinity ($p < 0.01$), DIC ($0.05 > p > 0.01$), Ω_{CA} ($0.1 > p > 0.05$), salinity ($0.1 > p > 0.05$), and water mass density ($0.05 > p > 0.01$) (**Table 7**). The distribution of pteropods is significantly correlated ($p < 0.01$) to depth in the water column, and all parameters from the carbonate water chemistry (AT, DIC, pH, pCO_2 and Ω_{AR}), salinity and water mass density (**Table 7**). This close correlation between pH or Ω_{AR}, and the distribution of pteropods (low abundance of pteropods correlate with low values of pH and Ω_{AR}) (**Table 7**) could possibly be a cause of effects of ocean acidification. However, since carbonate chemistry also correlate strongly with depth ($p < 0.01$) this is probably a causal relationship (one variable having a direct influence on another variable). Further studies on a seasonal basis covering at least one year are thus needed to understand the eventual effects of ocean acidification in the area.

The distribution of foraminiferal specimens among the different size fractions does not vary between the different depth intervals on a statistically significant basis (**Figure 4**). It is important to stress that this might be biased by the wide size fractions we are working with (most of the populations belongs to the size fractions between 90–250 μm) and by the very low numbers of foraminifera systematically found in the size classes >250 μm. As previously reported from the Arctic region, almost no foraminifera has been found in the 250–500 μm size fraction and none >500 μm (Carstens and Wefer, 1992; Carstens et al., 1997) similar to our study.

As also reported for the central Barents Sea and eastern Fram Strait (Carstens et al., 1997; Manno and Pavlov, 2014; Pados and Spielhagen, 2014; Ofstad et al., 2020), the highest concentration of planktic foraminifera occurs between 50–100 m

TABLE 7 | Correlation table between environmental parameters, carbonate chemistry and distribution of planktic foraminifera and pteropods.

	depth	AT	DIC	pH	pCO2	Ω_{CA}	Ω_{AR}	Salinity	Temperature	Density
AT	0.53***									
DIC	0.69***	0.94***								
pH	−0.72***	−0.83***	−0.95***							
pCO2	0.65***	0.83***	0.93***	−0.99***						
Ω_{CA}	−0.83***	−0.73***	−0.92***	0.92***	−0.88***					
Ω_{AR}	−0.83***	−0.72***	−0.91***	0.91***	−0.87***	1***				
Salinity	0.65***	0.96***	0.96***	−0.93***	0.93***	−0.82***	−0.81***			
Temperature	−0.18	0.23	0.08	−0.23	0.31	0.16	0.17	0.29		
Density	0.74***	0.92***	0.98***	−0.9***	0.86***	−0.91***	−0.91***	0.95***	−0.03	
Foraminifera	0.11	0.5***	0.43**	−0.32	0.3	−0.37*	−0.37**	0.37*	−0.28	0.46**
Pteropods	−0.66***	−0.61***	−0.69***	0.64***	−0.6***	0.73***	0.73***	−0.65***	0.3	−0.74***

*$0.1 > p > 0.05$; **$0.05 > p > 0.01$; ***$p < 0.01$.

and 100–200 m water depth correlating with water masses of Atlantic origin (**Figure 3**). At the same time, the abundance range presented here (7–34 ind m^{-3}) agrees well with previous results reporting between 3 and 29 ind m^{-3} in the early summer at the Fram Strait (Pados and Spielhagen, 2014). However, the abundances presented in our study are generally lower than previously reported abundances from the central Barents Sea for early summer (12–436 ind m^{-3}) (Ofstad et al., 2020) and in the western Barents Sea for late summer (0–400 ind m^{-3}) (Meilland et al., 2020). The discrepancy could be caused by seasonality and/or differences in environmental conditions (higher sea surface temperature and higher surface salinity) and regime (Atlantic), confirmed by dominance of Atlantic or sub-polar species (mainly *T. quinqueloba*) in these more southerly locations than in our study area in the north. In addition, the stations in the central Barents Sea are affected by methane seepage, which may have contributed to the higher concentrations and productivity (Ofstad et al., 2020). Methane seepage have been considered as areas of increased primary productivity [Ofstad et al. (2020) and referenced therein]. However, in both the central Barents Sea and northern Svalbard margin, planktic foraminifera show similar vertical distribution patterns in the water column. Considering the differences in sampling time (day/night), foraminiferal distribution in the study area seems to not be affected by diurnal vertical migration [as also reported by Ofstad et al. (2020)] and as reported from the subtropical North Atlantic (Meilland et al., 2020). This agrees with previous studies reporting no evidence of diel vertical migration in the Fram Strait of *N. pachyderma* and *T. quinqueloba* during the midnight-sun season (Manno and Pavlov, 2014) and in the Arctic and North Atlantic of *N. pachyderma* (Greco et al., 2019).

Medium-sized pteropods (>250 μm) dominate the upper 100 meters of the water column and are scarcely present at depth below 200 m (**Figures 4**, **5**). The absolute abundance of pteropods is generally higher between 0 and 50 m water depth in summer in the central Barents Sea, as previously reported by Ofstad et al. (2020). This pattern is also observed in other polar regions (Indian sector of the Antarctic Ocean) where over 90% of *L. helicina* were found in the upper 100 m of the water column (Akiha et al., 2017). Pteropods are concentrated in the upper water column at night [Fabry (1989) and references therein]. Specifically in the Arctic, patterns of diurnal vertical migrations of the pteropod *L. helicina* have been observed during autumn (Falk-Petersen et al., 2008). Adults of *L. helicina* are able to descend to deep waters during the day and ascend to the surface during the night to avoid predation, mainly from cods (Falk-Petersen et al., 2008). However, the negligible concentrations (average < 15% of the total assemblage) found in our study below 100 m do not follow any particular pattern regarding the presence or absence of light and the sampling time.

Species Distribution – Relative Abundance

In summer in the Fram Strait, Pados and Spielhagen (2014) attributed the distribution of the polar species *N. pachyderma* to polar water masses [characterized by lower temperature, pH and $CaCO_3$ saturation (Shadwick et al., 2013)] and the sub-polar species *T. quinqueloba*, to the Atlantic water masses (characterized by higher pH and $CaCO_3$ saturation). The polar species *N. pachyderma* thus might be more resistant and/or better adapted to waters with lower pH and $CaCO_3$ saturation than the subpolar species *N. incompta*, *T. quinqueloba* and *G. bulloides*. The highest integrated vertical concentration of planktic foraminifera and pteropods (32.72 ind m^{-3}) (from 0 to 300 m depth) is found at slope station 4 (**Table 4**). This station is crossed by the Atlantic current which brings warm and nutrient rich waters to the Arctic Ocean and an influx of various planktic organisms [Hop et al. (2019) and references therein] (**Figure 1**). This station is also characterized by a high surface pH (8.2) and a relatively high Ω_{CA} and Ω_{AR} typical for the Atlantic water mass (**Figure 2**). The integrated upper 300 m concentration from this station is caused by the high concentrations of planktic foraminifera and pteropods found between 100 and 200 m (**Figure 3**). This depth range, characterized by relatively cold Atlantic Water (2°C), is dominated by foraminifera in the size fractions between 90–250 μm (**Figure 5**). The dominant species are *N. pachyderma* and *N. incompta*. The presence of other warmer water species such as *T. quinqueloba* and *G. bulloides* (**Table 4**) might be indicative of a highly productive

environment and high food availability (Volkmann, 2000). The lowest integrated vertical concentrations of foraminifera and pteropods (10.09 ind m^{-3}) are found at shelf station 1, the westernmost station. The station, which also records the lowest abundances at each depth, is dominated by small specimens (90–100 μm) of *N. pachyderma*. The low abundances of warmer water species recorded at this station from surface to 300 m, which are the lowest found in the whole transect, might be indicative of low productivity and food availability and no input from warmer waters, which in general correlate with low concentrations of marine calcifiers.

The high proportion of both the polar species *N. pachyderma* and the subpolar species *T. quinqueloba* at the northern Svalbard margin agrees well with results reported in previous studies from the Fram Strait (Carstens et al., 1997; Volkmann, 2000; Husum and Hald, 2012; Manno and Pavlov, 2014; Pados and Spielhagen, 2014) and Nansen Basin (Carstens and Wefer, 1992). However, studies in the Arctic Ocean from plankton tows and sediment reconstructions from the Holocene reported a monospecific faunal assemblage consisting of *N. pachyderma* [Bauch (1999) and references therein]. In our study the highest relative abundance of *N. pachyderma* usually occurs in the upper 100 m of the water column. The distribution observed here agrees with a previous study at high northern latitudes reporting that *N. pachyderma* is found all along the upper water column, but being most abundant in the subsurface below 50 m (Greco et al., 2019). Thus, *N. pachyderma* does not behave as a deep-dweller species [as reported for high latitudes by Kohfeld et al. (1996) and references therein] and as previously observed in the Sea of Okhotsk (Bauch et al., 2002). The depth of calcification of this species has been reported to be between 25 to 70 m in the western part of the Fram Strait (Simstich et al., 2003). The depth of calcification is thought to be related to their optimum habitat and environmental conditions [Weinkauf et al. (2016) and references therein]. The relative abundance of *N. pachyderma* presented here (average: 55.9%; range 33–74%) is lower than the percentages reported recently in the Fram Strait (76–90%) (Pados and Spielhagen, 2014). Here, the highest percentages (90%) of *N. pachyderma* were found at sea-ice covered stations, where a higher absolute abundance was found as well (Pados and Spielhagen, 2014). Thus, we can possibly attribute our lower values to the absence of sea ice in our sampling area. The highest relative abundance of *T. quinqueloba* is found between 100 and 200 m below the surface (**Figure 6**). In the Barents Sea in general, it prefers the deeper waters between 100 and 200 m and areas influenced by relatively warm Atlantic waters (Volkmann, 2000). This species dominates (>80%) the faunal composition in the south-western Svalbard margin, followed by *N. pachyderma* (>10%) and *G. uvula* and *N. incompta* (<5%) (Zamelczyk et al., 2020). The relative abundance of *T. quinqueloba* found in this transect (average: 21.7%; range 8–41%) surpass previous values reported from the Fram Strait (5–23%) (Pados and Spielhagen, 2014). As suggested by the authors, the maximum productivity of this species is expected to occur in early autumn (Pados and Spielhagen, 2014), which was the time when our samples were collected.

The relative abundance of *N. incompta* observed in our samples (average: 13.5%; range 7–34%) exceeds the values that have been published before. In the Fram Strait, Pados and Spielhagen (2014) reported that this species contributed, together with *G. bulloides*, less than 9% of the total assemblage. Also, a recent study observed an average percentage of *N. incompta* of 1% in June 2016 along a transect in the central Barents Sea (Ofstad et al., 2020). In the central Barents Sea, the relative abundances of subarctic species such as *N. incompta*, are increasing compared to preindustrial records (Jonkers et al., 2019; Meilland et al., 2020; Ofstad et al., 2020). The higher relative abundances observed can be a result of the so-called 'Atlantification.' This process is caused by an increasing influence (both in volume and heat) of warm Atlantic water inflow (Årthun et al., 2012). Moreover, the seasonal difference might be a factor affecting the relative abundances of this species, where the June samples in the central Barents Sea [Ofstad et al. (2020) would be recording spring characteristics], whereas September, represents late summer or early fall. In addition, the northern Svalbard margin could be more affected by the Atlantic inflow and to the 'Atlantification' processes than the central Barents Sea. A previous study conducted in the same area north of Svalbard has reported the presence of tropical adiolarian associated with an episode of strong and warm Atlantic inflow (Bjørklund et al., 2012).

Earlier studies of planktic foraminiferal faunas collected by plankton tows in the Arctic Ocean have reported absence of *G. bulloides* (Volkmann, 2000). However, it has been suggested that this species can be transported sporadically to the Arctic Ocean by the Atlantic water masses (Volkmann, 2000). In our study, we attribute the presence and relatively high concentrations of living *G. bulloides* (average: 5.2%; range < 12.9%) and of *N. incompta*, to an 'Atlantification' process.

It is noteworthy that we only considered living specimens (containing cytoplasm) of planktic foraminifera and pteropods, thus our results suggest that certain subpolar planktic foraminferal and pteropod species can survive in this high-Arctic environment, probably as long as 'Atlantic' conditions prevail.

A recent study by Kacprzak et al. (2017) have reported pteropod abundances from both Arctic and Atlantic water masses in the Nordic Seas. They found absolute abundances of *L. helicina* ranging from 0.056 to 12 ind m^{-3} and *L. retroversa* from 0.002 to 52 ind m^{-3}. The highest abundance of *L. helicina*, which is comparable to our results (1.6–5.9 ind m^{-3}), were found in Arctic water (Kacprzak et al., 2017). The high abundance of *L. retroversa* reported by Kacprzak et al. (2017) is indicative of an Atlantic-influenced environment. The presence of the subpolar pteropod *L. retroversa* at slope stations 3, 4 and 6 could be interpreted as a stronger influence of the warmer Atlantic waters on the northern Svalbard margin. An increase in the Atlantic water inflow was observed in this area between summer and late fall of 2018 (Kolås et al., 2020).

Biogenic Carbonate Standing Stocks and Export Production

The organic-inorganic carbon ratio (C_{ORG}/C_{INORG}) from planktic foraminifera and pteropods is estimated to be between

0.28 and 0.32 (**Tables 8**, **9**). Thus, the inorganic carbon from planktic foraminifera and pteropods represents between 76 and 79% of the total carbon they generate (relative to the sum of estimated organic and inorganic carbon) (**Tables 8**, **9**). The inorganic contribution (76%) of pteropods is lower than the foraminiferal contribution (82−87%) (**Tables 8**, **9**). This agrees well with results from other polar regions where foraminiferal inorganic carbon represents between 67 and 85% of the total carbon (Meilland et al., 2018). Hence, we focus the discussion on the inorganic standing stocks and export production from the planktic foraminifera and pteropods.

Despite the higher absolute abundances of planktic foraminifera in the upper 100 m of the water column (**Figures 3**, **5**), pteropods contribute 66–96% to the inorganic carbon standing stocks compared to 4–34% by the planktic foraminifera (**Table 8**). This suggests that the estimates of inorganic carbon standing stocks largely depends on the size of the organisms. In this study, the foraminiferal test size is smaller than pteropods from the same size fraction on average (**Table 2**). Moreover, negligible abundances of planktic foraminifera are found in the larger size fractions, with few individuals in the size fraction 250–500 μm and none >500 μm (**Figure 5**). The inorganic carbon standing stocks and flux (export production) reported in the present study are derived from living individuals; hence there could be an underestimation. Considering empty shells of dead individuals could lead to larger standing stocks and production values.

The highest inorganic carbon standing stocks in the upper 100 m of the water column (shelf station 2 and slope stations 3 and 6) are the stations where large pteropods (>500 μm) show high abundances (0.6–5.7 ind m^{-3}) (**Table 8** and **Figure 5**). In these stations we also find the subpolar species *L. retroversa* (**Table 4**) and the highest influence of Atlantic Water. The lowest inorganic carbon standing stock (basin station 7) is where the contribution of pteropods is the lowest (66.6%) (**Table 8**). This station is only represented by the subsurface samples (due to loss of the surface sample 0–50 m), therefore this value is most probably an underestimation.

The highest standing stocks of foraminifera are found at slope station 4 and basin station 7 (**Table 8**), where the lowest surface temperatures and salinities are found (2.76°C and 33.77; 1.15°C and 32.94, respectively). However, the values from station 7 could be overestimated because of the loss of the surface sample 0–50 m. The highest standing stocks from pteropods are found at the slope station 3, with relatively cold and fresh surface waters (T < 3° C and S < 34). The lowest standing stocks from pteropods are found at the slope station 4 and basin station 7, which are strongly influenced by low surface salinity from melting sea ice (33.77 and 32.94, respectively). However, the lower standing stocks from pteropods found at station 7 could be an underestimation. As previously discussed, in general pteropods are more abundant from 0 to 50 m depth and this sample is missing.

The absolute abundances found between 50 and 100 m depth are mainly from planktic foraminifera (38.8–91.8%), rather than pteropods (8.2–61.2%). Even though the inorganic carbon flux estimates come from those abundances, pteropods contribute significantly more (56.7–98.4%) to the total inorganic carbon export production than the planktic foraminifera (1.6–43.4%)

TABLE 8 | Total, and foraminiferal and pteropod organic:inorganic carbon ratio, foraminifera and pteropod inorganic contribution to the total carbon and foraminifera and pteropod inorganic contribution to the total inorganic standing stocks.

	Total OC:IC	Foraminifera OC:IC	Foraminifera IC/TC (%)	Pteropod OC:IC	Pteropod IC/TC (%)	Foraminifera/total CaCO3 (%)	Pteropod/total CaCO3 (%)
Station 1	0.3	0.2	84.8	0.3	75.5	7.6	92.4
Station 2	0.3	0.2	84.7	0.3	75.5	13.5	86.5
Station 3	0.3	0.2	84.9	0.3	75.5	4.4	95.6
Station 4	0.3	0.2	84.7	0.3	75.5	29.6	70.4
Station 5	0.3	0.2	84.1	0.3	75.5	8.5	91.5
Station 6	0.3	0.2	84.2	0.3	75.5	7.7	92.3
Station 7*	0.3	0.2	82.5	0.3	75.5	33.8	66.3

**The surface sample of the Nansen Basin station 7 was missing, therefore the values presented here are considering only the subsurface samples.*

TABLE 9 | Total, and foraminiferal and pteropod organic:inorganic carbon ratio, foraminifera and pteropod inorganic contribution to the total carbon and foraminifera and pteropod inorganic contribution to the total inorganic export production.

	Total OC:IC	Foraminifera OC:IC	Foraminifera IC/TC (%)	Pteropod OC:IC	Pteropod IC/TC (%)	Foraminifera/total CaCO3 (%)	Pteropod/total CaCO3 (%)
Station 1	0.3	0.2	82.1	0.3	75.3	27.4	72.6
Station 2	0.3	0.2	82.5	0.3	75.5	4.5	95.5
Station 3	0.3	0.2	84.1	0.3	75.5	1.6	98.4
Station 4	0.3	0.2	83.2	0.3	75.7	43.6	56.9
Station 5	0.3	0.2	83.7	0.3	75.5	13.0	87.0
Station 6	0.3	0.2	86.7	0.3	75.5	8.5	91.5
Station 7	0.3	0.2	83.1	0.3	75.5	16.6	83.4

(**Table 9**). The high contribution of pteropods agrees with a previous study reporting that pteropods represents between 60 and 100% of the vertical productivity of calcium carbonate in autumn in the Lofoten Basin in the Norwegian Sea (Drits et al., 2020), and between 55 and 83% in the northern Scotia Sea (Manno et al., 2018). The highest inorganic carbon export production (slope stations 3 and 6 and shelf station 2) are the stations where pteropods contribute the most (91–98%), whereas the lowest (shelf station 1 and slope station 4), they contribute 56–72% (**Table 9**). The highest inorganic carbon flux at slope station 3 is caused by a relatively high abundance (7.8 ind m^{-3}) of pteropods >500 μm between 50 and 100 m compared to the other stations (0.008–1.96 ind m^{-3}). Even though the highest inorganic carbon standing stocks and flux are found at the same stations, they are not directly proportional to one another (**Tables 5**, **6**). This is particularly true for shelf station 2 and slope station 6. The differences between the standing stocks and the flux at stations 2 and 6 are caused by the greater abundances of large specimens in the size fraction 250–500 μm at station 6 compared to station 2, which is dominated by individuals <100 μm.

Only few studies have reported the contribution of planktic foraminifera and pteropods to the inorganic carbon budgets and production from plankton tows (Bednaršek et al., 2012a; Buitenhuis et al., 2013). In these studies, there are no agreement about the mesh-size used (100, 150, 180, 200, 300, and 333 μm) or the sampling depth (upper 200, upper 300 m or to the bottom), which influences the size and abundance of organisms captured by the nets (Bednaršek et al., 2012a). In any of these studies, authors combine data of planktic foraminifera and shelled pteropods in the northern Svalbard margin. Thus, in order to be able to compare the standing stocks and flux of these organisms, it is important to standardize the sampling strategy.

A polar study (Meilland et al., 2018) has reported planktic foraminiferal standing stocks of 205.05–618.9 μg m^{-3} and flux of 25.16–92.03 mg m^{-2} day^{-1} along the southern Polar Front (between 50 and 60°S). Recently, it has been reported that Arctic foraminiferal shells are heavier (containing more calcite) and thicker than the specimens inhabiting the Antarctic and Sub-Antarctic sector (Schiebel et al., 2017). However, the average foraminiferal shell weights estimated from the northern Svalbard margin reported in our study (on average 6.68 μg from the 250–500 μm size fraction and 2.22 μg from the 100–250 μm size fraction) agrees well with the shell weights reported from the Sub-Antarctic (Meilland et al., 2018). Nevertheless, the difference on the mesh size used to sample [100 μm in Meilland et al. (2018)] could influence the size distribution, collecting larger individuals and, therefore, likely heavier individuals. We combine the weight of 257 planktic foraminiferal specimens following the equations published in Meilland et al. (2018). These equations, based on specimens from the sub-Antarctic, lead to an estimated mass of 6.77 μg (250–500 μm), 1.71 μg (100–250 μm), and 0.46 (90–100 μm). Hence, we might be inducing just a negligible bias on our estimates.

In case of the shelled pteropods, Bednaršek et al. (2012a) reviewed published abundance and biomass data from all over the world. Abundances of 10.87 and 18.52 ind m^{-3} from veligers (250–500 μm) and adults of *L. helicina* with an associated biomass of 0.27 and 11.11 mg m^{-3}, respectively, were reported in the Northern Barents Sea (Blachowiak-Samolyk et al., 2008). Highest values were recorded over the Western Svalbard margin while the lowest values were obtained closer to our sampling area. However, those values are difficult to compare because of the different mesh size used [90 μm in our study compared to 180 μm in Blachowiak-Samolyk et al. (2008)].

Ocean Acidification Perspectives

The Arctic Ocean in general is expected to be a 'hotspot' of ocean acidification (Orr et al., 2005; Sugie et al., 2020). Indeed, Chierici et al. (2019) estimated continued CO_2 uptake by the ocean at the West Spitsbergen shelf and on the slope north of Svalbard. With the effect of ocean acidification, the planktic foraminifera and pteropods shells are expected to be more fragile, to produce thinner and smaller shells, require more energy to clacify, and to be prone to dissolution (Moy et al., 2009; Bednaršek et al., 2012b; Manno et al., 2018). Lower shell weights and, therefore, lower test sinking velocity associated with each size fraction, could result in decreased carbonate standing stocks and export production from these marine calcifiers. The impact of ocean acidification to their calcification process and the lower export of their inorganic shells to the sea floor are expected to alter the carbonate compensation depth in the near future and, when less of these shells dissolve, decrease the carbonate ion concentration on the longer term [Middelburg et al. (2020) and references therein]. Ultimately, a decrease in sinking velocity, would affect the inorganic carbon pump turning it less effective (Bednaršek et al., 2014). Experiments show that exposing *L. helicina antarctica* to an aragonite saturation state (Ω_{AR}) of 0.8 for 100 days, would reduce the shell weight by half and reduce its sinking velocity proportionally [Bednaršek et al. (2014) and references therein]. A previous experiment reported that ocean acidification would decrease the terminal sinking velocity of the subpolar *L. retroversa* after being maintained at medium (800 μatm) and high (1200 μatm) controlled levels of CO_2 (Bergan et al., 2017). *Limacina retroversa* is more able to tolerate wider ranges of temperature (2.0–7.0°C) and salinity (30.1–36.0) than *L. helicina*, thus the former species could have more chance to survive in a warning climate than the latter (Manno et al., 2012).

Pteropods with shells built of aragonite, are more susceptible to dissolution than organisms with shells of calcite, and are expected to be more vulnerable toward changes in the seawater carbonate chemistry. Due to their high vulnerability and contribution to the inorganic standing stocks and productivity, ocean acidification might have considerable and unpredicted effects on the standing stocks and export production in the northern Svalbard shelf and Arctic deep basin.

CONCLUSION

In the northern Barents Sea and Svalbard margin, the vertical distribution patterns of planktic foraminifera and shelled pteropods, not affected by diurnal vertical migration, show a clear depth zonation. Large (>500 μm) and medium sized (250–500 μm) pteropods dominate in the upper 50 m of the water column. In general, no pteropods were found below 100 m depth. Both medium sized (100–250 μm) and

small sized (90–100 μm) foraminifera dominate from 50 to 300 m depth. The foraminiferal community is dominated by the polar species *Neogloboquadrina pachyderma* (33–67%), the subpolar species *Turborotalita quinqueloba* (6–32%) and *Neogloboquadrina incompta* (8–34%). The pteropod community is largely dominated by *Limacina helicina* (>94.2%). Based on our data we attribute the increase in subpolar species of foraminifera (*N. incompta* and *T. quinqueloba*) and pteropods (*L. retroversa*) to the "Atlantification" process.

Despite their lower abundance, the estimated contribution of shelled pteropods to late summer inorganic carbon standing stocks and export production drastically exceeds the contribution of planktic foraminifera. The inorganic standing stocks and export production from pteropods represent 66.6–96.5 and 56.7–98−4% of the total inorganic carbon, respectively. The organic standing stocks and export production from pteropods, represent 75.0 – 97.5 and 67.4–99.1% of the total organic carbon, respectively. The sensitivity of their shells toward changes in the environment should be considered when predicting how ocean acidification might affect the carbonate standing stocks and fluxes. Due to the lack of seasonal sampling, it is difficult to estimate the pelagic production, budgets and fluxes that would reflect the annual variability.

The combined potential effect of ocean acidification and "Atlantification" in the Barents Sea remains poorly understood. "Atlantification" processes could lead to a dominance of subpolar species, higher abundances and productivity and larger shells. In contrast, ocean acidification is expected to make the shells of calcifiers more fragile and affect their growth, thus reducing their contribution to the inorganic carbon cycle. In the future one could therefore expect that subpolar species increase their relative abundance, but decrease their shell thickness and size, since subpolar species might be less adapted to low pH.

DATA AVAILABILITY STATEMENT

The raw data supporting the conclusion of this article will be made available by the authors, without undue reservation.

AUTHOR CONTRIBUTIONS

GA-O analyzed the plankton samples, calculated standing stocks and production, and drafted the manuscript. TR contributed with cruise data, samples and finances, and original research plan. The study was designed by TR, GA-O, PZ, KZ, and JM. KZ contributed to the species identification. JM and PZ contributed to the standing stocks and production part of the study. JM contributed to the statistical analyses. MC and AF performed the carbonate chemistry analyses. The manuscript was finalized with contributions from GA-O, KZ, JM, PZ, MC, AF, and TR. All authors contributed to the article and approved the submitted version.

FUNDING

The study was carried out as part of the Research Council of Norway through the project "The Nansen Legacy" (RCN #276730) and partly within the framework of the Flagship research program "Ocean Acidification and effects in northern waters" within the FRAM – High North Research Centre for Climate and the Environment at the Norwegian Polar Institute, Norway. This work was also supported by the Centre for Arctic Gas Hydrate, Environment and Climate (CAGE), the Research Council of Norway through its Centers of Excellence scheme (Grant #223259) and CALMED (#CTM2016-79547-R) projects of the Spanish Ministry of Science and Innovation, and the Generalitat de Catalunya MERS (#2017 SGR-1588).

ACKNOWLEDGMENTS

We are grateful to the captain and crew from RV Helmer Hansen and all cruise participants, especially S. Ofstad and N. El bani Altuna for collecting the samples. We also thank the AMGG (Arctic Marine Geology and Geophysics) Research School for supporting the cruise.

SUPPLEMENTARY MATERIAL

The Supplementary Material for this article can be found online at: https://www.frontiersin.org/articles/10.3389/fmars.2021.661158/full#supplementary-material

REFERENCES

Akiha, F., Hashida, G., Makabe, R., Hattori, H., and Sasaki, H. (2017). Distribution in the abundance and biomass of shelled pteropods in surface waters of the Indian sector of the Antarctic Ocean in mid-summer. *Polar Sci.* 12, 12–18. doi: 10.1016/j.polar.2017.02.003

Anderson, L. G., and Macdonald, R. W. (2015). Observing the Arctic Ocean carbon cycle in a changing environment. *Polar Res.* 34:26891. doi: 10.3402/polar.v34.26891

Årthun, M., Eldevik, T., Smedsrud, L., Skagseth, Ø, and Ingvaldsen, R. (2012). Quantifying the influence of Atlantic heat on Barents Sea ice variability and retreat. *J. Clim.* 25, 4736–4743. doi: 10.1175/jcli-d-11-00466.1

Bates, N., and Mathis, J. (2009). The Arctic Ocean marine carbon cycle: evaluation of air-sea CO 2 exchanges, ocean acidification impacts and potential feedbacks. *Biogeosciences* 6, 2433–2459. doi: 10.5194/bg-6-2433-2009

Bauch, D., Erlenkeuser, H., Winckler, G., Pavlova, G., and Thiede, J. (2002). Carbon isotopes and habitat of polar planktic foraminifera in the Okhotsk Sea: the 'carbonate ion effect'under natural conditions. *Mar. Micropaleontol.* 45, 83–99. doi: 10.1016/s0377-8398(02)00038-5

Bauch, H. A. (1999). "Planktic foraminifera in Holocene sediments from the Laptev Sea and the Central Arctic Ocean: species distribution and paleobiogeographical implication," in *Land-Ocean Systems in the Siberian Arctic*, eds H. Kassens, H. A. Bauch, I. A. Dmitrenko, H. Eicken, H.-W. Hubberten, M. Melles et al. (Berlin: Springer), 601–613. doi: 10.1007/978-3-642-60134-7_46

Bednaršek, N., Feely, R. A., Howes, E. L., Hunt, B. P., Kessouri, F., León, P., et al. (2019). Systematic review and meta-analysis toward synthesis of thresholds of ocean acidification impacts on calcifying pteropods and interactions with warming. *Front. Mar. Sci.* 6:227. doi: 10.3389/fmars.2019.00227

Bednaršek, N., Možina, J., Vogt, M., O'brien, C., and Tarling, G. (2012a). The global distribution of pteropods and their contribution to carbonate and carbon biomass in the modern ocean. *Earth Syst. Sci. Data* 4, 167–186. doi: 10.5194/essd-4-167-2012

Bednaršek, N., Tarling, G., Bakker, D., Fielding, S., Jones, E., Venables, H., et al. (2012b). Extensive dissolution of live pteropods in the Southern Ocean. *Nat. Geosci.* 5, 881–885. doi: 10.1038/ngeo1635

Bednaršek, N., Tarling, G. A., Bakker, D. C., Fielding, S., Cohen, A., Kuzirian, A., et al. (2012c). Description and quantification of pteropod shell dissolution: a sensitive bioindicator of ocean acidification. *Glob. Change Biol.* 18, 2378–2388. doi: 10.1111/j.1365-2486.2012.02668.x

Bednaršek, N., Tarling, G. A., Bakker, D. C., Fielding, S., and Feely, R. A. (2014). Dissolution dominating calcification process in polar pteropods close to the point of aragonite undersaturation. *PLoS One* 9:e109183. doi: 10.1371/journal.pone.0109183

Beer, C. J., Schiebel, R., and Wilson, P. A. (2010). Technical note: on methodologies for determining the size-normalised weight of planktic foraminifera. *Biogeosciences* 7, 2193–2198. doi: 10.5194/bg-7-2193-2010

Bergan, A. J., Lawson, G. L., Maas, A. E., and Wang, Z. A. (2017). The effect of elevated carbon dioxide on the sinking and swimming of the shelled pteropod *Limacina retroversa*. *ICES J. Mar. Sci.* 74, 1893–1905. doi: 10.1093/icesjms/fsx008

Bjørklund, K. R., Kruglikova, S. B., and Anderson, O. R. (2012). Modern incursions of tropical Radiolaria into the Arctic Ocean. *J. Micropalaeontol.* 31, 139–158. doi: 10.1144/0262-821x11-030

Blachowiak-Samolyk, K., Søreide, J. E., Kwasniewski, S., Sundfjord, A., Hop, H., Falk-Petersen, S., et al. (2008). Hydrodynamic control of mesozooplankton abundance and biomass in northern Svalbard waters (79–81 N). *Deep Sea Res. 2 Top. Stud. Oceanogr.* 55, 2210–2224. doi: 10.1016/j.dsr2.2008.05.018

Bluhm, B., Kosobokova, K., and Carmack, E. (2015). A tale of two basins: an integrated physical and biological perspective of the deep Arctic Ocean. *Progr. Oceanogr.* 139, 89–121. doi: 10.1016/j.pocean.2015.07.011

Buitenhuis, E., Vogt, M., Moriarty, R., Bednarsek, N., Doney, S. C., Leblanc, K., et al. (2013). MAREDAT: towards a world atlas of MARine Ecosystem DATa. *Earth Syst. Sci. Data* 5, 227–239. doi: 10.5194/essd-5-227-2013

Buitenhuis, E. T., Le Quere, C., Bednaršek, N., and Schiebel, R. (2019). Large contribution of Pteropods to shallow CaCO3 export. *Glob. Biogeochem. Cycles* 33, 458–468. doi: 10.1029/2018gb006110

Carstens, J., Hebbeln, D., and Wefer, G. (1997). Distribution of planktic foraminifera at the ice margin in the Arctic (Fram Strait). *Mar. Micropaleontol.* 29, 257–269. doi: 10.1016/s0377-8398(96)00014-x

Carstens, J., and Wefer, G. (1992). Recent distribution of planktonic foraminifera in the Nansen Basin, Arctic Ocean. *Deep Sea Res. A. Oceanogr. Res. Papers* 39, S507–S524.

Chang, Y., and Yen, J. (2012). Swimming in the intermediate reynolds range: kinematics of the pteropod *Limacina helicina*. *Integr. Comp. Biol.* 52, 597–615. doi: 10.1093/icb/ics113

Chierici, M., and Fransson, A. (2018). "Arctic chemical oceanography at the edge: focus on carbonate chemistry (chapter 13)", in *At the Edge*, ed. P. Wassmann, 343.

Chierici, M., Vernet, M., Fransson, A., and Børsheim, K. Y. (2019). Net community production and carbon exchange from winter to summer in the Atlantic water inflow to the Arctic Ocean. *Front. Mar. Sci.* 6:528. doi: 10.3389/fmars.2019.00528

Davis, C. V., Rivest, E. B., Hill, T. M., Gaylord, B., Russell, A. D., and Sanford, E. (2017). Ocean acidification compromises a planktic calcifier with implications for global carbon cycling. *Sci. Rep.* 7:2225.

Descamps, S., Aars, J., Fuglei, E., Kovacs, K. M., Lydersen, C., Pavlova, O., et al. (2017). Climate change impacts on wildlife in a High Arctic archipelago–Svalbard, Norway. *Glob. Change Biol.* 23, 490–502. doi: 10.1111/gcb.13381

Dickson, A. (1990). Standard potential of the (AgCl (s)+ 1/2H2 (g)= Ag (s)+ HCl (aq)) cell and the dissociation constant of bisulfate ion in synthetic sea water from 273.15 to 318.15 K. *J. Chem. Thermodyn.* 22, 113–127. doi: 10.1016/0021-9614(90)90074-z

Dickson, A., and Millero, F. J. (1987). A comparison of the equilibrium constants for the dissociation of carbonic acid in seawater media. *Deep Sea Res. A Oceanogr. Res. Papers* 34, 1733–1743. doi: 10.1016/0198-0149(87)90021-5

Dickson, A. G., Sabine, C. L., and Christian, J. R. (2007). *Guide to Best Practices for Ocean CO2 Measurements*. Sydney, VIC: North Pacific Marine Science Organization.

Drits, A., Klyuvitkin, A., Kravchishina, M., Karmanov, V., and Novigatsky, A. (2020). Fluxes of sedimentary material in the lofoten basin of the Norwegian Sea: seasonal dynamics and the role of zooplankton. *Oceanology* 60, 501–517. doi: 10.1134/s0001437020040074

Fabry, V. J. (1989). Aragonite production by pteropod molluscs in the subarctic Pacific. *Deep Sea Res. A Oceanogr. Res. Papers* 36, 1735–1751. doi: 10.1016/0198-0149(89)90069-1

Fabry, V. J. (2008). Marine calcifiers in a high-CO2 ocean. *Science* 320, 1020–1022. doi: 10.1126/science.1157130

Fabry, V. J., Seibel, B. A., Feely, R. A., and Orr, J. C. (2008). Impacts of ocean acidification on marine fauna and ecosystem processes. *ICES J. Mar. Sci.* 65, 414–432. doi: 10.1093/icesjms/fsn048

Falk-Petersen, S., Leu, E., Berge, J., Kwasniewski, S., Nygård, H., Røstad, A., et al. (2008). Vertical migration in high Arctic waters during autumn 2004. *Deep Sea Res. 2 Top. Stud. Oceanogr.* 55, 2275–2284. doi: 10.1016/j.dsr2.2008.05.010

Fox, L., Stukins, S., Hill, T., and Miller, C. G. (2020). Quantifying the effect of anthropogenic climate change on calcifying plankton. *Sci. Rep.* 10:1620.

Greco, M., Jonkers, L., Kretschmer, K., Bijma, J., and Kucera, M. (2019). Depth habitat of the planktonic foraminifera *Neogloboquadrina pachyderma* in the northern high latitudes explained by sea-ice and chlorophyll concentrations. *Biogeosciences* 16, 3425–3437. doi: 10.5194/bg-16-3425-2019

Guinotte, J. M., and Fabry, V. J. (2008). Ocean acidification and its potential effects on marine ecosystems. *Ann. N. Y. Acad. Sci.* 1134, 320–342. doi: 10.1196/annals.1439.013

Hop, H., Assmy, P., Wold, A., Sundfjord, A., Daase, M., Duarte, P., et al. (2019). Pelagic ecosystem characteristics across the Atlantic water boundary current from Rijpfjorden, Svalbard, to the Arctic Ocean during summer (2010-2014). *Front. Mar. Sci.* 6:181. doi: 10.3389/fmars.2019.00181

Husum, K., and Hald, M. (2012). Arctic planktic foraminiferal assemblages: implications for subsurface temperature reconstructions. *Mar. Micropaleontol.* 96, 38–47. doi: 10.1016/j.marmicro.2012.07.001

Jonkers, L., Hillebrand, H., and Kucera, M. (2019). Global change drives modern plankton communities away from the pre-industrial state. *Nature* 570, 372–375. doi: 10.1038/s41586-019-1230-3

Kacprzak, P., Panasiuk, A., Wawrzynek, J., and Weydmann, A. (2017). Distribution and abundance of pteropods in the western Barents Sea. *Oceanol. Hydrobiol. Stud.* 46:393. doi: 10.1515/ohs-2017-0039

Katz, M. E., Cramer, B. S., Franzese, A., Hönisch, B.r, Miller, K. G., Rosenthal, Y., et al. (2010). Traditional and emerging geochemical proxies in foraminifera. *J. Foraminifer. Res.* 40, 165–192. doi: 10.2113/gsjfr.40.2.165

Kohfeld, K. E., Fairbanks, R. G., Smith, S. L., and Walsh, I. D. (1996). *Neogloboquadrina pachyderma* (sinistral coiling) as paleoceanographic tracers in polar oceans: evidence from Northeast Water Polynya plankton tows, sediment traps, and surface sediments. *Paleoceanography* 11, 679–699. doi: 10.1029/96pa02617

Kolås, E. H., Koenig, Z., Fer, I., Nilsen, F., and Marnela, M. (2020). Structure and transport of Atlantic Water north of Svalbard from observations in summer and fall 2018. *J. Geophys. Res. Oceans* 125:e2020JC016174.

Lalli, C. M., and Gilmer, R. W. (1989). *Pelagic Snails: the Biology of Holoplanktonic Gastropod Mollusks*. Stanford, CA: Stanford University Press.

Langer, M. R. (2008). Assessing the Contribution of Foraminiferan Protists to Global Ocean Carbonate Production 1. *J. Eukaryot. Microbiol.* 55, 163–169. doi: 10.1111/j.1550-7408.2008.00321.x

Lee, K., Kim, T.-W., Byrne, R. H., Millero, F. J., Feely, R. A., and Liu, Y.-M. (2010). The universal ratio of boron to chlorinity for the North Pacific and North Atlantic oceans. *Geochim. Cosmochim. Acta* 74, 1801–1811. doi: 10.1016/j.gca.2009.12.027

Lee, Y. J., Matrai, P. A., Friedrichs, M. A., Saba, V. S., Antoine, D., Ardyna, M., et al. (2015). An assessment of phytoplankton primary productivity in the

Arctic Ocean from satellite ocean color/in situ chlorophyll−a based models. *J. Geophys. Res. Oceans* 120, 6508–6541. doi: 10.1002/2015jc011018

Lischka, S., and Riebesell, U. (2012). Synergistic effects of ocean acidification and warming on overwintering pteropods in the Arctic. *Glob. Change Biol.* 18, 3517–3528. doi: 10.1111/gcb.12020

Manno, C., Bednaršek, N., Tarling, G. A., Peck, V. L., Comeau, S., Adhikari, D., et al. (2017). Shelled pteropods in peril: assessing vulnerability in a high CO2 ocean. *Earth Sci. Rev.* 169, 132–145. doi: 10.1016/j.earscirev.2017.04.005

Manno, C., Giglio, F., Stowasser, G., Fielding, S., Enderlein, P., and Tarling, G. (2018). Threatened species drive the strength of the carbonate pump in the northern Scotia Sea. *Nat. Commun.* 9:4592.

Manno, C., Morata, N., and Primicerio, R. (2012). *Limacina retroversa*'s response to combined effects of ocean acidification and sea water freshening. *Estuar. Coast. Shelf Sci.* 113, 163–171. doi: 10.1016/j.ecss.2012.07.019

Manno, C., and Pavlov, A. (2014). Living planktonic foraminifera in the Fram Strait (Arctic): absence of diel vertical migration during the midnight sun. *Hydrobiologia* 721, 285–295. doi: 10.1007/s10750-013-1669-4

Mehrbach, C., Culberson, C., Hawley, J., and Pytkowicx, R. (1973). Measurement of the apparent dissociation constants of carbonic acid in seawater at atmospheric pressure 1. *Limnol. Oceanogr.* 18, 897–907. doi: 10.4319/lo.1973.18.6.0897

Meilland, J., Howa, H., Hulot, V., Demangel, I., Salaun, J., and Garlan, T. (2020). Population dynamics of modern planktonic foraminifera in the western Barents Sea. *Biogeosciences* 17, 1437–1450. doi: 10.5194/bg-17-1437-2020

Meilland, J., Schiebel, R., Monaco, C. L., Sanchez, S., and Howa, H. (2018). Abundances and test weights of living planktic foraminifers across the Southwest Indian Ocean: implications for carbon fluxes. *Deep Sea Res.2 Oceanogr. Res. Papers* 131, 27–40. doi: 10.1016/j.dsr.2017.11.004

Meyer, A., Sundfjord, A., Fer, I., Provost, C., Villacieros Robineau, N., Koenig, Z., et al. (2017). Winter to summer oceanographic observations in the Arctic Ocean north of Svalbard. *J. Geophys. Res. Oceans* 122, 6218–6237. doi: 10.1002/2016jc012391

Middelburg, J. J., Soetaert, K., and Hagens, M. (2020). Ocean alkalinity, buffering and biogeochemical processes. *Rev. Geophys.* 58:e2019RG000681.

Millero, F. J. (1979). Effects of pressure and temperature on activity coefficients. *Act. Coefficients Electrolyte Solututions* 2, 63–151.

Moy, A. D., Howard, W. R., Bray, S. G., and Trull, T. W. (2009). Reduced calcification in modern Southern Ocean planktonic foraminifera. *Nat. Geosci.* 2, 276–280. doi: 10.1038/ngeo460

Mucci, A. (1983). The solubility of calcite and aragonite in seawater at various salinities, temperatures, and one atmosphere total pressure. *Am. J. Sci.* 283, 780–799. doi: 10.2475/ajs.283.7.780

NOAA NCFEI. (2018). *Climate at a Glance: Global Mapping* [Online]. Available online at: https://www.ncdc.noaa.gov/snow-and-ice/extent/ (accessed May 13, 2021).

Ofstad, S., Meilland, J., Zamelczyk, K., Chierici, M., Fransson, A., Gründger, F., et al. (2020). Development, productivity, and seasonality of living planktonic foraminiferal faunas and *Limacina helicina* in an Area of intense methane seepage in the Barents Sea. *J. Geophys. Res. Biogeosci.* 125: e2019JG005387.

Onarheim, I. H., Smedsrud, L. H., Ingvaldsen, R. B., and Nilsen, F. (2014). Loss of sea ice during winter north of Svalbard. *Tellus A Dyn. Meteorol. Oceanogr.* 66:23933. doi: 10.3402/tellusa.v66.23933

Orr, J. C., Fabry, V. J., Aumont, O., Bopp, L., Doney, S. C., Feely, R. A., et al. (2005). Anthropogenic ocean acidification over the twenty-first century and its impact on calcifying organisms. *Nature* 437, 681–686. doi: 10.1038/nature04095

Pados, T., and Spielhagen, R. F. (2014). Species distribution and depth habitat of recent planktic foraminifera in Fram Strait. Arctic Ocean. *Polar Res.* 33, 22483. doi: 10.3402/polar.v33.22483

Peck, V. L., Oakes, R. L., Harper, E. M., Manno, C., and Tarling, G. A. (2018). Pteropods counter mechanical damage and dissolution through extensive shell repair. *Nat. Commun.* 9:264.

Pierrot, D., Lewis, E., and Wallace, D. (2006). *MS Excel Program Developed for CO2 System Calculations*. Oak Ridge, TN: Oak Ridge National Laboratory, 10.

Renner, A., Sundfjord, A., Janout, M., Ingvaldsen, R. B., Beszczynska−Möller, A., Pickart, R. S., et al. (2018). Variability and redistribution of heat in the Atlantic water boundary current north of Svalbard. *J. Geophys. Res. Oceans* 123, 6373–6391. doi: 10.1029/2018jc013814

Riley, J., and Tongudai, M. (1967). The major cation/chlorinity ratios in sea water. *Chem. Geol.* 2, 263–269. doi: 10.1016/0009-2541(67)90026-5

Roy, T., Lombard, F., Bopp, L., and Gehlen, M. (2015). Projected impacts of climate change and ocean acidification on the global biogeography of planktonic Foraminifera. *Biogeosciences* 12, 2873–2889. doi: 10.5194/bg-12-2873-2015

Sakshaug, E. (1997). Biomass and productivity distributions and their variability in the Barents Sea. *ICES J. Mar. Sci.* 54, 341–350. doi: 10.1006/jmsc.1996.0170

Salter, I., Schiebel, R., Ziveri, P., Movellan, A., Lampitt, R., and Wolff, G. A. (2014). Carbonate counter pump stimulated by natural iron fertilization in the Polar Frontal Zone. *Nat. Geosci.* 7, 885–889. doi: 10.1038/ngeo2285

Schiebel, R. (2002). Planktic foraminiferal sedimentation and the marine calcite budget. *Glob. Biogeochem. Cycles* 16, 3-1-3-21.

Schiebel, R., Barker, S., Lendt, R., Thomas, H., and Bollmann, J. (2007). Planktic foraminiferal dissolution in the twilight zone. *Deep Sea Res. 2 Top. Stud. Oceanogr.* 54, 676–686. doi: 10.1016/j.dsr2.2007.01.009

Schiebel, R., and Hemleben, C. (2000). Interannual variability of planktic foraminiferal populations and test flux in the eastern North Atlantic Ocean (JGOFS). *Deep Sea Res. 2 Top. Stud. Oceanogr.* 47, 1809–1852. doi: 10.1016/s0967-0645(00)00008-4

Schiebel, R., Spielhagen, R. F., Garnier, J., Hagemann, J., Howa, H., Jentzen, A., et al. (2017). Modern planktic foraminifers in the high-latitude ocean. *Mar. Micropaleontol.* 136, 1–13. doi: 10.1007/978-3-662-50297-6_1

Schneider, C. A., Rasband, W. S., and Eliceiri, K. W. (2012). NIH Image to ImageJ: 25 years of image analysis. *Nat. Methods* 9, 671–675. doi: 10.1038/nmeth.2089

Shadwick, E., Trull, T., Thomas, H., and Gibson, J. (2013). Vulnerability of polar oceans to anthropogenic acidification: comparison of Arctic and Antarctic seasonal cycles. *Sci. Rep.* 3:2339.

Simstich, J., Sarnthein, M., and Erlenkeuser, H. (2003). Paired δ18O signals of *Neogloboquadrina pachyderma* (s) and *Turborotalita quinqueloba* show thermal stratification structure in Nordic Seas. *Mar. Micropaleontol.* 48, 107–125. doi: 10.1016/s0377-8398(02)00165-2

Sugie, K., Fujiwara, A., Nishino, S., Kameyama, S., and Harada, N. (2020). Impacts of temperature, CO2, and salinity on phytoplankton community composition in the Western Arctic Ocean. *Front. Mar. Sci.* 6:821. doi: 10.3389/fmars.2019.00821

Sundfjord, A., Assmann, K. M., Lundesgaard, Ø, Renner, A. H. H., Lind, S., and Ingvaldsen, R. B. (2020). *Suggested Water Mass Definitions for the Central and Northern Barents Sea, and the Adjacent Nansen Basin: Workshop Report.", in: The Nansen Legacy Report Series 8/2020*. Tromsø: The Nansen Legacy.

Takahashi, K., and Bé, A. (1984). Planktonic foraminifera: factors controlling sinking speed. *Deep Sea Res. A Oceanogr. Res. Papers* 31, 1477–1500. doi: 10.1016/0198-0149(84)90083-9

Volkmann, R. (2000). Planktic foraminifers in the outer Laptev Sea and the Fram Strait—Modern distribution and ecology. *J. Foraminifer. Res.* 30, 157–176. doi: 10.2113/0300157

Wassmann, P., Slagstad, D., and Ellingsen, I. H. (2019). Advection of Mesozooplankton into the Northern svalbard shelf region. *Front. Mar. Sci.* 6:458. doi: 10.3389/fmars.2019.00458

Weinkauf, M. F., Kunze, J. G., Waniek, J. J., and Kučera, M. (2016). Seasonal variation in shell calcification of planktonic foraminifera in the NE Atlantic reveals species-specific response to temperature, productivity, and optimum growth conditions. *PLoS One* 11:e0148363. doi: 10.1371/journal.pone.0148363

Zamelczyk, K., Rasmussen, T. L., Raitzsch, M., and Chierici, M. (2020). The last two millennia: climate, ocean circulation and palaeoproductivity inferred from planktic foraminifera, south-western Svalbard margin. *Polar Res.* 39. doi: 10.33265/polar.v39.3715

Ziveri, P., de Bernardi, B., Baumann, K.-H., Stoll, H. M., and Mortyn, P. G. (2007). Sinking of coccolith carbonate and potential contribution to organic carbon ballasting in the deep ocean. *Deep Sea Research Part II: Topical Studies in Oceanography* 54, 659–675. doi: 10.1016/j.dsr2.2007.01.006

Conflict of Interest: The authors declare that the research was conducted in the absence of any commercial or financial relationships that could be construed as a potential conflict of interest.

frontiers

Supplementary Material

Supplementary Figure 1 CTD profiles focusing on the upper 300 m of the water column (delimited with the grey line). The top panel (A) represents from left to right the shelf stations 1 and 2, the middle panel (B) from left to right, slope stations 3 (1019 m), 4 (to 510 m), 5 (2166 m) and 6 (853 m), and lower panel (C), the basin station 7 (3094 m). In orange the temperature profile and in dark blue, the salinity.

W → E

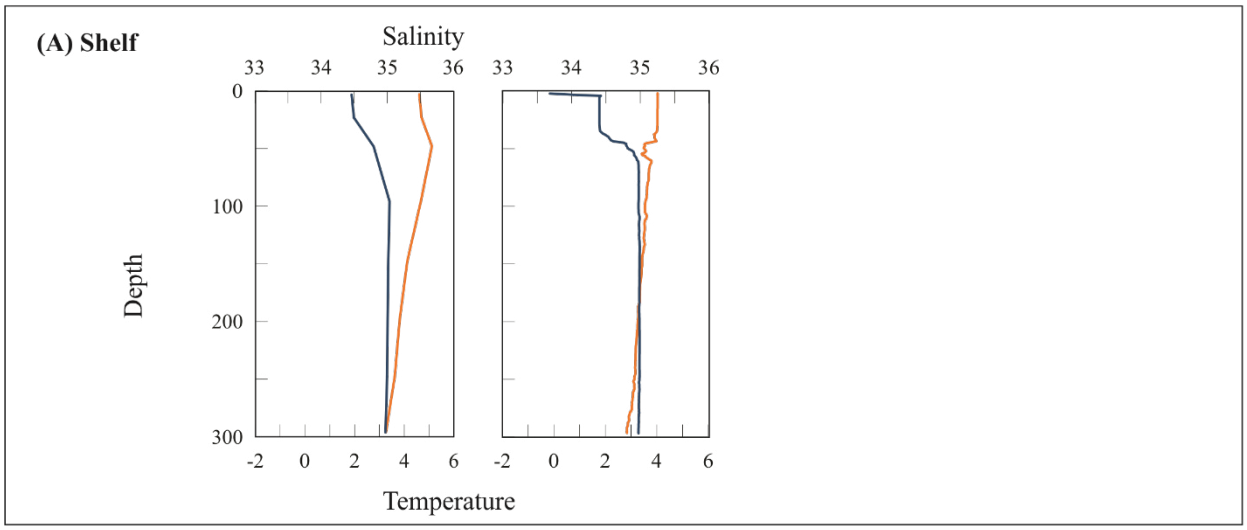
(A) Shelf
Salinity
33 34 35 36 33 34 35 36
0
100
200
300
Depth
-2 0 2 4 6 -2 0 2 4 6
Temperature

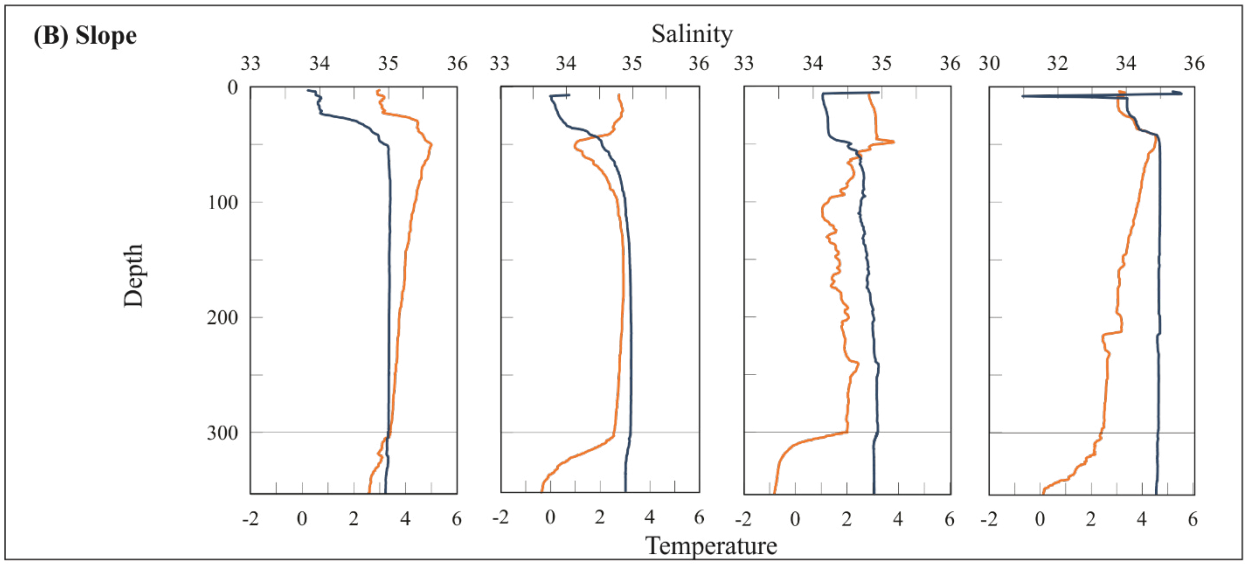
(B) Slope
Salinity
33 34 35 36 33 34 35 36 33 34 35 36 30 32 34 36
0
100
200
300
Depth
-2 0 2 4 6 -2 0 2 4 6 -2 0 2 4 6 -2 0 2 4 6
Temperature

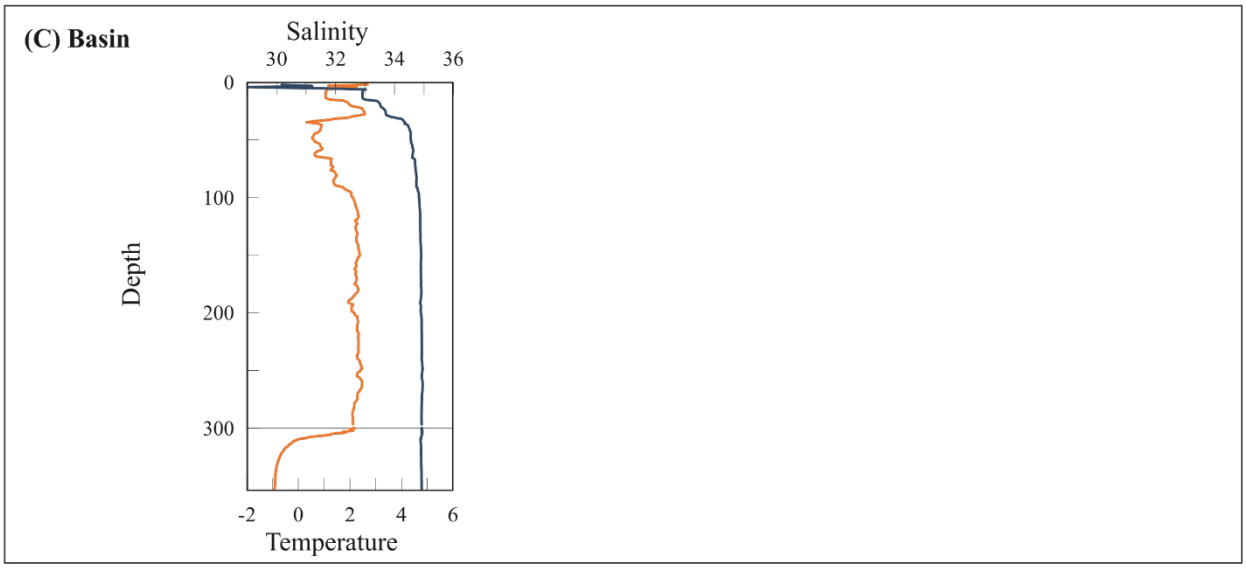
(C) Basin
Salinity
30 32 34 36
0
100
200
300
Depth
-2 0 2 4 6
Temperature

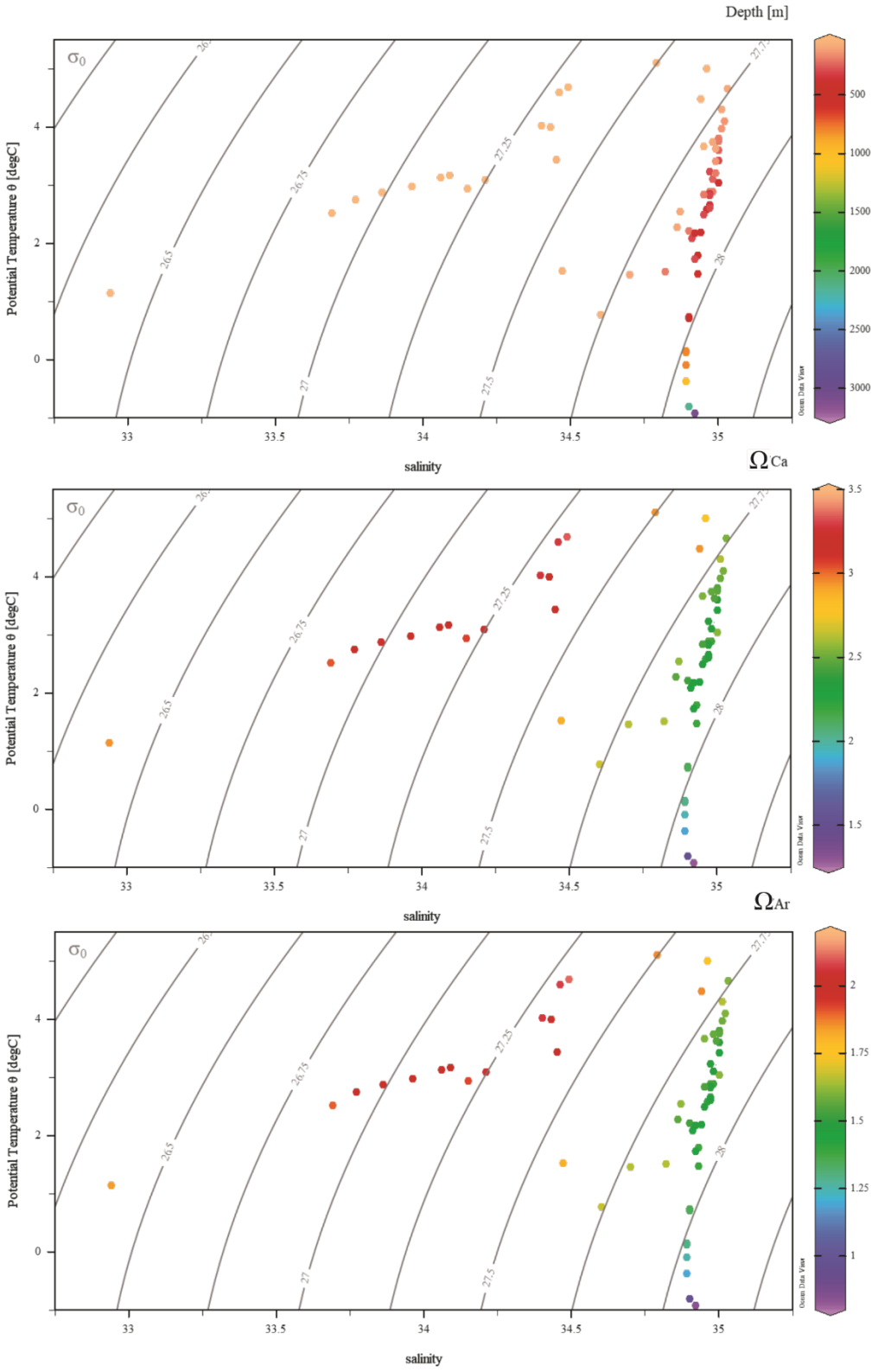

Supplementary Figure 2 Temperature-Salinity profile regarding depth, Ω Calcite and Ω Aragonite.

	Depth	Counted foraminifera					Absolute abundance foraminifera				
		> 500 µm	250-500 µm	100-250 µm	63-100 µm	Total	> 500 µm (ind m^{-3})	250-500 µm (ind m^{-3})	100-250 µm (ind m^{-3})	63-100 µm (ind m^{-3})	Total (ind m^{-3})
Station 1	0-50	0	1	21	7	29	0.0	0.1	1.6	0.5	2.3
Station 1	50-100	0	0	64	69	133	0.0	0.0	5.0	5.4	10.4
Station 1	100-200	0	0	52	175	227	0.0	0.0	2.0	6.9	8.9
Station 1	200-300	0	0	33	115	148	0.0	0.0	1.3	4.5	5.8
Station 2	0-50	0	0	89	55	144	0.0	0.0	7.0	4.3	11.3
Station 2	50-100	0	0	88	145	233	0.0	0.0	6.9	11.4	18.3
Station 2	100-200	0	0	170	162	332	0.0	0.0	6.7	6.3	13.0
Station 2	200-300	0	0	92	103	195	0.0	0.0	3.6	4.0	7.6
Station 3	0-50	0	3	37	26	66	0.0	0.2	2.9	2.0	5.2
Station 3	50-100	0	1	91	181	273	0.0	0.1	7.1	14.2	21.4
Station 3	100-200	0	0	54	224	278	0.0	0.0	2.1	8.8	10.9
Station 3	200-300	0	0	85	129	214	0.0	0.0	3.3	5.1	8.4
Station 4	0-50	0	3	40	27	70	0.0	0.2	3.1	2.1	5.5
Station 4	50-100	0	0	220	220	440	0.0	0.0	17.2	17.2	34.5
Station 4	100-200	0	5	783	553	1341	0.0	0.2	30.7	21.7	52.6
Station 4	200-300	0	9	381	360	750	0.0	0.4	14.9	14.1	29.4
Station 5	0-50	0	3	3	41	47	0.0	0.2	0.2	3.2	3.7
Station 5	50-100	0	0	122	15	137	0.0	0.0	9.6	1.2	10.7
Station 5	100-200	0	0	341	292	633	0.0	0.0	13.4	11.4	24.8
Station 5	200-300	0	0	223	136	359	0.0	0.0	8.7	5.3	14.1

Station 6	0-50	0	2	16	27	45	0.0	0.2	1.3	2.1	3.5
Station 6	50-100	0	15	118	93	226	0.0	1.2	9.2	7.3	17.7
Station 6	100-200	0	1	181	212	394	0.0	0.0	7.1	8.3	15.4
Station 6	200-300	0	2	174	96	272	0.0	0.1	6.8	3.8	10.7
Station 7											
Station 7	50-100	0	0	135	145	280	0.0	0.0	10.6	11.4	21.9
Station 7	100-200	0	0	183	320	503	0.0	0.0	7.2	12.5	19.7
Station 7	200-300	0	0	73	177	250	0.0	0.0	2.9	6.9	9.8

Supplementary Table 1. Counts of foraminifera per size fraction and depth with the associated absolute abundance.

	Depth	Counted pteropods					Absolute abundance pteropods				
		> 500 µm	250-500 µm	100-250 µm	63-100 µm	**Total**	> 500 µm (ind m^{-3})	250-500 µm (ind m^{-3})	100-250 µm (ind m^{-3})	63-100 µm (ind m^{-3})	**Total** (ind m^{-3})
Station 1	0-50	1	102	33	9	145	0.1	8.0	2.6	0.7	11.4
Station 1	50-100	2	0	5	0	7	0.2	0.0	0.4	0.0	0.5
Station 1	100-200	0	4	14	3	21	0.0	0.2	0.5	0.1	0.8
Station 1	200-300	0	0	3	3	6	0.0	0.0	0.1	0.1	0.2
Station 2	0-50	0	64	0	15	79	0.0	5.0	0.0	1.2	6.2
Station 2	50-100	14	40	14	5	73	1.1	3.1	1.1	0.4	5.7
Station 2	100-200	5	0	1	4	10	0.2	0.0	0.0	0.2	0.4
Station 2	200-300	0	0	3	14	17	0.0	0.0	0.1	0.5	0.7
Station 3	0-50	46	56	16	13	131	3.6	4.4	1.3	1.0	10.3
Station 3	50-100	100	22	4	5	131	7.8	1.7	0.3	0.4	10.3
Station 3	100-200	3	1	7	0	11	0.1	0.0	0.3	0.0	0.4
Station 3	200-300	1	0	5	5	11	0.0	0.0	0.2	0.2	0.4
Station 4	0-50	3	51	15	7	76	0.2	4.0	1.2	0.5	6.0
Station 4	50-100	2	4	3	14	23	0.2	0.3	0.2	1.1	1.8
Station 4	100-200	1	2	1	3	7	0.0	0.1	0.0	0.1	0.3
Station 4	200-300	0	2	14	8	24	0.0	0.1	0.5	0.3	0.9
Station 5	0-50	5	94	13	18	130	0.4	7.4	1.0	1.4	10.2
Station 5	50-100	1	8	9	142	160	0.1	0.6	0.7	11.1	12.5
Station 5	100-200	0	0	3	1	4	0.0	0.0	0.1	0.0	0.2
Station 5	200-300	0	1	3	3	7	0.0	0.0	0.1	0.1	0.3

Station 6	0-50	8	91	80	93	272	0.6	7.1	1.3	7.3	21.3
Station 6	50-100	25	16	25	17	83	2.0	1.3	9.2	1.3	6.5
Station 6	100-200	0	3	9	8	20	0.0	0.1	7.1	0.3	0.8
Station 6	200-300	0	6	65	2	73	0.0	0.2	6.8	0.1	2.9
Station 7											
Station 7	50-100	4	18	1	2	25	0.3	1.4	0.1	0.2	2.0
Station 7	100-200	2	1	0	0	3	0.1	0.0	0.0	0.0	0.1
Station 7	200-300	0	0	5	6	11	0.0	0.0	0.2	0.2	0.4

Supplementary table 2. Counts of pteropods per size fraction and depth with the associated absolute abundance.

Paper II

Progress in Oceanography 218 (2023) 103121

Contents lists available at ScienceDirect

Progress in Oceanography

journal homepage: www.elsevier.com/locate/pocean

Seasonality of marine calcifiers in the northern Barents Sea: Spatiotemporal distribution of planktonic foraminifers and shelled pteropods and their contribution to carbon dynamics

Griselda Anglada-Ortiz [a,*], Julie Meilland [b], Patrizia Ziveri [c,d], Melissa Chierici [e], Agneta Fransson [f], Elizabeth Jones [e], Tine L. Rasmussen [a]

[a] Department of Geosciences UiT, The Arctic University of Norway, 9037 Tromsø, Norway
[b] MARUM, Center for Marine Environmental Sciences, University of Bremen, Leobener Str. 8, 28359 Bremen, Germany
[c] Institute of Environmental Science and Technology (ICTA-UAB), Universitat Autònoma de Barcelona, 08193, Barcelona, Spain
[d] Institució Catalana de Recerca i Estudis Avançats, ICREA, 08010, Barcelona, Spain
[e] Institute of Marine Research (IMR), 9296 Tromsø, Norway
[f] Norwegian Polar Institute (NPI), 9296 Tromsø, Norway

ARTICLE INFO

Keywords:
Planktonic calcifiers
Abundances
Inorganic carbon
Organic carbon
Standing stocks
Export production

ABSTRACT

The Barents Sea is presently undergoing rapid warming and the sea-ice edge and the productive zones are retreating northward at accelerating rates. Planktonic foraminifers and shelled pteropods are ubiquitous marine calcifiers that play an important role in the carbon budget and being particularly sensitive to ocean biogeochemical changes and ocean acidification. Their distribution at high latitudes have rarely been studied, and usually only for the summer season. Here we present results of their distribution patterns in the upper 300 m in the water column (individuals m^{-3}), protein content and size distribution on a seasonal basis to estimate their inorganic and organic carbon standing stocks (μg m^{-3}) and export production (mg m^{-2} d^{-1}). The study area constitutes a latitudinal transect in the northern Barents Sea from 76° N to 82° N including seven stations through both Atlantic, Arctic, and Polar surface water regimes and the marginal and seasonal sea-ice zones. The transect was sampled in 2019 (August and December) and 2021 (March, May, and July). The highest carbon standing stocks and export production were found at the Polar seasonally sea-ice covered shelf stations with the contribution from shelled pteropods being significantly higher than planktonic foraminifers during all seasons. We recorded the highest production of foraminifers and pteropods in summer (August 2019 and July 2021) and autumn (December 2019) followed by spring (May 2021), and the lowest in winter (March 2021).

1. Introduction

The rapid increase in anthropogenic carbon dioxide (CO_2) in the atmosphere and the ocean uptake have changed and continue to change the water carbonate chemistry by reducing the pH, the carbonate ion concentration ($[CO_3^{2-}]$) and the calcium carbonate saturation state ($\Omega CaCO_3$) (Feely et al., 2004). This process, known as ocean acidification, is thought to have irreversible consequences for marine calcifiers, such as planktonic foraminifers and thecosome (shelled) pteropods. In the past the reduction of calcification rates and biogenic calcium carbonate ($CaCO_3$) production, as well as damages to (aragonitic; Ar) shells have been attributed to ocean acidification and $CaCO_3$ undersaturation ($\Omega < 1$) of the surface waters (Schiebel, 2002; Fabry, 2008; Hunt et al., 2008; Moy et al., 2009; Manno et al., 2017; Peck et al., 2018; Bednaršek et al., 2019 and references therein). However, damages to the aragonitic shell of the pteropod *Limacina helicina* have been observed even in supersaturated ($\Omega_{Ar} > 1$) conditions of $\Omega_{Ar} = 1.5$ (Bednaršek et al., 2014a; Bednaršek et al., 2019). Because of their sensitivity to $\Omega CaCO_3$, the calcareous shells of planktonic foraminifers and pteropods are considered biological indicators of ocean acidification (Orr et al., 2005; Fabry 2008; Moy et al., 2009; Bednaršek et al., 2012b). Furthermore, they have been reported to play an important role in the marine carbonate cycle and can affect the buffer capacity of the ocean by $CaCO_3$ production, export and dissolution (Schiebel, 2002; Ziveri et al., 2007; Langer, 2008; Bednaršek et al., 2012a; Buitenhuis et al., 2019; Subhas et al., 2022; Ziveri et al., 2023).

* Corresponding author.
E-mail address: Griselda.a.ortiz@uit.no (G. Anglada-Ortiz).

https://doi.org/10.1016/j.pocean.2023.103121

Available online 7 September 2023

Planktonic foraminifers are protists with a shell made of calcite and are found in all oceans, from low to high latitudes. They mainly inhabit the upper 300 m of the water column and are transported passively by ocean currents (Hemleben et al., 1989). Previous studies have reported the absence of diel vertical migration in high latitudes (Manno and Pavlov, 2013; Greco et al., 2019; Meilland et al., 2020; Ofstad et al., 2020; Anglada-Ortiz et al., 2021). When they die, their shells sink and accumulate on the seafloor and in the sediment. They preserve in the sediment when the seabed is above the calcite compensation depth (CCD) or dissolve otherwise, hereby playing an important role in the marine carbonate cycle and alkalinity budget (Schiebel, 2002; Jonkers and Kučera, 2015). Even though the seasonal distribution of living foraminifers has been studied for a long time (Allan, 1960) there is only a limited number of studies focusing on Arctic areas and the southern Barents Sea (Ofstad et al., 2020) especially outside of the summer period.

Shelled pteropods are holoplanktonic gastropods found in all oceans. Their shells are made of aragonite, a metastable form of $CaCO_3$, which is more sensitive to changes in the water carbonate chemistry than calcite (Bednaršek et al., 2012b; Manno et al., 2017). The presence of pteropod shells in the fossil record is restricted to sediments above the aragonite compensation depth, shallower than the CCD (Gerhardt and Henrich, 2001; Peijnenburg et al., 2020). However, they also play an important role in the carbonate cycle by exporting (mainly) inorganic carbon from the ocean surface (e.g. Anglada-Ortiz et al. (2021); Knecht et al. (2023); Ziveri et al. (2023)). To our knowledge, and similar to the foraminiferal fauna, the northern Barents Sea has never been studied to track the seasonality of the pteropod fauna.

The Barents Sea (Arctic Ocean) is a relatively shallow shelf sea (average water depth ~230 m) which currently experiences rapid warming, in both the atmosphere and the ocean (Dalpadado et al., 2014; Descamps et al., 2017). Coupled with a decline in sea-ice cover, the direct gas exchange with the atmosphere is predicted to increase (Bates and Mathis, 2009). The northern Barents Sea region of the Arctic is expected to be more affected by ocean acidification because of its already low carbonate saturation state (Ω) of calcite and aragonite and the higher solubility of CO_2 in cold waters (Chierici and Fransson, 2018). The study area is characterized by strong seasonal changes in light intensity and sea-ice cover. These parameters mainly drive the primary production and the availability of nutrients, together with surface stratification (Bluhm et al., 2015). Over the last few decades an increase in primary and secondary production have been observed in the Barents Sea and Arctic Ocean (Dalpadado et al., 2014; Arrigo and van Dijken, 2015; Lewis et al., 2020). In the northern Barents Sea, the primary production is characterized by a spring (phytoplankton) bloom, occurring between April and July, when the sea ice melts and retreats (Sakshaug, 1997; Lee et al., 2015). The spring bloom may be followed by a second bloom in late summer (Wassmann et al., 2019). These blooms are the most important food source for the zooplankton (Sakshaug, 1997 and references therein). Advection of Atlantic and Arctic/Polar Waters bring not only nutrients but phytoplankton and zooplankton to the northern Svalbard margin (Wassmann et al., 2019).

The marginal ice zone (MIZ) is a frontal system between Atlantic and Arctic/Polar Water (Sakshaug and Skjoldal, 1989) and characterized by high productivity and seasonality, mainly close to the sea-ice edge (Reigstad et al., 2002). This production is strongly linked to mixing of Atlantic and Arctic Water, meteorological and sea-ice conditions (Wassmann et al., 1999 and references therein). The MIZ has been expanding northwards since 1870 and accelerating since 1970 (Kinnard et al., 2008). The MIZ also affects the benthic community. A study by Saher et al. (2012) on the benthic foraminifers *Nonionellina labradorica*, a sea-ice edge indicator, showed that its distribution has been pushed northwards (100 km) as the summer sea-ice edge has moved northward during the last few decades compared to c. 40 years old data previously reported by Steinsund (1994). The seasonal ice zone (SIZ) is the transitional zone between the winter and the summer sea-ice edges (Wadhams, 1986), where the seasonally retreating and expanding sea ice generates a productive area between the open sea and the drifting pack ice (Wassmann and Reigstad, 2011).

Despite the vulnerability to ocean acidification and strong seasonality of the Northern Barents Sea, little is known about the distribution of marine calcifiers, their present state of calcification and how they would respond to ocean acidification. A recent study from the northern Svalbard margin reported that large (>500 μm) and medium-sized (250–500 μm) pteropods dominated the upper 50 m of the water column in late summer (September 2018), while medium (100–250 μm) and small-sized (<100 μm) foraminifers, dominated from 50 to 300 m at the same time (Anglada-Ortiz et al., 2021). The study also suggested that, in this region of the Arctic Ocean, pteropods compared to planktonic foraminifers contributed the most to the inorganic carbon standing stocks (66.6–96.5 %) and export production (56.7–98.4%) (Anglada-Ortiz et al., 2021). A study from the northern Barents Sea reported that adults and juveniles (>500 μm) of *L. helicina* dominated the assemblages from 0 to 300 m water depth in December 2019 during the polar night (Zamelczyk et al., 2021).

Our present study provides a seasonal quantification of carbonate contributions from foraminifers and pteropods from this remote and rarely studied Arctic region (Fig. 1). We estimate the seasonal and vertical distribution of the planktonic foraminifers and pteropods and their contribution to the inorganic and organic carbon standing stocks (μg m^{-3}) and export production (mg m^{-2} d^{-1}) over a 650 km long south-north transect from the central Barents Sea into the Arctic Ocean slope and Nansen Basin. These new data shed light on the contribution of the planktonic calcifying organisms to the carbon pump and their life cycle. This work will contribute to improve projections of environmental changes (e.g. ocean acidification) in the region and the reconstruction of past environments based on their fossil shells in sedimentary record. The sampling transect spans the Atlantic zone south of the Polar Front, over the marginal and seasonal ice zone north of the front comprising seven seasonally sampled stations.

2. Material and methods

2.1. Study area

The Barents Sea (annual mean Area = 1.47 10^6 km^2, annual mean Sea Surface Temperature = 0.9℃, annual mean Sea Surface Salinity = 34.2 (Sakshaug and Slagstad, 1991, Smedsrud et al., 2022)), is a shelf sea in the Arctic Ocean. It is influenced by both warm and relatively saline Atlantic Water flowing into the Arctic Ocean, and cold and relatively fresh Arctic Water coming in from the Arctic Ocean, this part being seasonally sea-ice covered (Sundfjord et al., 2020, Lundesgaard et al., 2022) (Fig. 1a). The Atlantic Water reaches the Barents Sea via the Norwegian Atlantic Current until it meets the southward flowing Arctic Water to form the Polar Front, where the first and southernmost station of this study is located (P1) (Fig. 1a). Environmental parameters, such as winds and currents, play an important role on mixing the water column south of the Polar Front, while north of the front a strong pycnocline between the light Polar surface Water and Atlantic Water exists during the productive season (March–October) (Sakshaug and Slagstad, 1991). North of the Polar Front, the stations P2 to P5 are influenced by the Arctic/Polar Water (Fig. 1a). These waters are created by different mixing processes, including surface cooling, sea-ice edge interactions, inflows of meltwater and Atlantic Water (Lundesgaard et al., 2022). The northernmost stations (P6 and P7), located at the northern Svalbard slope and Nansen Basin respectively, are influenced by cold Arctic/Polar Water, as well as Atlantic inflow through the West Spitsbergen Current (Fig. 1a). The strength of the Atlantic inflow varies seasonally, having its maximum during winter and minimum in summer (Vernet et al., 2019; Fer et al., 2022). Previous studies in the last decades have reported an increase in Atlantic (and warmer and more saline) inflow and an increasing abundance of subpolar organisms advected through the west

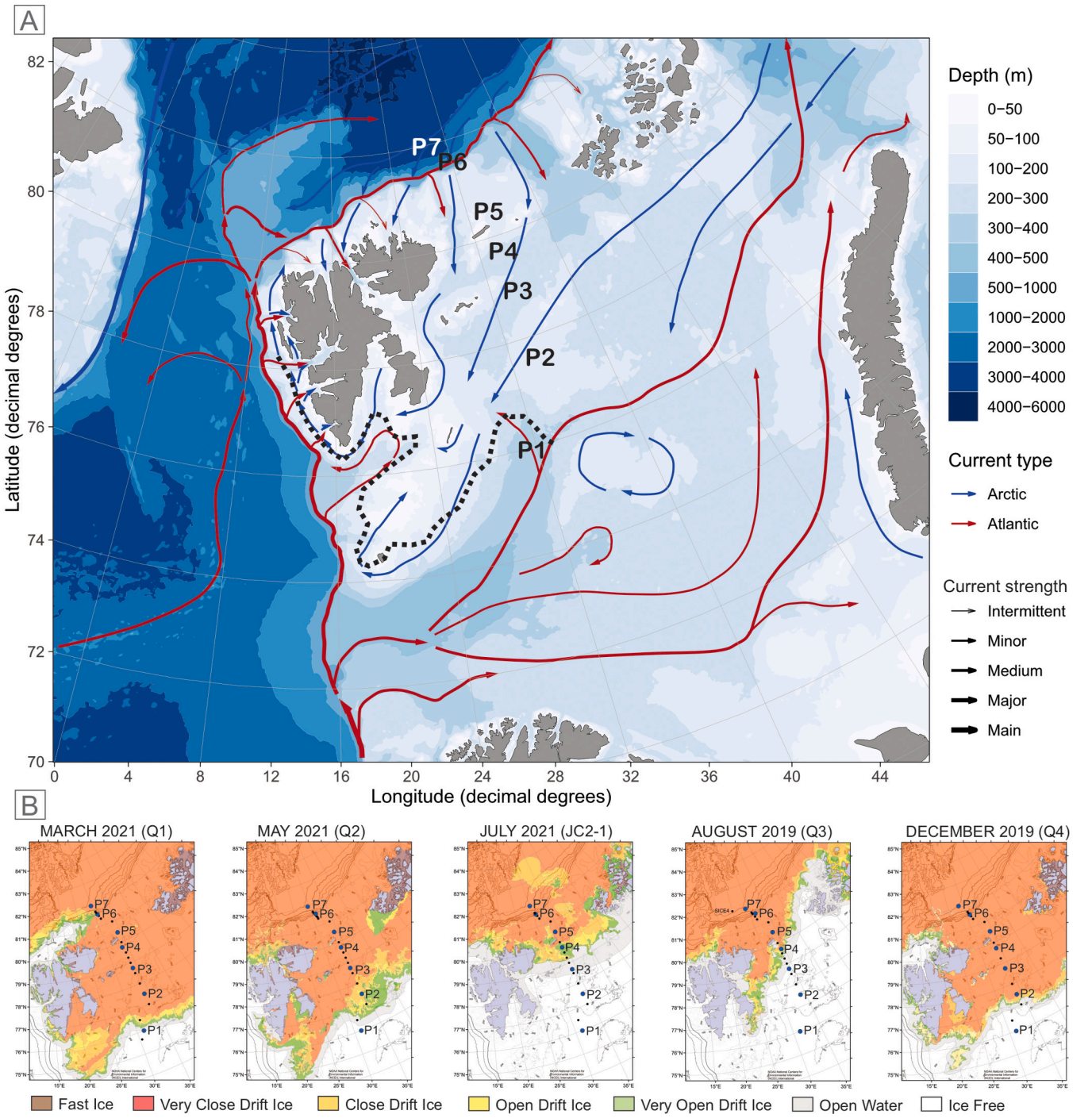

Fig. 1. (A) Location map of study area, including bathymetry and main currents (Atlantic, red arrows, and Polar ("Arctic"), blue arrows)) and strength ("current width") from R package Vihtakari (2020), and location of the Polar Front (black dashed line) from Loeng (1991). (B) Sea ice extent during the sampling months from the Norwegian Ice Service–MET Norway and bathymetry from NOAA National Centers for Environmental Information (NCEI); International Bathymetric Chart of the Arctic Ocean (IBCAO); General Bathymetric Chart of the Oceans (GEBCO).

Spitsbergen current to the northern Svalbard margin, termed "Atlantification" (Bjørklund et al., 2012; Polyakov et al., 2020; Anglada-Ortiz et al., 2021).

Station P1, south of the Polar Front, is ice-free year-round. The location of the sea ice edge changes seasonally and interannually, being at its maximum during March and at minimum during the month of September (Fetterer et al., 2017). In 2019, the sea-ice margin retreated from 75N (1st March 2019) to 80N (16th September 2019), and in 2021 from (below) 75N (1st of March 2021) to 82N (16th September 2021) (from Norwegian Meteorological Institute Ice service, 2022). The stations P2–P7 were seasonally sea-ice covered during the study period (see Fig. 1b), however the sea-ice edge in this region retreated to above 82 N in September and October 2018 (e.g. Anglada-Ortiz et al. (2021); Pieńkowski et al. (2021)). No fast ice (sea ice attached to land (Jacobs et al., 1975)) was recorded during the sampling period in the region (see Fig. 1b).

The general characteristics of the water masses present in the study area are: *Polar Water* (conservative temperature (CT) $\leq$ 0.0℃, density (σ_0) $\leq$ 27.97 kg m^{-3}), *warm Polar Water* (0.0 ℃ < CT < 4.0 ℃, absolute salinity (S_A) < 35.06 g kg^{-1}), *Atlantic Water* (CT > 2.0 ℃, $S_A \geq$ 35.06 g

kg^{-1}), and *modified Atlantic Water* (0.0 ℃ < CT ≤ 2.0 ℃, $S_A \geq 35.06$ g kg^{-1}) following the water mass classification suggested by Sundfjord et al. (2020) (Fig. 2).

2.2. Sampling and sample analyses

Plankton samples were collected onboard the RV *Kronprins Haakon* during the seasonal cruises of the Norwegian national *Nansen Legacy Project* to the Barents Sea in 2019 and 2021 (Table 1). Seven stations were sampled along a latitudinal transect east of the Svalbard archipelago (28.8°–34° E), from 76° N to 82° N covering the shelf, slope, and deep Nansen Basin, and crossing the Polar Front, the SIZ and MIZ (Fig. 1). The stations are numbered from south to north and classified as the Atlantic shelf station (south of the Polar Front) (P1), shelf stations P2–P5 (north of the Polar Front and in the MIZ), slope station (P6) and Nansen Basin station (P7) (Table 1 and Fig. 1). Data from the December cruise (absolute and relative abundance of planktonic foraminifers and pteropods) have been published in Zamelczyk et al. (2021). Data of normalized size, protein content, organic and inorganic standing stocks, and export production of the planktonic foraminifers and pteropods sampled in December 2019 are new to this study as are all other data from the other seasons in 2019 and 2021.

Samples for temperature, salinity and dissolved oxygen, nutrients (nitrite + nitrate, phosphate, silicate, $NO_2^- + NO_3^-$, PO_4^{-3} and $SiOH_4$, respectively), chlorophyll a, and carbonate chemistry were collected during all cruises and published in Reigstad (2022), Søreide (2022), Gerland (2022), Ludvigsen (2022), Jones (2022), Chierici et al. (2021a, 2021b), Jones et al. (2022a, 2022b, 2022c), Vader (2022), and Jones et al. (this issue). Ocean acidification variables (pH, calcite and aragonite saturation states, Ω_{Ca} and Ω_{Ar}, respectively) were determined from the carbonate chemistry samples following methods described in Zamelczyk et al. (2021).

Planktonic foraminifers and pteropods were collected using a midi zooplankton multinet (Hydrobios 64 μm mesh size, net opening of 50 × 50 cm = 0.25 m^2). This mesh size is the most commonly used (Manno and Pavlov 2013; Pados and Spielhagen 2014; Ofstad et al., 2020; Zamelczyk et al., 2021), together with 90 μm (Manno et al., 2012; Anglada-Ortiz et al., 2021) and 100 μm (Meilland et al., 2020) in Arctic and subarctic studies. The non-standardization of methods to collect zooplankton (e.g. by different mesh sizes of plankton nets or sediment traps), is considered to affect the quality and quantity of the collected material (Bednaršek et al., 2012a). The upper 300 m of the water column were vertically towed at regular intervals of 0–50 m, 50–100 m, 100–150 m, 150–200 m, 200–300 m in August 2019 and 0–20 m, 20–50, 50–100, 100–200, 200–300 m (200–290 m in case of P3) in March, May, and July 2021 (Table S1 (*supplementary material*)). Stations shallower than 300 m (Table 1) were sampled using the same intervals down to 170 m and 150 m in case of P2 and P5, respectively. Samples from December 2019 were collected at the intervals: 0–20 m, 20–50 m, 50–100 m, 100–200 m, 200–300 m (P1, P4, and P7); 0–20 m, 20–50 m, 50–80 m, 80–100 m, 100–170 m (P2) or 100–125 m (P5); 0–20 m, 20–50 m, 50–100 m, 100–200 m, 200–280 m (P3); and 0–20 m, 20–50 m, 50–200 m, 200–600 m, 600–750 m (P6) (Zamelczyk et al., 2021) (Table S1).

Immediately after the recovery, the samples were wet sieved though a cascade of sieves of mesh sizes 500, 250, 100 and 64 μm. Living specimens of pteropods and planktonic foraminifers from all size fractions obtained (>500 μm = large size fraction, 250–500 μm = medium size fraction, 100–250 μm = small-medium size fraction, and 63–100 μm = small fraction) were wet picked from the upper 100 m of the water column for protein extraction and measurements (see ***2.3** Organic and inorganic carbon contribution*) and frozen at −80 °C. The rest of the samples were frozen at −20 °C and were analyzed in the laboratory of the Department of Geosciences, UiT the Arctic University of Norway (Tromsø, Norway).

Each frozen sample was thawed and planktonic foraminifers containing cytoplasm and pteropod shells with the animal inside were wet picked and counted. The absolute abundance (individuals per cubic meter (ind m^{-3})) was calculated dividing the number of specimens by the volume of water sampled with the multinet. The volume of water was calculated by the equation:

$$Volume\,[m^3] = -1.2482 + (0.3298 * D\,[m])$$

with **D** being the sampled depth interval.

We classified the foraminifers by size fractions as follows: 63–100 μm as small, 100–250 μm as medium, and 250–500 μm as large. For pteropods, we have attributed each size fraction to the life stage of individuals as follows: 63–100 μm (early veliger stages), 100–250 μm (veliger or early juveniles), 250–500 μm (juveniles), and >500 μm (adults).

Based on the absolute abundances per season, station, and depth, and the average shell diameter of planktonic foraminifers and pteropods (see ***2.3** Organic and inorganic carbon contribution*), we calculated the average normalized size of a model organism of a planktonic foraminifer and a pteropod (see ***3.2** Seasonal and spatial distribution of marine calcifiers*).

2.2.1. Statistical analysis

The statistical analyses were performed using the *ggplot2* package from H (2016) from the *Rstudio* (version 4.2.1) software. To study the relation between our dataset and the environment (salinity and temperature, nutrients, chlorophyll *a*, pH, calcite and aragonite saturation states we have performed a Principal Component Analysis (PCA) and fit the distribution of planktonic foraminifers and shelled pteropods (separately) and the water masses. Moreover, we have performed a multiple linear regression and an Analysis of Variance (ANOVA) to assess the effects of environmental parameters on the abundance of foraminifers and pteropods separately, and to understand which factors best explain their distribution.

2.3. Organic and inorganic carbon contributions

The organic carbon was estimated as the individual protein content (as reported by Meilland et al. (2016) and Schiebel and Movellan (2012)) of 148 specimens of planktonic foraminifers and 300 specimens of pteropods that were individually and randomly picked from all stations and seasons onboard and were frozen at −80℃ (see ***2.2** Sampling and sample analyses*). The individual protein content is used as a proxy to estimate the organic carbon content of the organism, where 1 mg of protein equals to 1 mg of organic carbon. We followed the BCA (bicinchoninic acid) protocol from Meilland et al. (2016) using the nanospectrophotometer (NanoDrop 2000®) at the Department of Arctic and Marine Biology, UiT the Arctic University of Norway (Tromsø, Norway). This technique does not affect their aragonitic and calcitic shells, allowing us to use them for further analyses, e.g. size measurements (diameter and mass) or scanning electron microscopy (SEM).

The mass of solid inorganic carbon ($CaCO_3$) of planktonic foraminifers and pteropods was estimated by measuring the shell diameter of the specimens analyzed for protein content, applying the equations previously reported for foraminifers ($y_w = 2.04*10^{05}x^{2.2}$ from Meilland et al. (2018)) and pteropods (for *L. helicina)* ($DW = 0.137*D^{1.5055}$ from Bednaršek et al. (2012a)) separately. The 148 planktonic foraminifers (*48* specimens from 63 to 100 μm; *92* from 100 to 250 μm; and *8* from 250 to 500 μm) and 300 pteropods (*24* from the 63–100 μm size fraction; *67* from 100 to 250 μm; *59* from 250 to 500 μm; and *150* > 500 μm) were photographed with a DMC4500 camera attached to a Leica Z16 APO binocular (magnification × 0.57–9.2). We measured their diameter (pteropods) and minimum diameter (foraminifers) (see Fig. S1) using the ImageJ software (Schneider et al., 2012).

The carbon standing stocks (μg m^{-3}) of foraminifers and pteropods have been estimated by extrapolating their protein content and shell diameter, for the organic or inorganic contribution, respectively (see ***3.3***

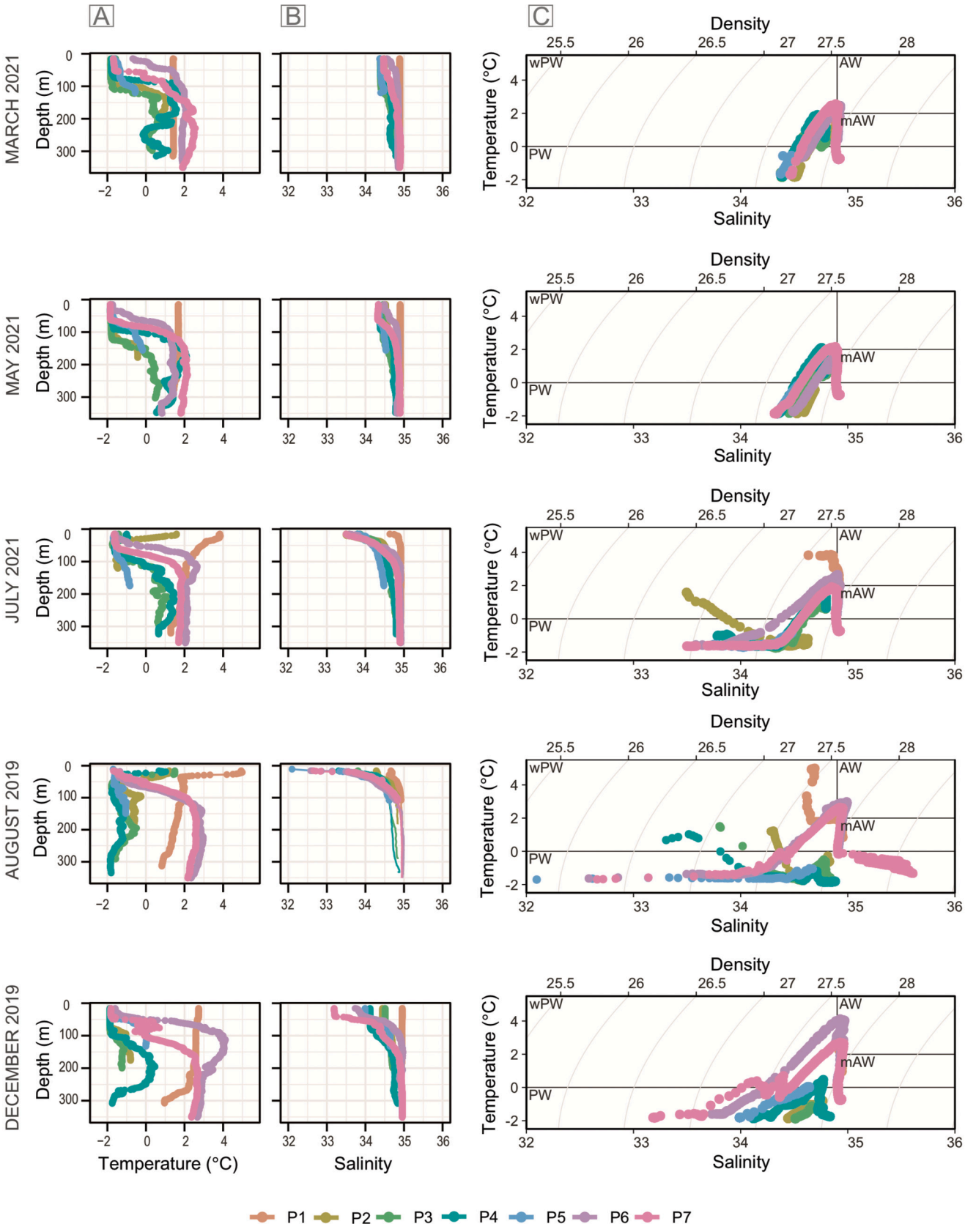

Fig. 2. Vertical temperature (A) and salinity (B) of the transect from the different seasons. Temperature-Salinity (T-S) profile (C) with water mass classification from Sundfjord et al., 2020: Polar Water (PW), warm Polar Water (wPW), Atlantic Water (AW), and modified Atlantic Water (mAW).

Table 1
Location, latitude, longitude, water depth, multinet sampling intervals (August, March, May, and July) and multinet sampling dates from each cruise (Q3 = August 2019, Q4 = December 2019, Q1 = March 2021, Q2 = May 2021, JC2-1 = July 2021).

	Location	Latitude (N)	Longitude (E)	Water depth (m)	Sampling interval(m)	Date (Q3)	Date (Q4)	Date (Q1)	Date (Q2)	Date (JC2-1)
P1	Shelf	76	31.22	322	0–300	08.08.2019	12.12.2019	05.03.2021	30.04.2021	14.07.2021
P2	Shelf	77.5	34	190	0–170	12.08.2019	10.12.2019	07.03.2021	02.05.2021	15.07.2021
P3	Shelf	78.7	34	307	0–300	–	09.12.2019	08.03.2021	03.05.2021	17.07.2021
P4	Shelf	79.7	34.23	332	0–300	14.08.2019	08.12.2019	09.03.2021	05.05.2021	18.07.2021
P5	Shelf	80.5	33.96	158	0–150	16.08.2019	06.12.2019	12.03.2021	07.05.2021	19.07.2021
P6	Slope	81.5	31.5	840	0–300	18.08.2019	05.12.2019	16.03.2021	10.05.2021	22.07.2021
P7	Basin	82	28.8	3120	0–300	21.08.2019	02.12.2019	17.03.2021	14.05.2021	24.07.2021

Organic and inorganic carbon of marine calcifiers) and integrating their absolute abundances from the upper 100 m of the water column following the published literature (Schiebel and Hemleben, 2000; Schiebel, 2002; Bednaršek et al., 2012a; Meilland et al., 2016; Anglada-Ortiz et al., 2021). Similarly, the export productions (mg m^{-2} d^{-1}) have been estimated using protein content and shell diameter, their abundances between 50 and 100 m (or 80–100 m), except for station P6 in December, which was 200 m, and their test sink velocity (Schiebel and Hemleben, 2000; Schiebel, 2002; Bednaršek et al., 2012a; Meilland et al., 2016; Anglada-Ortiz et al., 2021).

3. Results

3.1. Environmental properties of water masses

In summer (August and July) and late autumn (December) we observed a wider range in temperatures and salinities, associated with the higher atmospheric temperatures and melting of sea ice, compared to winter (March) and spring (May) (Fig. 2a, 2b). In terms of temperature, the slope station (P6) and basin station (P7) (ice covered during all cruises, see Fig. 1b) varied less along the seasons than the other stations (see Fig. 2a). Moreover, we observed lower surface salinities in July, August, and December (Fig. 2b). The stations P5, P6 and P7 were associated with very closed drift ice during all sampling seasons, while stations P2 and P4 were associated with variable sea ice conditions, consisting of very open drift ice, open drift ice, and very close drift ice in August, July and May, respectively (Fig. 1b). In all seasons, the surface water (20–50 m) consisted of Atlantic and modified Atlantic Water at the stations P1, P6 and P7, while the other stations (P2–P5) were characterized by Polar Water and warm Polar Waters (Fig. 2c).

3.2. Seasonal and spatial distribution of marine calcifiers

A clear seasonal pattern of temporal and spatial distribution of the studied planktonic calcifiers has been identified. The overall highest seasonal absolute abundances of living planktonic foraminifers and pteropods (ind m^{-3}) were observed in August 2019, followed by July

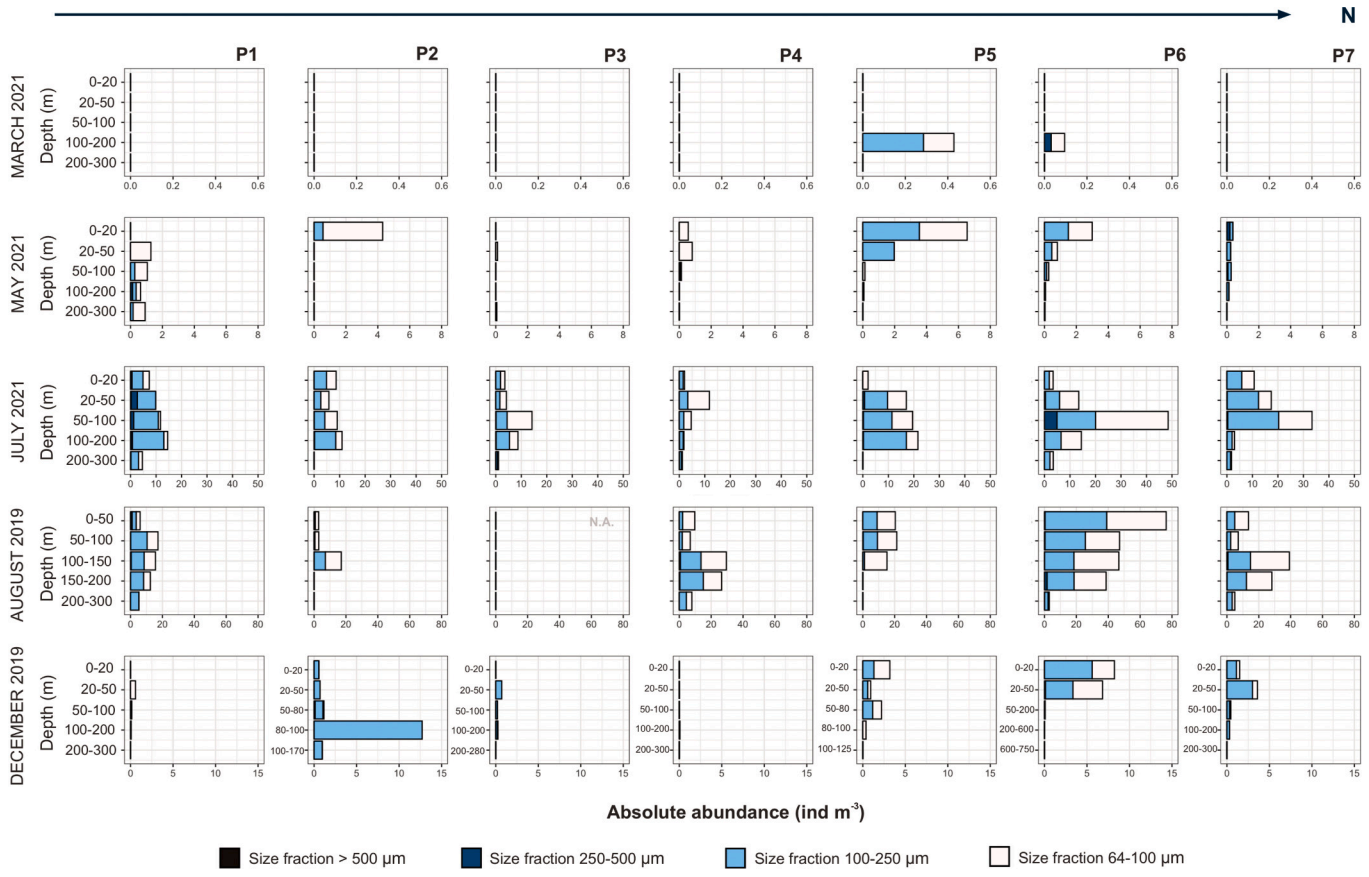

Fig. 3. Absolute abundances (ind m^{-3}) of planktonic foraminifers containing cytoplasm in the various size fractions (note change in x-axis) along P stations (columns) and seasons (rows). December data from Zamelczyk et al. (2021) (note different y-axes).

2021 and May 2021, with the lowest in March 2021 (Figs. 3, 4 and 9). Regarding the vertical distribution of marine calcifiers and their group relative abundance (planktonic foraminifers vs pteropods) and the environmental conditions, from now on we will refer to the stations with the following categories: shelf station south of the Polar Front (Atlantic station P1), shelf stations north of the Polar Front (Polar stations P2–P5), slope station (P6), and basin station (P7). The environmental parameters seem to follow a depth distribution, and in general the abundance of shelled pteropods is the highest when the temperature is low (Fig. S2).

In March, the highest abundances (22 ind m^{-3}) of calcifiers were found at P2 at depth (100 –200 m), while the lowest (0 ind m^{-3}) at P1 throughout the water column (0–20, 20–50, 50–100, and 100–200 m), P2 at the surface and subsurface (0–20, 20–50, and 50–100 m), and P3 at the surface (0–20 m) (Figs. 3 and 4). Foraminifers were only present at stations P5 and P6 at depth (100–200 m) in very low abundances (0.4 and 0.1 ind m^{-3}, respectively), while pteropods completely dominated the assemblages (av 99%, min 87%, max 100%) (Figs. 3, 4 and 9a). The foraminiferal community was dominated by medium sized organisms, while the pteropod community was dominated by small veliger larvae (Figs. 3 and 4) (see *supplementary material* for details).

In May, the highest abundance (50 ind m^{-3}) of calcifiers occurred at P2 at subsurface (50–100 m). In this season we observed an increasing presence of planktonic foraminifers (av 30%) when compared to March and to pteropods (av 70%) (Figs. 3 and 9a). The basin station was the only one dominated by planktonic foraminifers, while pteropods dominated the upper 300 m of the water column at the Polar stations and represented (approximately) half of both groups at the Atlantic and slope stations, (Fig. 9a) (see *supplementary material* for details). The foraminiferal community was dominated by small-medium sized organisms, while the pteropod community was dominated by veliger/young juveniles (Figs. 3 and 4).

In July, the highest abundance (60 ind m^{-3}) of calcifiers was found at P3 at subsurface (20–50 m), and the lowest (1 ind m^{-3}) at depth (200–300 m) (Figs. 3 and 4). Foraminifers dominated the assemblages (av 74%), while pteropods were less abundant at depth and at the northernmost stations (av 26%) (Figs. 3, 4 and 9a). In general foraminifers dominated throughout the upper water column at the Atlantic station, slope, and basin stations, while pteropods dominated the Polar stations, except at P5 (Fig. 9a) (see *supplementary material* for details). The planktonic foraminiferal community was dominated by small and small-medium specimens, while pteropods by juveniles/young adults (Figs. 3 and 4).

In August the highest (82 ind m^{-3}) abundances of calcifiers were found at station P5 at depth (100–150 m) and the lowest (4 ind m^{-3}) at stations P6 at depth (200–300 m) (Figs. 3 and 4). Opposite to the other stations, where high abundances were found at the surface (0–50 m) and decreasing with depth, the abundances at P5 (mainly pteropods) increase at depth (100–150 m) (Fig. 4). Almost no pteropods were collected from the slope (P6) and basin (P7) stations in this (or any) season (Fig. 4). In general, foraminifers dominated the upper 300 m of the water column at the Atlantic station, slope, and basin stations, while pteropods at the Polar stations, with exception of P4 (Fig. 9a, 9b). The planktonic foraminiferal community was dominated by small and small-medium specimens, while pteropods by juveniles/young adults (Figs. 3 and 4) (see *supplementary material* for more details).

In December, the highest abundance (43 ind m^{-3}) of calcifiers was found at P5 at surface (0–50 m), while the lowest (<0.04 ind m^{-3}) at P1, P6, and P7 all at depth below 200 m (Figs. 3 and 4). On average, the abundance of pteropods (57%) was higher than the foraminifers along the transect and they dominated the assemblage in the Polar stations (av 82%, min 0%, max 100%) (Figs. 3, 4 and 9a, 9b). The foraminiferal community was dominated by medium and small-medium specimens,

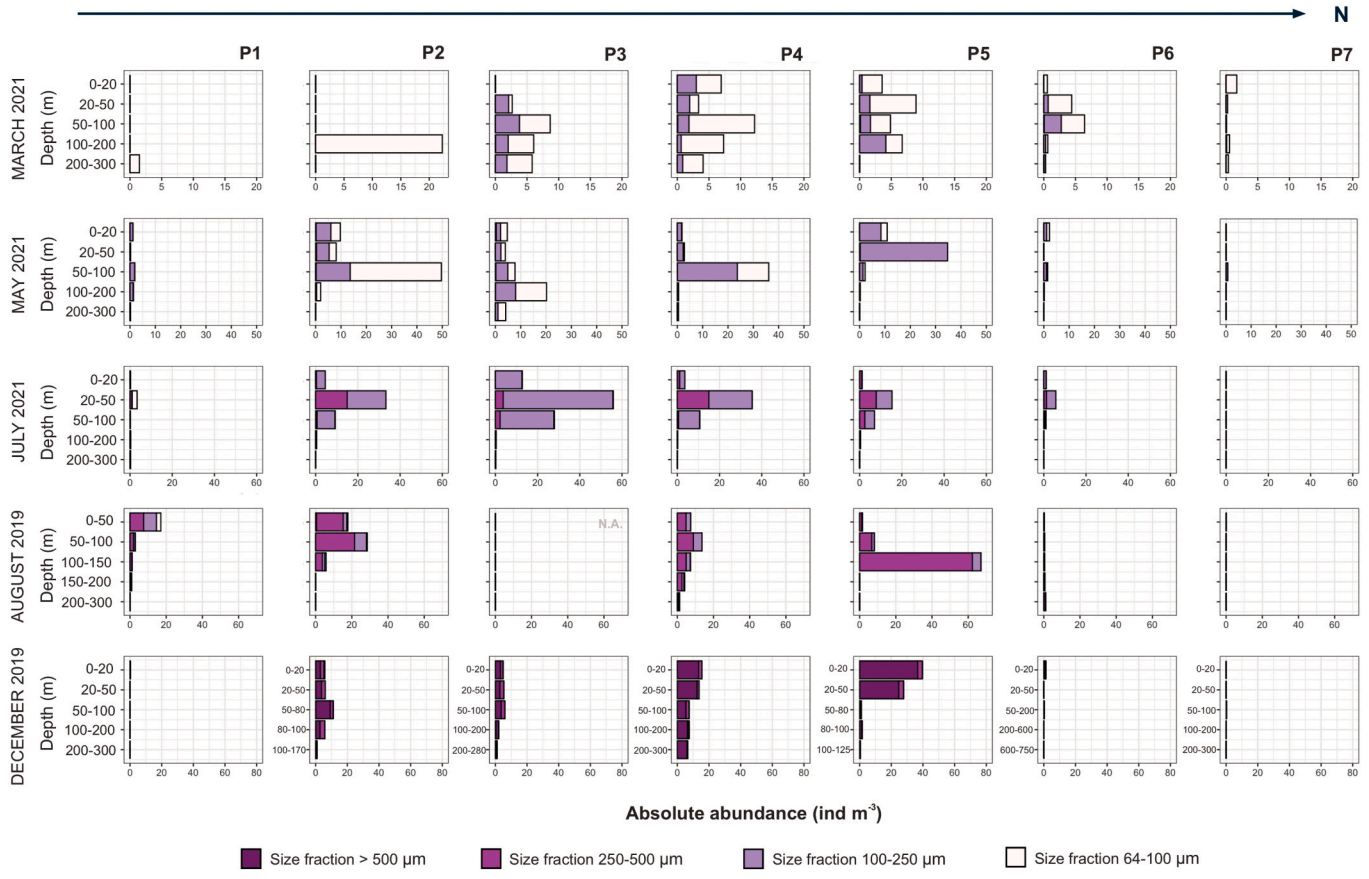

Fig. 4. Absolute abundances (ind m^{-3}) of pteropod shells containing the animal in the various size fractions (note change in x-axis) along P stations (columns) and seasons (rows). December data from Zamelczyk et al.(2021) (note different y-axes).

while the pteropods by adults (see Figs. 3, 4 and Zamelczyk et al. (2021)).

3.3. Organic and inorganic carbon of marine calcifiers

3.3.1. Protein content of foraminifers and pteropods

The protein content of 148 and 300 living foraminifers and pteropods, respectively, was correlated to the length of the organisms, being directly proportional for foraminifers and logarithmic for pteropods (Fig. 5). The protein-length of pteropods was better correlated than in the case of planktonic foraminifers (R^2 = 0.68 and R^2 = 0.2, respectively) (Fig. 5). The protein content of foraminifers, as well as their size, were significantly smaller in terms of values and variability compared to pteropods (Fig. 5).

3.3.2. Seasonal variability of planktonic foraminifers and pteropod size distribution

The normalized size of calcifiers based on their abundance, changed along the seasons. For both planktonic foraminifers and pteropods, we observed larger average sizes in December 2019, followed by August 2019, July 2021, and May 2021, and the lowest, in March 2021 (Fig. 6). The size range of foraminifers from 0 to 300 m and the upper 100 m was widest in December 2019 and May 2021 (Fig. 6a, 6b), and in the case of pteropods, in August and December 2019 and May 2021 (Fig. 6d, 6e). Below 100 m water depth, the highest size range of foraminifers was in March 2021 (Fig. 6g) and for pteropods, December 2019 (Fig. 6f). We did not observe larger organisms below 100 m that could suggest ontogenic vertical migration.

3.4. Seasonal and spatial variability in carbon dynamics

3.4.1. Carbon standing stock in the upper 0–100 m water depth [μg m^{-3}]

We have recorded the highest carbon standing stocks of both pteropods and foraminifers combined in December 2019 (av 458 ± 520 μg m^{-3}; min 3 μg m^{-3}; max 1401 μg m^{-3}), followed by August 2019 (av 269 ± 368 μg m^{-3}; min 7 μg m^{-3}; max 1002 μg m^{-3}), July 2021 (av 79 ± 75 μg m^{-3}; min 21 μg m^{-3}; max 233 μg m^{-3}), and May 2021 (av 52 ± 51 μg m^{-3}; min 3 μg m^{-3}; max 113 μg m^{-3}), and the lowest in March 2021 (av 12 ± 12 μg m^{-3}; min 0 μg m^{-3}; max 29 μg m^{-3}) (Fig. 7a and Table S2). The highest carbon standing stocks were found along the polar stations (P2 in August and May, P5 in December, P4 in March, and P3 in July), and lowest at the Atlantic, slope and basin stations (P1 in December and March, and P7 in August, May, and July) (Fig. 7b, Table S2). On average, the organic contribution to the total carbon of each group is different, because pteropods are larger (av 15%) than foraminifers (av 0.1%). In all seasons, pteropods dominate the total (both organic and inorganic) carbon standing stocks of the planktonic calcifiers (av 50%), recording their highest contribution at the shelf stations (av c. 70–100%) (Table S2) (see also *supplementary material* for more details).

3.4.2. Carbon export production at 100 m water depth [mg m^{-2} d^{-1}]

We recorded the highest carbon export production of foraminifers and pteropods together in August 2019 (av 149 ± 249 mg m^{-2} d^{-1}; min 0.4 mg m^{-2} d^{-1}; max 647 mg m^{-2} d^{-1}), followed by December 2019 (av 76 ± 93 mg m^{-2} d^{-1}; min 0.02 μg m^{-3}; max 232 mg m^{-2} d^{-1}), July 2021 (av 32 ± 31 mg m^{-2} d^{-1}; min 5 mg m^{-2} d^{-1}; max 95 mg m^{-2} d^{-1}), and May 2021 (av 29 ± 38 mg m^{-2} d^{-1}; min 0.9 mg m^{-2} d^{-1}; max 77 mg m^{-2} d^{-1}), and the lowest in March 2021 (av 8 ± 8 mg m^{-2} d^{-1}; min 0 mg m^{-2} d^{-1}; max 17 mg m^{-2} d^{-1}) (Fig. 8a). The highest carbon export production was found along the polar stations (P2 in August, P3 in March and July, and P4 in December and May), while the lowest at the Atlantic, slope and basin stations (P1 in December and March, P6 in May, and P7 in August and July) (Fig. 8b). The organic contribution of pteropods was larger (av 14%) than foraminifers (av 0.07%). In all seasons, pteropods drove the total (organic and inorganic) carbon export production (av >66%), recording their highest contribution along the shelf stations (c. 75–100%). In general, the export production followed the same trend as

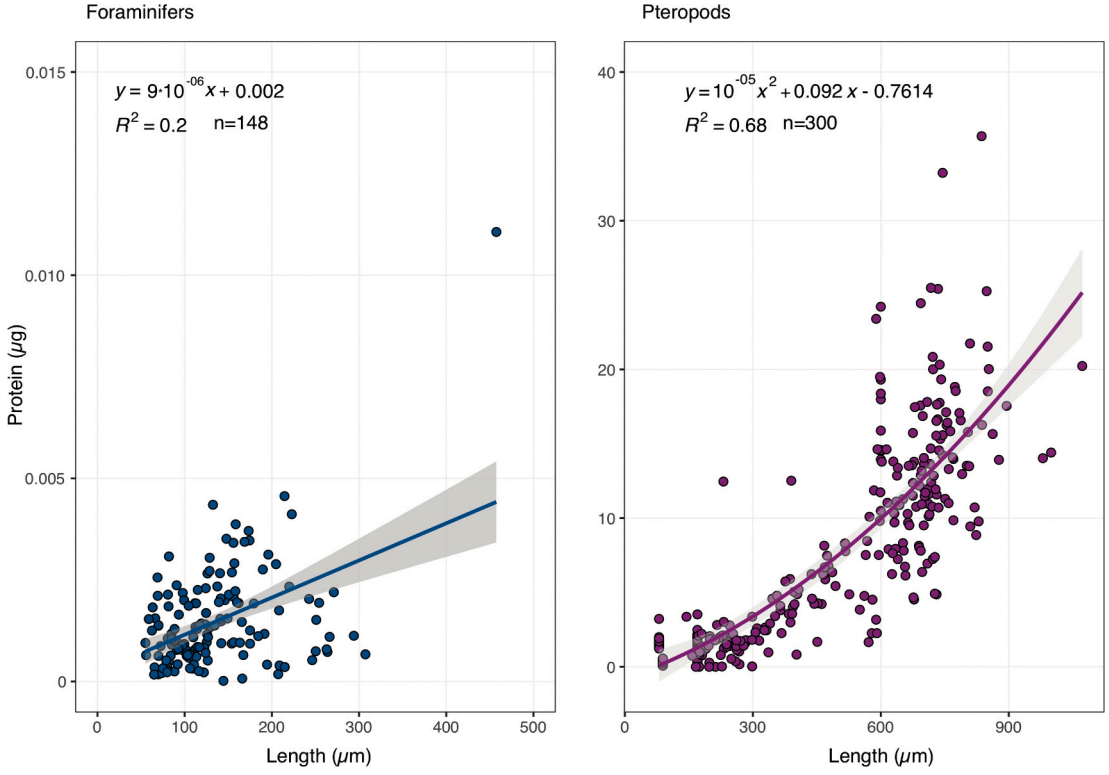

Fig. 5. Protein content (μg) of foraminifers (left) and pteropods (right) relative to shell length (μm) with the equations used to estimate organic content (see 2.3 Organic and inorganic carbon contribution). Note different scales on the x- and y-axis.

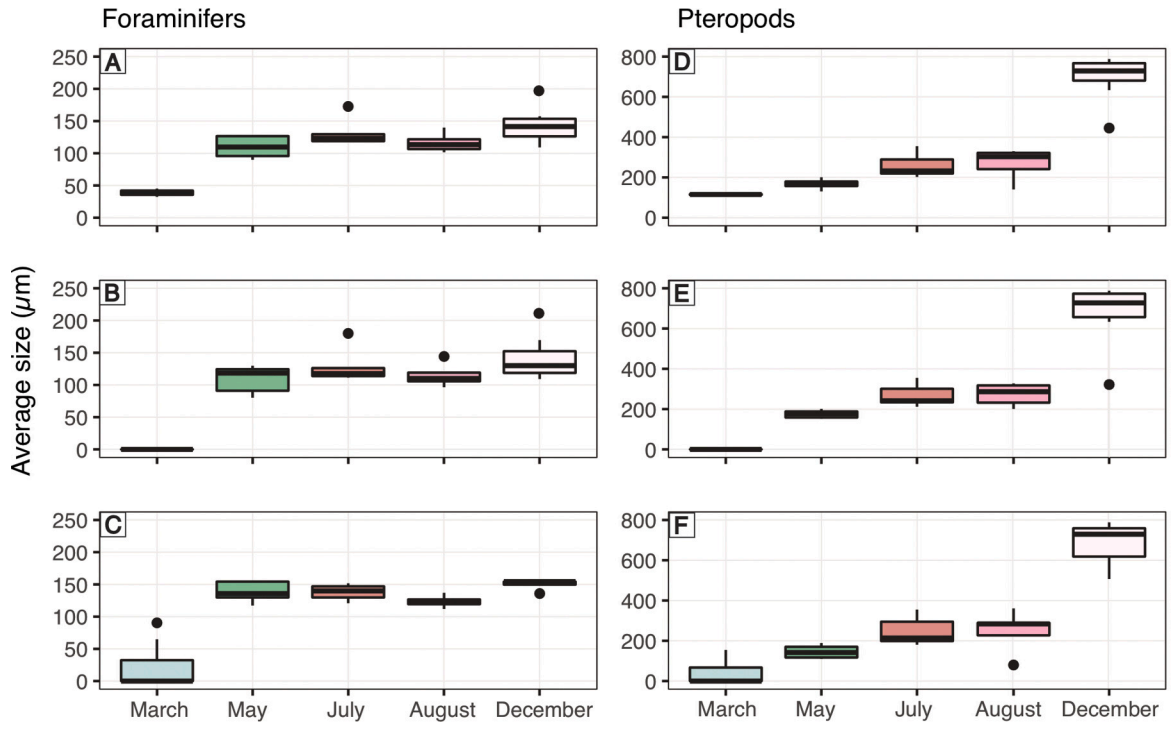

Fig. 6. Average size (μm) of foraminifers (integrating 0–300 m (A), 0–100 m (B), and below 100 m (C)) and pteropods (integrating 0–300 m (D), 0–100 m (E), and below 100 m (F) for each season. The black dots are outliers from the seasonal measurements. Note different scales on the y-axes.

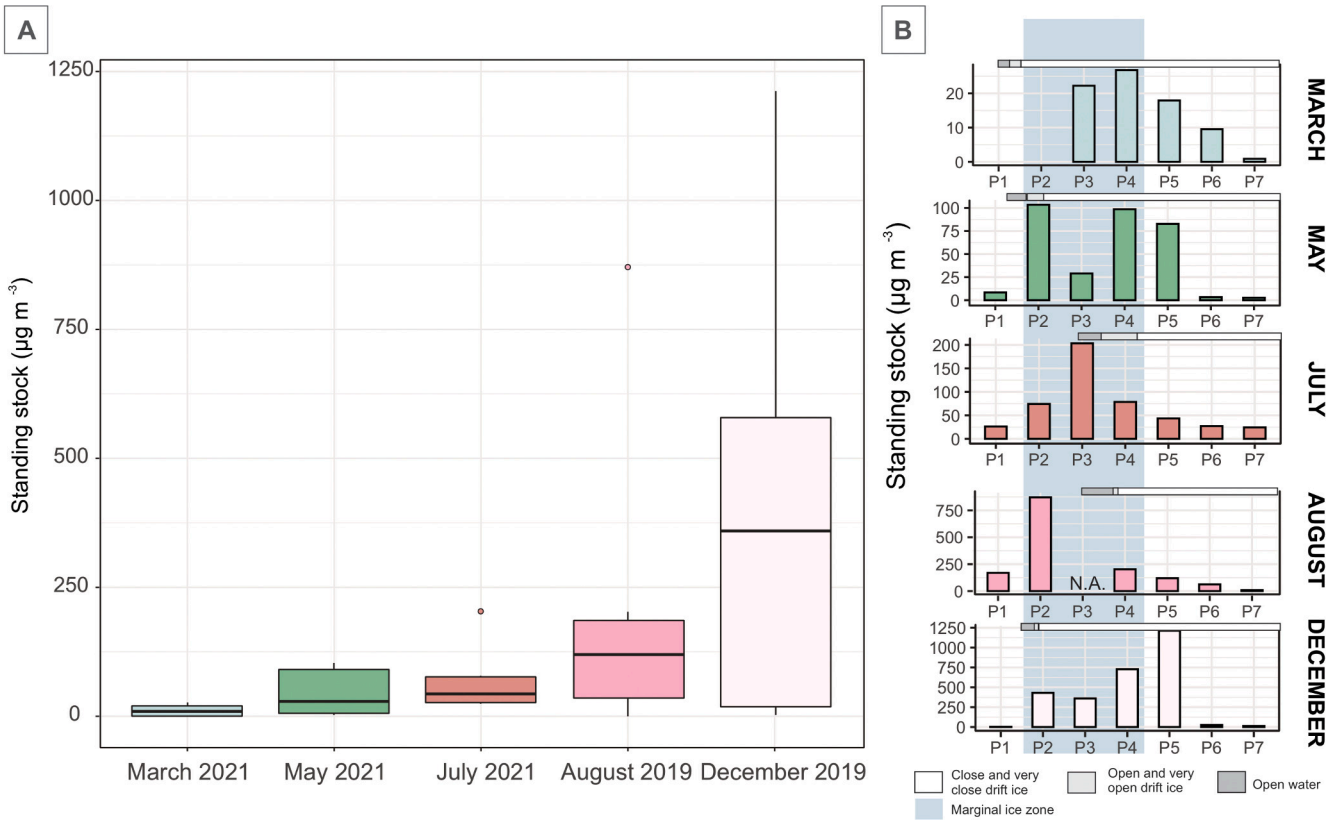

Fig. 7. Panel A: Total carbon (organic and inorganic) standing stocks (from 0 to 100 m depth, μg m^{-3}) from planktonic foraminifers and shelled pteropods in five different seasons, each of them represented by a different color (August 2019: pink; December 2019: light pink; March 2021: light blue; May 2021: green; and July 2021: orange). Panel B: Detailed standing stocks at each station during the different seasons and information about sea ice cover (close and very close drift ice: white; open and very open drift ice: light grey; open water: grey) and seasonal ice zone (blue) (note different y-axes at panel B).

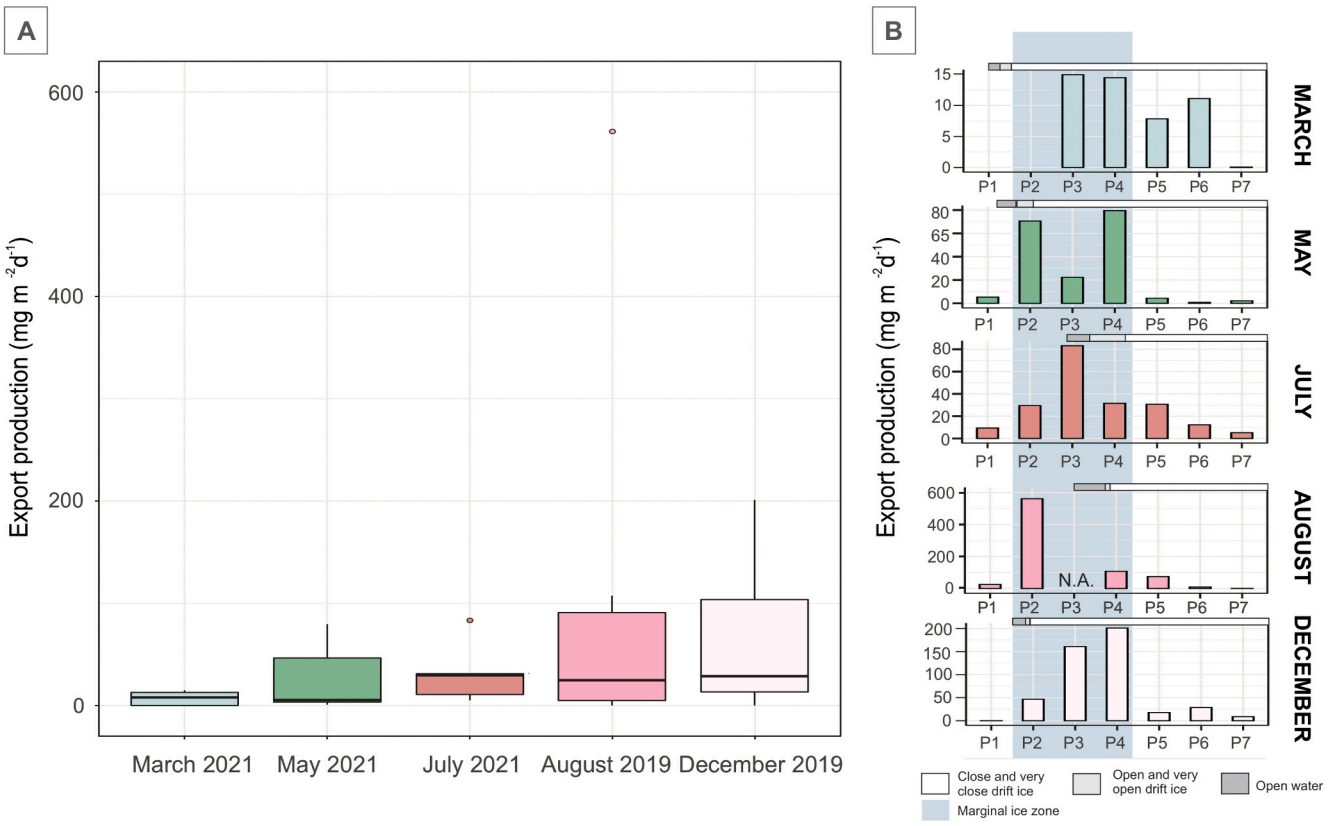

Fig. 8. Panel A: Total carbon (organic and inorganic) export production (at 100 m depth, mg $m^{-2}d^{-1}$) from planktonic foraminifers and shelled pteropods in five different seasons, each of them represented by a different color (August 2019: pink; December 2019: light pink; March 2021: light blue; May 2021: green; and July 2021: orange). Panel B: Detailed export production at each station during the different seasons and information about sea ice cover (close and very close drift ice: white; open and very open drift ice: light grey; open water: grey) and seasonal ice zone (blue) (note different y-axes at panel B).

the carbon standing stocks (Figs. 7 and 8). The values that differ the most were found at P5 in December (Figs. 7 and 8), with high abundances of pteropods (young adults) at the surface (0–50 m) (Fig. 4) (see also *supplementary material* for more details).

4. Discussion

In this study we have observed the highest abundance of planktonic foraminifers and pteropods in August and July, followed by December and May, and with a minimum in March. However, the largest diameter of calcifiers and the associated total carbon standing stock and export production were estimated for December, followed by August and July, May, and March. We find the highest production of foraminifers in summer in the Atlantic zones south of the Polar front and in the Arctic Ocean in the northern part of the MIZ (P1, P6 and P7; Fig. 3). For pteropods production is highest in the polar stations and along the MIZ and SIZ during most seasons (P2–P5; Fig. 4).

4.1. Pattern in abundance, seasonality and water masses

Due to difficulties of sampling and accessibility in the Arctic region, most studies have been carried out during the summer season. From all Arctic regions, planktonic foraminifers have been mostly studied in the Fram Strait (e.g. Carstens et al., 1997; Volkmann, 2000; Stangeew, 2001; Manno and Pavlov, 2013; Pados and Spielhagen, 2014; Greco et al., 2022). Here, the abundances of living planktonic foraminifers are 30–60 ind m^{-3} in June-July-early August (Volkmann, 2000; Manno and Pavlov, 2013; Pados and Spielhagen, 2014), while the mean abundance of foraminifers in the Arctic Basin was 25.4 ind m^{-3} (Tell et al., 2022). Carstens et al. (1997) reported different maxima in abundances along the Fram Strait in August of 1250 ind m^{-3} and 100 ind m^{-3} at 78° and 80°N, respectively. The abundances in the Barents Sea (6–12 ind m^{-3}) (Volkmann, 2000), are comparable to the current study (5–15 ind m^{-3}, and 10–35 ind m^{-3} in July and August, respectively). Ofstad et al. (2020) reported abundances in the southern Barents Sea in April (0–6 ind m^{-3}) comparable to May in the current study; while the highest were found in June (436 ind m^{-3}) and exceeding any of the abundances found in the summer months in the northern Barents Sea (Fig. 3). The higher values compared to this study could be attributed to a higher productivity in the southern Barents Sea compared to the northern part and/or influence of strong seepage of methane probably causing upwelling (Ofstad et al., 2020). The abundances found along the north Svalbard margin in September (2.3–52.6 ind m^{-3}, Anglada-Ortiz et al., 2021) agrees with the values found in the northern Barents Sea in July and August (Fig. 3).

In general for pteropods, lower abundances were reported compared to the present study in the southern Barents Sea (Ofstad et al., 2020) and the northern Svalbard margin (Anglada-Ortiz et al., 2021), probably related to local differences in water masses and presence/absence of sea ice. Abundances from the Atlantic shelf station (P1) from August and July are comparable to the results from the southern Barents Sea in June and April, respectively (Ofstad et al., 2020).

The stations P1 (south of the SIZ), and P6–P7 (north of the SIZ) have generally the lowest (total) abundances in all seasons. Planktonic foraminifers are more abundant in the Atlantic influenced stations (P1, P6 and P7), while pteropods are more abundant in the Arctic productive stations P2–P5 (Figs. 9 and S3). The distribution of planktonic foraminifers observed in the current study is associated with temperature, with higher abundances in warmer waters (Atlantic influenced stations P1, P6 and P7) (Figs. 3, S2 and S3). Their vertical distribution does not follow a specific depth pattern, but it changes through seasons (Fig. 3). In spring and winter, their highest abundances are found at the upper

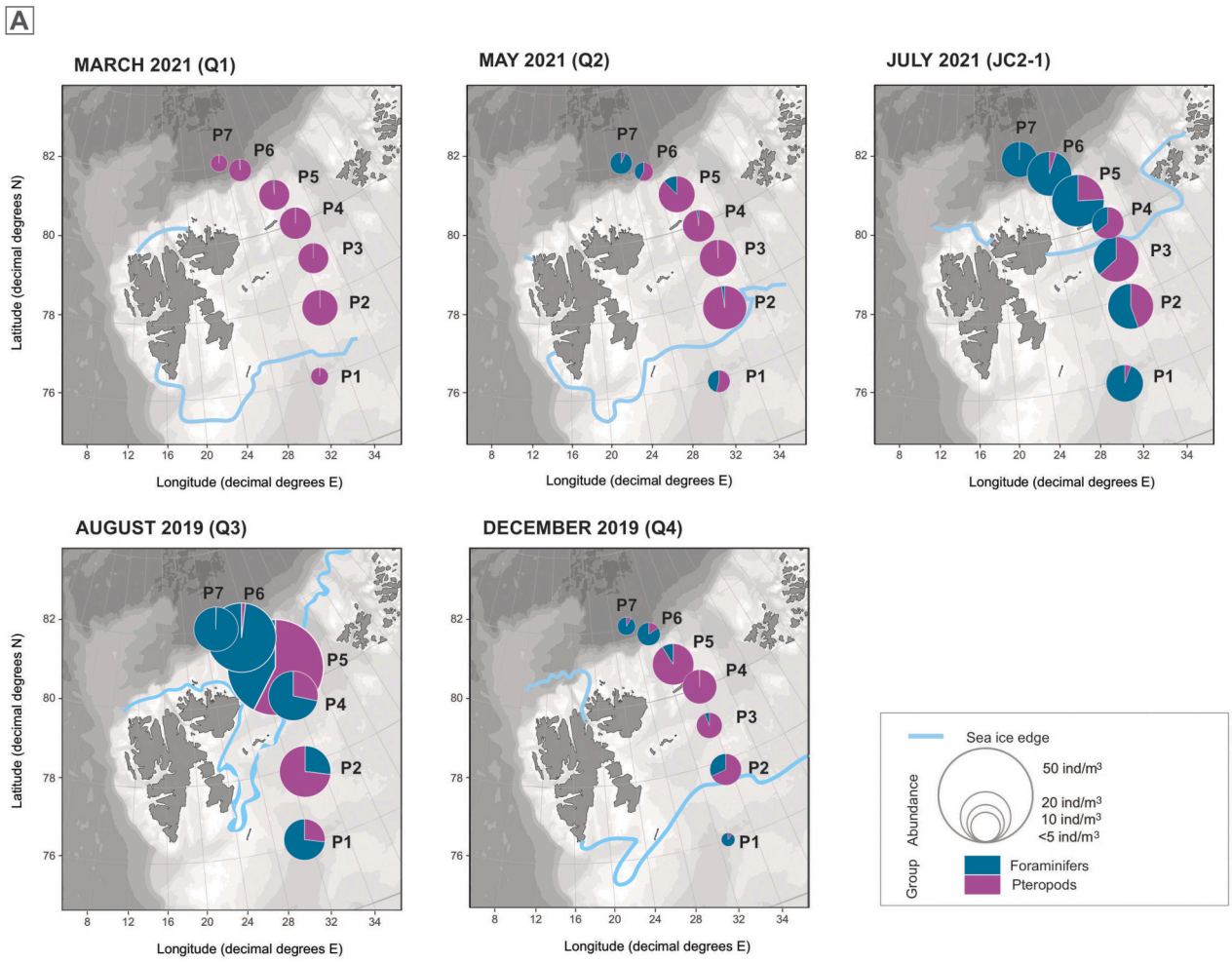

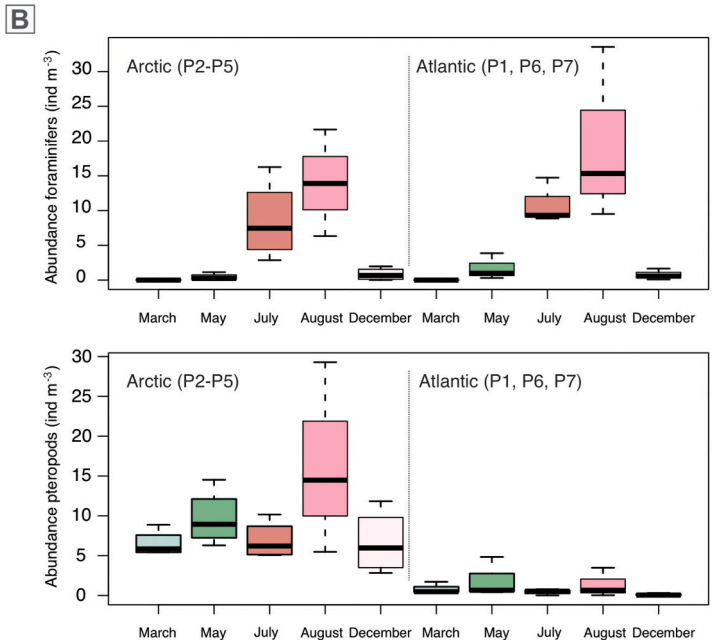

	p value
Abundance/season	0.223
Abundance/water mass	0.408
Season/Water mass	0.817

	p value
Abundance/season	0.868
Abundance/water mass	0.0000302 ***
Season/Water mass	0.612

Fig. 9. Panel A: Depth integrated abundance (ind m^{-3}) of all size fractions of planktonic foraminifers (dark blue) and shelled pteropods (purple) from the upper 300 m of the water column (with exception of station P6 in December, which only considers the upper 200 m), and sea-ice edge from the Norwegian Ice Service–MET Norway (in light blue). The size of the circles represents the total absolute abundance. Panel B: Distribution and results of the two-way ANOVA test of planktic foraminifers (upper panels) and pteropods (lower panels) in the Arctic (P2 – P5) and Atlantic (P1, P6 and P7) influenced stations during all seasons. ***$p < 0.01$.

50–100 m of the water column, while in summer they are spread throughout the water column (Fig. 3) and potentially following the distribution of food. Their abundances and distribution are significantly explained ($p < 0.05$) by the temperature and nutrients (NO_2^-, NO_3^- and $SiOH_4$) (Table S6). Reported possible controlling factors of the distribution of calcifiers, foraminifers specifically, are temperature and chlorophyll (as a measure of surface productivity), but also sea-ice cover and therefore, inorganic nutrient availability (Volkmann, 2000; Pados and Spielhagen, 2014; Greco et al., 2019). Several studies found the highest abundances of planktonic foraminifers along the productive sea-ice margins in the Arctic Ocean (Carstens et al., 1997; Volkmann, 2000; Pados and Spielhagen, 2014). These studies were mainly carried out during the late spring or summer months (June-August) and some of them also included the dead (=empty) foraminifers. Our observations of the highest abundances of planktonic foraminifers and pteropods during the summer months (July and August) and at the stations located close to the sea ice edge and in the SIZ in all studied seasons concur well with previous data (Fig. 9a).

The absence (zero abundance) of planktonic foraminifers during winter (March) and the increasing values during spring (May) suggest two possible scenarios: planktonic foraminifers are either seasonally advected from the south by the Atlantic currents and/or during winter they are in a dormant stage resting within the sea ice (as reported by Nigam (2005); Ross and Hallock (2016); Meilland et al. (2022)). The repeatedly higher abundances found at the slope (P6) and basin (P7) stations, influenced by Atlantic currents, combined by the zero abundances found in March, suggest that both processes were at work and followed by their capacity to reproduce rapidly asexually, as observed in the Greenland Sea (Meilland et al., 2022). In the western Barents Sea (Storfjorden) planktonic foraminifers and shelled pteropods were found under ice in late winter (March 2003) (Werner, 2005). We believe therefore, a "nursery" role of the sea ice could exist during winter months for pteropods, but especially for foraminifers. This is the case for other groups such as copepods (Søreide et al., 2010). Specimens of *N. pachyderma* would overwinter as they do in Antarctica (Lipps and Krebs, 1974; Spindler and Dieckmann, 1986) and use a multigenerational strategy combining sexual and asexual reproduction to repopulate the environment successfully within a short time frame (Meilland et al., 2022). Recent laboratory experiments on living individuals of *N. pachyderma* captured from the Greenland Sea documented dormancy and inactivity stages (Westgård et al., 2023).

The low abundances of pteropods together with the smaller sizes in late winter might be due to presence of offspring from the late summer populations. The increasing proportion of larger organisms, as well as their normalized size may be indicative of their life cycle (Fig. 6). The pteropod species *Limacina helicina*, one of the most ubiquitous species in the Arctic, can be found from temperate to polar regions (Bednaršek et al., 2014b; Peck et al., 2016). It is most abundant in the Arctic stations P2–P5 likely following the spring and summer blooms of phytoplankton and zooplankton. *Limacina helicina* is considered an omnivore collecting food using their mucous webs (Lalli and Gilmer, 1989; Gannefors et al., 2005; Conley et al., 2018). At the same time, *L. helicina*, serves as an important food source for larger zooplankton, including the non-shelled pteropod *Clione limacina*, but also for fish, such as polar cod, and sea birds (Gannefors et al., 2005 and references therein). In our study *L. helicina* is most abundant in summer and autumn with large specimens, and less abundant and with juveniles in winter (March) and spring (May) (Fig. 4). The very low abundances found in March agree with the scarce presence (almost zero) reported during pre-spring bloom in a Canadian fjord (Wang et al., 2017). Our observed seasonal pattern is furthermore similar to other studies. In Kongsfjorden, Svalbard, *L. helicina* has a life span of one year, with one or two new generations per year (in spring and summer) (Gannefors et al., 2005). They reach their maximum abundance in late summer and can reach a maximum size of 13 mm (Gannefors et al., 2005; Wang et al., 2017). The highest flux of pteropods in deep sediment traps from the Norwegian Sea (Lofoten Basin at 69° N, Bear Island at 76° N and Fram Strait at 79° N) was recorded in October (Meinecke and Wefer, 1990). Shallow sediment traps from the Fram Strait recorded a rapidly increasing flux of pteropods in summer (July–August) or early autumn (September–October) when it becomes stable until February (Busch et al., 2015). The distribution of shelled pteropods from our study is also associated with temperature, finding higher abundances in colder waters, (Arctic stations P2–P5) (Figs. 4 and S3). In general, they are mainly found in the upper 100 m of the water column (Fig. 4). However, in March we found veliger stages throughout the whole water column (Fig. 4). Their abundances are significantly explained ($p < 0.01$) by a combination of salinity, temperature, and nutrients (NO_3^-), thus showing association with Arctic waters (Table S6).

4.2. Seasonality in carbon standing stocks and export production

Despite the similar absolute abundances of planktonic foraminifers and shelled pteropods in the upper 100 m during summer months (August and July) (Figs. 3 and 4), foraminifers contribute on average 34% to the total (organic and inorganic) export production at 100 m, while pteropods, contributes c. 66% (Table S3).

The carbon standing stocks and export production is well correlated with the seasons. We suggest that the seasonality of carbon standing stocks and export production could be partially associated with the sea-ice edge, the MIZ and SIZ where we find the fresher polar surface water. The calcifiers follow the production of phytoplankton, specially diatoms (Wassmann et al., 1999) and the distribution of zooplankton such as copepods (Falk-Petersen et al., 1999). The highest values of export production recorded along the transect were found in the Arctic stations, P2–P5, where the MIZ was located during all sampling seasons (Figs. 8 and 9). The ice edge, the MIZ and SIZ have been previously described as the most seasonally productive zone for phytoplankton and other organisms that will likely be consumed by foraminifers and pteropods. In particular, the distribution pattern of the foraminifers along the transect in relation to productivity and sea ice distribution is relevant for studies that use foraminifers as proxies to reconstruct past climate and environment. The spatial and temporal variability of foraminifers are also key to better reconstruct past productivity in the fossil record based on the abundance and flux of their shells. In the northern Barents Sea, we have observed the highest foraminiferal export productions in early summer (July, 3.5 ± 3.38 mg $CaCO_3$ m^{-2} d^{-1}) followed by late summer (August, 2.32 ± 1.93 mg $CaCO_3$ m^{-2} d^{-1}) (Table S2). This is later than the peak phytoplankton bloom in the ice-covered northern Barents Sea (Wassmann and Reigstad, 2011), which results in an even more delayed foraminiferal export production (Fig. 8). This late foraminiferal production peak could also be because 2021 was a particularly cold year, keeping a larger (in terms of area) sea-ice cover in the study area and for a longer time than in 2019 (Fig. 1). The Arctic Ocean in general, and our study area in particular, have been reported as extremely variable in degree of sea-ice cover and light availability, resulting in a very strong seasonality and variability of biological production.

The seasonal chlorophyll concentration (=chlorophyll *a*) has been measured at all stations and previously published by Vader (2022). The highest values are found in July, followed by August, and May (Fig. S3). Planktonic foraminifers and pteropods are heterotrophs, feeding on both phytoplankton and smaller zooplankton. We would therefore assume that the higher production of these organisms would occur after the phytoplankton bloom. This has been observed in modelled seasonal distribution of mesozooplankton by Wassmann et al. (2019). However, the production of the calcifiers could be increasing at a slower rate (compared to smaller zooplankton) and their maximum delayed: the July-August maximum may have developed from the spring bloom, while the still high production combined with the larger sizes in December, from a potential late summer phytoplankton bloom. In May and July we observed the highest carbon standing stocks and export productions at the stations closest to the ice edge (P2–P4) and at the time

of maximum spring and early summer phytoplankton productivity (Figs. 7 and 8). Moreover, we need to acknowledge the interannual variability in the Barents Sea region. It is still unclear if years with a higher influence of Atlantic Water (e.g. 2018) could develop a higher production the following year that would hamper the comparison between years. In September 2018 we observed larger carbon standing stocks and export production north of Svalbard (Anglada-Ortiz et al., 2021) than in August and December. We could hypothesize that the carbon standing stock and export production in this region increase until October where it reaches its maximum and subsequently starts decreasing. However, we could also attribute the higher carbon standing stocks from Anglada-Ortiz et al. (2021) to that 2018 was a warmer year than usual, with no ice cover at 82° N in late summer (September) retreating further to 83° N in October (Rasmussen et al., 2018; Husum et al., 2020). In contrast to what we have observed during this seasonal study, in 2018 pteropods were found along the North Svalbard margin in the Arctic Ocean. Given the northward location of the MIZ in late summer 2018, the Arctic zone had spread far north and most likely the production moved along following the retreating sea-ice edge.

5. Conclusions

We identified a clear seasonal pattern in terms of production, size distribution and species abundances and export production of planktonic foraminifers and pteropods, observing the highest values in summer and autumn, and the lowest, in winter (March), as follows:

- In winter (March 2021), with the largest sea-ice extent and with the edge of open and close drift ice located at its southernmost position (76.4° N), is when the lowest abundances of calcifiers were found. The negligible abundance of planktonic foraminifers (<0.4 ind m^{-3}), and the low abundance of pteropods (early veligers) resulted in the lowest carbon standing stock and export production.
- In spring (May 2021) when the sea ice started retreating and where the sea-ice edge between open and close ice drift was located at P2, the abundance of foraminifers and pteropods slowly increased and hence, the carbon standing stock and export production increased compared to late winter. The pteropod community was dominated by both veligers and early veligers, while the planktonic foraminifers, by small and medium sized specimens.
- In summer months, with decreasing sea-ice cover along the transect (P4 very open drift ice in July, and at the edge of open and close drift ice in August) the abundance values reached their highest. The significant abundances of large planktonic foraminifers (>250 μm) and the increased abundance of juvenile pteropods in August 2019 resulted in a higher carbon standing stock and export production compared to July 2021 (they do not differ strongly from the values found in May 2021).
- In late autumn (December 2019), the sea ice covered all stations except the Atlantic station P1 and the southernmost polar station P2, which were at the edge of close and very close ice drift. The abundances in general did not increase, but the relative abundance of adult and juvenile pteropods (>500 μm) did and reached their maximum of all the seasons. In December, we observed the highest normalized size from all the seasons, and hence the highest average carbon standing stock. The average export production was slightly higher than in August.

Furthermore, we found the highest carbon standing stocks and export production of the calcifiers in the seasonal ice zone SIZ (P2–P4) during all seasons closely following the productivity patterns of phytoplankton and other zooplankton. The pteropod community dominates the total carbon standing stock and export production at all seasons, representing on average 83% of both estimates. The foraminiferal distribution pattern was explained by the combination of food availability and temperature and association with Atlantic Water, while the distribution pattern of pteropods was explained by the combination of temperature, salinity, and food availability and association with Arctic Water.

The abundances of marine calcifiers in the northern Barents Sea are expected to change under conditions of "Atlantification" and ocean acidification. The abundances of shelled pteropods will probably decline during years of increased Atlantic inflow, while foraminifers could be increasing. Decreased pH in the water column could result in a lower contribution from pteropods to the carbon standing stocks and export production.

Declaration of Competing Interest

The authors declare that they have no known competing financial interests or personal relationships that could have appeared to influence the work reported in this paper.

Data availability

Data will be published after the acceptance of the paper.

Acknowledgements

We are grateful to the captain and crew from RV *Kronprins Haakon*, cruise participants and cruise leaders (M. Reigstad and T. Gabrielsen; J. Søreide and R. Gradinger; S. Gerland and A. Wold; M. Ludvigsen and P. Assmy; E. Jones and M. Reigstad). We thank the physical oceanographers, L. Marsden, and M. Amargant-Arumí, Y. Bodur and È. Jordà-Molina for the water mass classification, data and *Rstudio* software support. We specially thank N. Espinel-Velasco and V. Pitusi for collecting the samples during the JC 2-1 cruise in July 2021; and K. Zamelczyk who contributed to the study design in 2018, shared the published data and collected the samples for protein measurements during the Q4 cruise in December 2019. We are grateful to M. M. Svenning and A. Didriksen for lending their equipment from the group of Arctic Infection Biology at the Arctic University of Norway, UiT. This study is funded by the Research Council of Norway through the project "The Nansen Legacy" (RCN#276730). This work is contributing to the Spanish Ministry of Science and Innovation, BIOCAL Project (PID2020-113526RB-I00). J.M. is funded through the Cluster of Excellence "The Ocean Floor- Earth's Uncharted Interface" (Receiver unit) of the Deutsche Forschungsgemeinschaft. We thank the four anonymous reviewers for comments and suggestions that greatly helped to improve the manuscript.

Appendix A. Supplementary data

Supplementary data to this article can be found online at https://doi.org/10.1016/j.pocean.2023.103121.

References

Allan, W.H.B., 1960. Ecology of recent planktonic foraminifera: part 2: bathymetric and seasonal distributions in the Sargasso sea off Bermuda. J. Micropaleontol. 6 (4), 373–392. https://doi.org/10.2307/1484218.

Anglada-Ortiz, G., Zamelczyk, K., Meilland, J., Ziveri, P., Chierici, M., Fransson, A., Rasmussen, T.L., 2021. Planktic foraminiferal and pteropod contributions to carbon dynamics in the arctic ocean (North Svalbard Margin). [Original Research]. Front. Mar. Sci. 8 (636) https://doi.org/10.3389/fmars.2021.661158.

Arrigo, K.R., van Dijken, G.L., 2015. Continued increases in Arctic Ocean primary production. Prog. Oceanogr. 136, 60–70.

Bates, N., Mathis, J., 2009. The Arctic Ocean marine carbon cycle: evaluation of air-sea CO 2 exchanges, ocean acidification impacts and potential feedbacks. Biogeosci. 6 (11).

Bednaršek, N., Možina, J., Vogt, M., O'brien, C., Tarling, G.,, 2012a. The global distribution of pteropods and their contribution to carbonate and carbon biomass in the modern ocean. Earth Syst. 4, 167–186.

Bednaršek, N., Tarling, G., Bakker, D., Fielding, S., Jones, E., Venables, H., Ward, P., Kuzirian, A., Lézé, B., Feely, R., 2012b. Extensive dissolution of live pteropods in the Southern Ocean. Nat. Geosci. 5 (12), 881–885.

Bednaršek, N., Tarling, G.A., Bakker, D.C., Fielding, S., Feely, R.A., 2014a. Dissolution dominating calcification process in polar pteropods close to the point of aragonite undersaturation. PLoS One 9 (10), e109183.
Bednaršek, N., Feely, R., Reum, J., Peterson, B., Menkel, J., Alin, S., Hales, B., 2014b. *Limacina helicina* shell dissolution as an indicator of declining habitat suitability owing to ocean acidification in the California Current Ecosystem. Proc. Royal Soc. B 281 (1785), 20140123.
Bednaršek, N., Feely, R.A., Howes, E.L., Hunt, B.P., Kessouri, F., León, P., Lischka, S., Maas, A.E., McLaughlin, K., Nezlin, N.P., 2019. Systematic review and meta-analysis toward synthesis of thresholds of ocean acidification impacts on calcifying pteropods and interactions with warming. Front. Mar. Sci. 6, 227.
Bjørklund, K.R., Kruglikova, S.B., Anderson, O.R., 2012. Modern incursions of tropical Radiolaria into the Arctic Ocean. J. Micropalaeontol. 31 (2), 139–158.
Bluhm, B., Kosobokova, K., Carmack, E., 2015. A tale of two basins: an integrated physical and biological perspective of the deep Arctic Ocean. Prog. Oceanogr. 139, 89–121.
Buitenhuis, E.T., Le Quere, C., Bednaršek, N., Schiebel, R., 2019. Large contribution of pteropods to shallow CaCO3 export. Glob. Biogeochem. Cycles 33 (3), 458–468.
Busch, K., Bauerfeind, E., Nöthig, E.-M., 2015. Pteropod sedimentation patterns in different water depths observed with moored sediment traps over a 4-year period at the LTER station HAUSGARTEN in eastern Fram Strait. Polar Biol. 38, 845–859.
Carstens, J., Hebbeln, D., Wefer, G., 1997. Distribution of planktic foraminifera at the ice margin in the Arctic (Fram Strait). Mar. Micropaleontol. 29 (3–4), 257–269.
Chierici, M., Fransson, A., 2018. Arctic chemical oceanography at the edge: focus on carbonate chemistry (chapter 13). In: Wassmann, P. (Ed.), At the edge.
Chierici, M., Jones, E., Lødemel, H.H., 2021a. Water column data on dissolved inorganic nutrients (nitrite, nitrate, phosphate and silicic acid) from the Nansen LEGACY joint cruise KH 2019706 with R.V. Kronprins Haakon, 5-27 August 2019. 10.21335/NMDC-1472517325.
Chierici, M., Jones, E., Lødemel, H.H., 2021b. Water column data on dissolved inorganic nutrients (nitrite, nitrate, phosphate and silicic acid) from the Nansen LEGACY seasonal cruise Q4, KH 2019711 with R.V. Kronprins Haakon. 10.21335/NMDC-1629206101.
Conley, K.R., Lombard, F., Sutherland, K.R., 2018. Mammoth grazers on the ocean's minuteness: a review of selective feeding using mucous meshes. Proc. R. Soc. B Biol. Sci. 285 (1878), 20180056.
Dalpadado, P., Arrigo, K.R., Hjøllo, S.S., Rey, F., Ingvaldsen, R.B., Sperfeld, E., van Dijken, G.L., Stige, L.C., Olsen, A., Ottersen, G., 2014. Productivity in the Barents Sea - response to recent climate variability. PLoS One 9 (5), e95273. https://doi.org/10.1371/journal.pone.0095273.
Descamps, S., Aars, J., Fuglei, E., Kovacs, K.M., Lydersen, C., Pavlova, O., Pedersen, Å.Ø., Ravolainen, V., Strøm, H., 2017. Climate change impacts on wildlife in a High Arctic archipelago–Svalbard, Norway. Glob. Change Biol. 23 (2), 490–502.
Fabry, V.J., 2008. Marine calcifiers in a high-CO2 ocean. Science 320 (5879), 1020–1022.
Falk-Petersen, S., Pedersen, G., Kwasniewski, S., Hegseth, E.N., Hop, H., 1999. Spatial distribution and life-cycle timing of zooplankton in the marginal ice zone of the Barents Sea during the summer melt season in 1995. J. Plankton Res. 21 (7).
Feely, R.A., Sabine, C.L., Lee, K., Berelson, W., Kleypas, J., Fabry, V.J., Millero, F.J., 2004. Impact of anthropogenic CO2 on the CaCO3 system in the oceans. Science 305 (5682), 362–366.
Fer, I., Peterson, A.K., Nilsen, F., 2022. Atlantic water boundary current along the southern Yermak Plateau, Arctic Ocean. J. Geophys. Res. Oceans e2023JC019645.
Fetterer, F., K. Knowles, W. N. Meier, M. Savoie, A. K. Windnagel., 2017. Sea Ice Index, Version 3 [Data Set]. Boulder, Colorado USA. National Snow and Ice Data Center.
Gannefors, C., Böer, M., Kattner, G., Graeve, M., Eiane, K., Gulliksen, B., Hop, H., Falk-Petersen, S., 2005. The Arctic sea butterfly *Limacina helicina*: lipids and life strategy. Mar. Biol. 147 (1), 169–177.
Gerland, S., 2022. CTD data from Nansen Legacy Cruise - Seasonal cruise Q1. 10.21335/NMDC-1491279668.
Greco, M., Jonkers, L., Kretschmer, K., Bijma, J., Kucera, M., 2019. Depth habitat of the planktonic foraminifera *Neogloboquadrina pachyderma* in the northern high latitudes explained by sea-ice and chlorophyll concentrations. Biogeosciences 16 (17), 3425–3437.
Greco, M., Werner, K., Zamelczyk, K., Rasmussen, T.L., Kucera, M., 2022. Decadal trend of plankton community change and habitat shoaling in the Arctic gateway recorded by planktonic foraminifera. Glob. Chang. Biol. 28 (5), 1798–1808.
Hemleben, C., Spindler, M., Anderson, O.R., 1989. Modern Planktonic Foraminifera. Springer-Verlag Neew York Inc. 10.1007/978-1-4612-3544-6.
Hunt, B.P.V., Pakhomov, E.A., Hosie, G.W., Siegel, V., Ward, P., Bernard, K., 2008. Pteropods in Southern Ocean ecosystems. Prog. Oceanogr. 78 (3), 193–221. https://doi.org/10.1016/j.pocean.2008.06.001.
Husum, K., Ninnemann, U., Rydningen, T.A., Alve, E., El Bani Altuna, N., Braaten, A.H., Eilertsen, V., Gamboa, V., Kjøller, M.R., Orme, L., Rutledal, S., Tessin, A., Zindorf, M., 2020. Paleo Cruise 2018: Cruise Report. The Nansen Legacy Report Series 3/2020.
Jacobs, J., Barry, R., Weaver, R., 1975. Fast ice characteristics, with special reference to the eastern Canadian Arctic. Polar Rec. 17(110), 521–536. 10.1017/S0032247400032484.
Jones, E., Chierici, M., Lødemel, H.H., Møgster, J., Fonnes, L.L., 2022a. Water column data on dissolved inorganic nutrients (nitrite, nitrate, phosphate and silicic acid) from Process (P) stations during the Nansen LEGACY joint cruise JC2-1, 2021708, with R.V. Kronprins Haakon, 14-24 July 2021. 10.21335/NMDC-1747434716.
Jones, E., Chierici, M., Lødemel, H.H., Møgster, J., Fonnes, L.L., 2022b. Water column data on dissolved inorganic nutrients (nitrite, nitrate, phosphate and silicic acid) from Process (P) stations during the Nansen LEGACY seasonal cruise Q1, 2021703, with R.V. Kronprins Haakon, 4-17 March 2021. 10.21335/NMDC-762320451.
Jones, E., Chierici, M., Lødemel, H.H., Møgster, J., Fonnes, L.L., 2022c. Water column data on dissolved inorganic nutrients (nitrite, nitrate, phosphate and silicic acid) from Process (P) stations during the Nansen LEGACY seasonal cruise Q2, 2021704, with R.V. Kronprins Haakon, 30 April–18 May 2021. 10.21335/NMDC-487023368.
Jones, E., Chierici, M., Fransson, A., Assman, K., Renner, A.H.H., Lødemel, H.H. (this issue). Inorganic carbon and nutrient dynamics in the marginal ice zone of the Barents Sea: seasonality and implications for ocean acidification.
Jones, E., 2022. CTD data from Nansen Legacy Cruise - Joint cruise 2-1. 10.21335/NMDC-2085836005.
Jonkers, L., Kučera, M., 2015. Global analysis of seasonality in the shell flux of extant planktonic Foraminifera. Biogeosciences 12 (7), 2207–2226.
Kinnard, C., Zdanowicz, C.M., Koerner, R.M., Fisher, D.A., 2008. A changing Arctic seasonal ice zone: Observations from 1870–2003 and possible oceanographic consequences. Geophys. Res. Lett. 35 (2).
Lalli, C.M., Gilmer, R.W., 1989. Pelagic Snails: The Biology of Holoplanktonic Gastropod Mollusks. Stanford University Press.
Langer, M.R., 2008. Assessing the contribution of foraminiferan protists to global ocean carbonate production 1. J. Eukaryot. Microbiol. 55 (3), 163–169.
Lee, Y.J., Matrai, P.A., Friedrichs, M.A., Saba, V.S., Antoine, D., Ardyna, M., Asanuma, I., Babin, M., Bélanger, S., Benoît-Gagné, M., 2015. An assessment of phytoplankton primary productivity in the Arctic Ocean from satellite ocean color/in situ chlorophyll-a based models. J. Geophys. Res. Oceans 120 (9), 6508–6541.
Lipps, J.H., Krebs, W.N., 1974. Planktonic foraminifera associated with Antarctic sea ice. J. Foramin. Res. 4 (2), 80–85.
Loeng, H., 1991. Features of the physical oceanographic conditions of the Barents Sea. Polar Res. 10 (1), 5–18.
Ludvigsen, M., 2022. CTD data from Nansen Legacy Cruise - Seasonal cruise Q2. 10.21335/NMDC-515075317.
Lundesgaard, Ø., Sundfjord, A., Lind, S., Nilsen, F., Renner, A.H.H., 2022. Import of Atlantic Water and sea ice controls the ocean environment in the northern Barents Sea. Ocean Sci. 18 (5), 1389–1418. https://doi.org/10.5194/os-18-1389-2022.
Manno, C., Bednaršek, N., Tarling, G.A., Peck, V.L., Comeau, S., Adhikari, D., Bakker, D. C., Bauerfeind, E., Bergan, A.J., Berning, M.I., 2017. Shelled pteropods in peril: assessing vulnerability in a high CO2 ocean. Earth Sci. Rev. 169, 132–145.
Manno, C., Morata, N., Primicerio, R., 2012. *Limacina retroversa*'s response to combined effects of ocean acidification and sea water freshening. Estuar. Coast. Shelf Sci. 113, 163–171.
Manno, C., Pavlov, A., 2013. Living planktonic foraminifera in the Fram Strait (Arctic): absence of diel vertical migration during the midnight sun. Hydrobiologia 721 (1), 285–295.
Meilland, J., Howa, H., Monaco, C.L., Schiebel, R., 2016. Individual planktic foraminifer protein-biomass affected by trophic conditions in the Southwest Indian Ocean, 30° S–60° S. Mar. Micropaleontol. 124, 63–74.
Meilland, J., Schiebel, R., Monaco, C.L., Sanchez, S., Howa, H., 2018. Abundances and test weights of living planktic foraminifers across the Southwest Indian Ocean: Implications for carbon fluxes. Deep Sea Res. Part I 131, 27–40.
Meilland, J., Howa, H., Hulot, V., Demangel, I., Salaun, J., Garlan, T., 2020. Population dynamics of modern planktonic foraminifera in the western Barents Sea. Biogeosciences 17 (6), 1437–1450.
Meilland, J., Ezat, M.M., Westgård, A., Manno, C., Morard, R., Siccha, M., Kucera, M., 2022. Rare but persistent asexual reproduction explains the success of planktonic foraminifera in polar oceans. J. Plankton Res. 1–18 https://doi.org/10.1093/plankt/fbac069.
Meinecke, G., Wefer, G., 1990. Seasonal pteropod sedimentation in the Norwegian Sea. Palaeogeogr. Palaeoclimatol. Palaeoecol. 79 (1), 129–147. https://doi.org/10.1016/0031-0182(90)90109-K.
Moy, A.D., Howard, W.R., Bray, S.G., Trull, T.W., 2009. Reduced calcification in modern Southern Ocean planktonic foraminifera. Nat. Geosci. 2 (4), 276–280.
Nigam, R., 2005. Sediment traps as a new tool for estimation of longevity of planktonic foraminifera.
Norwegian Meteorological Institute Ice service, 2022. https://cryo.met.no/en/ice-service.
Ofstad, S., Meilland, J., Zamelczyk, K., Chierici, M., Fransson, A., Gründger, F., Rasmussen, T.L., 2020. Development, productivity, and seasonality of living planktonic foraminiferal faunas and *Limacina helicina* in an Area of intense methane seepage in the Barents Sea. J. Geophys. Res. Biogeosci. 125(2), e2019JG005387.
Orr, J.C., Fabry, V.J., Aumont, O., Bopp, L., Doney, S.C., Feely, R.A., Gnanadesikan, A., Gruber, N., Ishida, A., Joos, F., 2005. Anthropogenic ocean acidification over the twenty-first century and its impact on calcifying organisms. Nature 437 (7059), 681–686.
Pados, T., Spielhagen, R.F., 2014. Species distribution and depth habitat of recent planktic foraminifera in Fram Strait. Arctic Ocean. Polar Res. 33 (1), 22483.
Peck, V.L., Tarling, G.A., Manno, C., Harper, E.M., Tynan, E., 2016. Outer organic layer and internal repair mechanism protects pteropod *Limacina helicina* from ocean acidification. Deep Sea Res., Part IITopical Studies in Oceanography 127, 41–52. https://doi.org/10.1016/j.dsr2.2015.12.005.
Peck, V.L., Oakes, R.L., Harper, E.M., Manno, C., Tarling, G.A., 2018. Pteropods counter mechanical damage and dissolution through extensive shell repair. Nat. Commun. 9 (1), 1–7.
Pieńkowski, A.J., Husum, K., Belt, S.T., Ninnemann, U., Köseoğlu, D., Divine, D.V., Smik, L., Knies, J., Hogan, K., Noormets, R., 2021. Seasonal sea ice persisted through the Holocene Thermal Maximum at 80°N. Commun. Earth Environ. 2 (1), 124. https://doi.org/10.1038/s43247-021-00191-x.

Polyakov, I.V., Alkire, M.B., Bluhm, B.A., Brown, K.A., Carmack, E.C., Chierici, M., Danielson, S.L., Ellingsen, I., Ershova, E.A., Gårdfeldt, K., 2020. Borealization of the Arctic Ocean in response to anomalous advection from sub-Arctic seas. Front. Mar. Sci. 7, 491.

Rasmussen, T.L., Laberg, J.S., Ofstad, S., Rydningen, T.A., Åström, E., El Bani Altuna, N., Lasabuda, A., Carrol, M., 2018. Cruise Report: AMGG Cruise to the Northern and Eastern Svalbard Margin, Department of Geosciences, UiT, Arctic University of Norway, N-9037. Tromsø, Norway.

Reigstad, M., Wassmann, P., Riser, C.W., Øygarden, S., Rey, F., 2002. Variations in hydrography, nutrients and chlorophyll a in the marginal ice-zone and the central Barents Sea. J. Mar. Syst. 38 (1–2), 9–29.

Reigstad, M., 2022. CTD data from Nansen Legacy Cruise - Seasonal cruise Q3. 10.21335/NMDC-1107597377.

Ross, B.J., Hallock, P., 2016. Dormancy in the foraminifera: a review. J. Foramin. Res. 46 (4), 358–368.

Saher, M., Kristensen, D.K., Hald, M., Pavlova, O., Jørgensen, L.L., 2012. Changes in distribution of calcareous benthic foraminifera in the central Barents Sea between the periods 1965–1992 and 2005–2006. Glob. Planet. Change 98–99, 81–96. https://doi.org/10.1016/j.gloplacha.2012.08.006.

Sakshaug, E., 1997. Biomass and productivity distributions and their variability in the Barents Sea. ICES Mar. Sci. Symp. 54 (3), 341–350.

Sakshaug, E., Skjoldal, H.R., 1989. Life at the ice edge. Ambio (Sweden).

Sakshaug, E., Slagstad, D., 1991. Sea ice and wind: effects on primary productivity in the Barents Sea. Atmos.-Ocean 30 (4), 579–591.

Schiebel, R., 2002. Planktic foraminiferal sedimentation and the marine calcite budget. Glob. Biogeochem. Cycles 16 (4), 3-1-3-21.

Schiebel, R., Hemleben, C., 2000. Interannual variability of planktic foraminiferal populations and test flux in the eastern North Atlantic Ocean (JGOFS). Deep-Sea Res. II: Top. Stud. Oceanogr. 47(9-11), 1809–1852.

Schiebel, R., Movellan, A., 2012. First-order estimate of the planktic foraminifer biomass in the modern ocean. Earth Syst. Sci. Data 4, 75–89.

Schneider, C.A., Rasband, W.S., Eliceiri, K.W., 2012. NIH Image to ImageJ: 25 years of image analysis. Nat. Methods 9 (7), 671–675.

Smedsrud, L.H., Muilwijk, M., Brakstad, A., Madonna, E., Lauvset, S.K., Spensberger, C., Born, A., Eldevik, T., Drange, H., Jeansson, E., 2022. Nordic Seas heat loss, Atlantic inflow, and Arctic sea ice cover over the last century. Rev. Geophys. 60(1), e2020RG000725.

Søreide, J.E., Leu, E.V., Berge, J., Graeve, M., Falk-Petersen, S., 2010. Timing of blooms, algal food quality and *Calanus glacialis* reproduction and growth in a changing Arctic. Glob. Chang. Biol. 16 (11), 3154–3163.

Søreide, J.E., 2022. CTD data from Nansen Legacy Cruise - Seasonal cruise Q4. 10.21335/NMDC-301551919.

Spindler, M., Dieckmann, G.S., 1986. Distribution and abundance of the planktic foraminifer Neogloboquadrina pachyderma in sea ice of the Weddell Sea (Antarctica). Polar Biol. 5 (3), 185–191.

Stangeew, E., 2001. Distribution and Isotopic Composition of Living Planktonic Foraminifera *N. pachyderma* (sinistral) and *T. quinqueloba* in the High Latitude North Atlantic. Christian-Albrechts Universität Kiel.

Steinsund, P., 1994. Benthic Foraminifera in Surface Sediments of the Barents and Kara Seas: Modern and Late Quaternary Applications. University of Tromsø, Tromsø, 111 pp.

Subhas, A.V., Dong, S., Naviaux, J.D., Rollins, N.E., Ziveri, P., Gray, W., Rae, J.W., Liu, X., Byrne, R.H., Chen, S., 2022. Shallow calcium carbonate cycling in the North Pacific Ocean. Glob. Biogeochem. Cycles e2022GB007388.

Sundfjord, A., Assmann, K.M., Lundesgaard, Ø., Renner, A.H.H., Lind, S., Ingvaldsen, R. B., 2020. Suggested water mass definitions for the central and northern Barents Sea, and the adjacent Nansen Basin: Workshop Report. (2703-7525). The Nansen Legacy Report Series 8/2020. 10.7557/nlrs.5707.

Tell, F., Jonkers, L., Meilland, J., Kucera, M., 2022. Upper-ocean flux of biogenic calcite produced by the Arctic planktonic foraminifera *Neogloboquadrina pachyderma*. Biogeosciences 19 (20), 4903–4927. https://doi.org/10.5194/bg-19-4903-2022.

Vader, A., 2022. Chlorophyll A and phaeopigments Nansen. Legacy. https://doi.org/10.21335/NMDC-1371694848.

Vernet, M., Ellingsen, I.H., Seuthe, L., Slagstad, D., Cape, M.R., Matrai, P.A., 2019. Influence of phytoplankton advection on the productivity along the Atlantic water inflow to the Arctic Ocean [Original Research]. Front. Mar. Sci. 6 (583) https://doi.org/10.3389/fmars.2019.00583.

Vihtakari., M., 2020. PlotSvalbard: PlotSvalbard - Plot research data from Svalbard on maps. Version R package version (9), 2. https://github.com/MikkoVihtakari/PlotSvalbard.

Volkmann, R., 2000. Planktic foraminifers in the outer Laptev Sea and the Fram Strait—Modern distribution and ecology. J. Foramin. Res. 30 (3), 157–176.

Wadhams, P., 1986. The Seasonal Ice Zone. In: Untersteiner, N. (Ed.), The Geophysics of Sea Ice. Springer, US, pp. 825-991. 10.1007/978-1-4899-5352-0_15.

Wang, K., Hunt, B.P., Liang, C., Pauly, D., Pakhomov, E.A., 2017. Reassessment of the life cycle of the pteropod *Limacina helicina* from a high resolution interannual time series in the temperate North Pacific. ICES Mar. Sci. 74 (7), 1906–1920.

Wassmann, P., Ratkova, T., Andreassen, I., Vernet, M., Pedersen, G., Rey, F., 1999. Spring bloom development in the marginal ice zone and the central Barents Sea. Mar. Ecol. 20 (3–4), 321–346.

Wassmann, P., Reigstad, M., 2011. Future Arctic Ocean seasonal ice zones and implications for pelagic-benthic coupling. Oceanography 24 (3), 220–231.

Wassmann, P., Slagstad, D., Ellingsen, I., 2019. Advection of mesozooplankton into the Northern Svalbard shelf region [original research]. Front. Mar. Sci. 6 (458) https://doi.org/10.3389/fmars.2019.00458.

Werner, I., 2005. Living conditions, abundance and biomass of under-ice fauna in the Storfjord area (western Barents Sea, Arctic) in late winter (March 2003). Polar Biol. 28 (4), 311–318.

Westgård, A., Ezat, M.M., Chalk, T.B., Chierici, M., Foster, G.L., Meilland, J., 2023. Large-scale culturing of *Neogloboquadrina pachyderma*, its growth in, and tolerance of, variable environmental conditions. J. Plankton Res.

Zamelczyk, K., Fransson, A., Chierici, M., Jones, E., Meilland, J., Anglada-Ortiz, G., Lødemel, H.H., 2021. Distribution and abundances of planktic foraminifera and shelled pteropods during the polar night in the sea-ice covered northern Barents Sea. Front Mar. Sci. 1516.

Ziveri, P., de Bernardi, B., Baumann, K.-H., Stoll, H.M., Mortyn, P.G., 2007. Sinking of coccolith carbonate and potential contribution to organic carbon ballasting in the deep ocean. Deep Sea Res. Part II 54 (5–7), 659–675.

Ziveri, P., Gray, W.R., Anglada-Ortiz, G., Manno, C., Grelaud, M., Incarbona, A., Rae, J. W.B., Subhas, A.V., Pallacks, S., White, A., Adkins, J.F., Berelson, W., 2023. Pelagic calcium carbonate production and shallow dissolution in the North Pacific Ocean. Nat. Commun. 14 (1), 805.

Supplementary material

Seasonality of marine calcifiers in the northern Barents Sea: Spatiotemporal distribution of planktonic foraminifers and shelled pteropods and their contribution to carbon dynamics

Griselda Anglada-Ortiz[1*], Julie Meilland [2], Patrizia Ziveri [3,4], Melissa Chierici [5], Agneta Fransson [6], Elizabeth Jones [5], and Tine L. Rasmussen [1].

[1] Department of Geosciences UiT, the Arctic University of Norway, 9037 Tromsø, Norway

[2] MARUM, Center for marine environmental sciences, university of Bremen, Leobener Str. 8, 28359 Bremen, Germany

[3] Institute of Environmental Science and Technology (ICTA-UAB), Universitat Autònoma de Barcelona, 08193, Barcelona, Spain

[4] Institució Catalana de Recerca i Estudis Avançats, ICREA, 08010, Barcelona, Spain

[5] Institute of Marine Research (IMR), 9296 Tromsø, Norway

[6] Norwegian Polar Institute (NPI), 9296 Tromsø, Norway

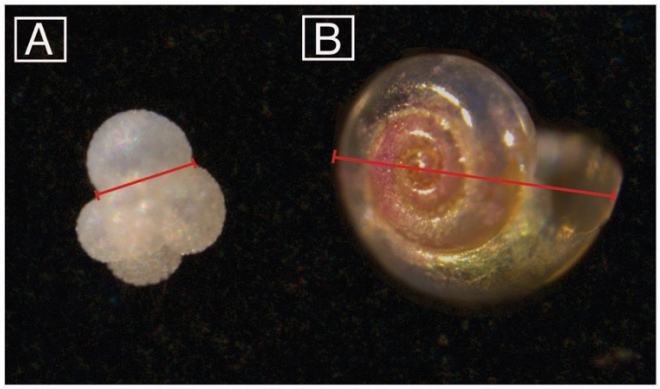

Figure S1. Length measurements of foraminifera (minimum size, panel A) and pteropods (diameter, panel B).

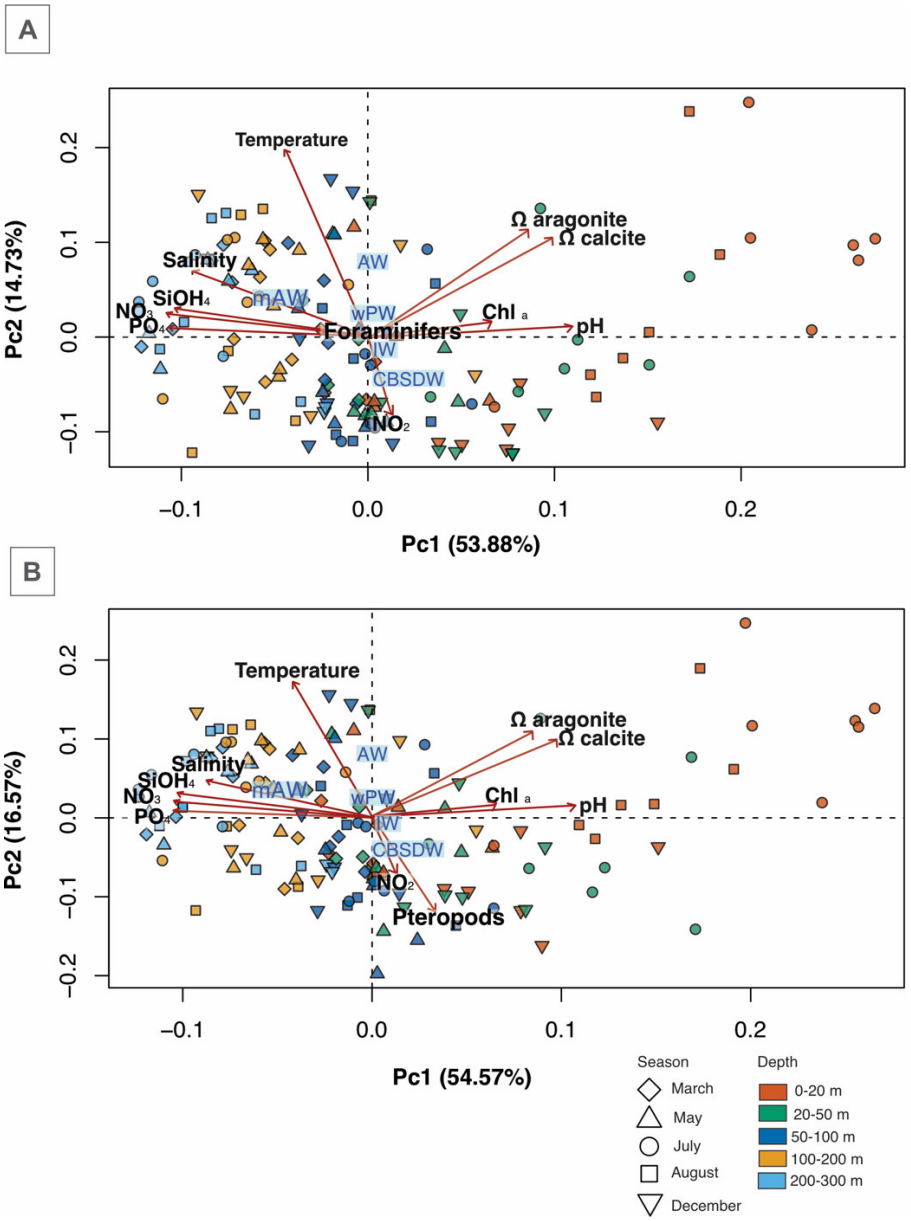

Figure S2. Principal component analysis plot with the abundance of foraminifers (A) and pteropods (B), and environmental parameters (salinity , temperature chl_a , calcite) and aragonite saturation states pH, and nutrients of NO_2^-, NO_3^-, PO_4^- and $SiOH_4$. Each season is represented by different shapes and the depth, by color. Distribution of water masses (AW=Atlantic Water, mAW=modified Atlantic Water, IW=Intermediate Water, CBSDW=Cold Barents Sea Deep Water) are enclosed in light blue rectangles.

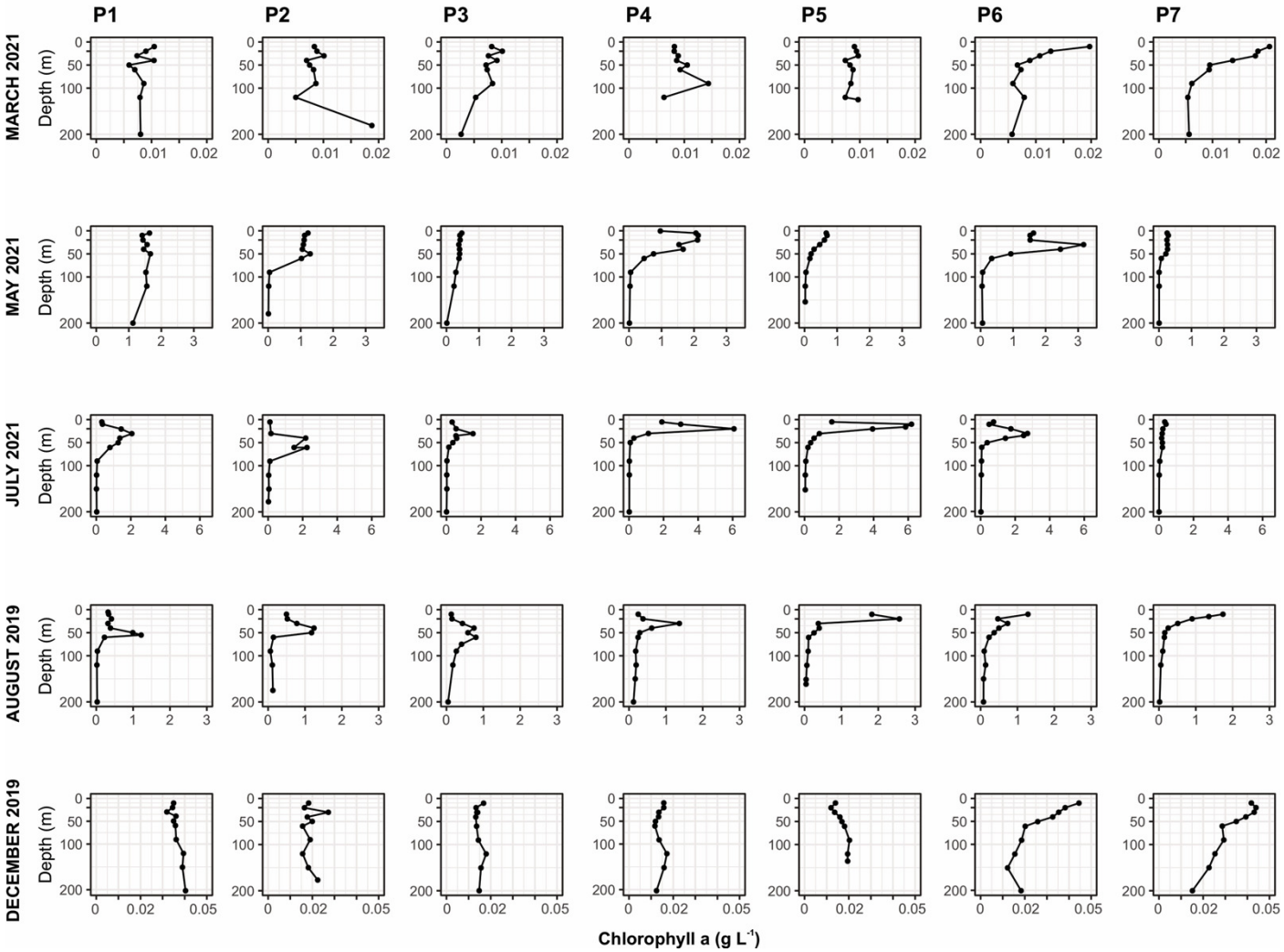

Figure S3. Vertical chlorophyll a concentration (g L^{-1}) along the P stations and seasons, from Vader (2022) .

Table S1. Sampling depths and time at every station and season (December data (*) from Zamelczyk et al. (2021)).

	MARCH	Time	MAY	Time	JULY	Time	AUGUST	Time *(UTC)*	DECEMBER*
P1	0-20, 20-50, 50-100, 100-200, 200-300	11:00h	0-20, 20-50, 50-100, 100-200, 200-300	12:10h	0-20, 20-50, 50-100, 100-200, 200-300	12:00h	0-50, 50-100, 100-150, 150-200, 200-300	11:35h	0-20, 20-50, 50-100, 100-200, 200-300
P2	0-20, 20-50, 50-100, 100-170	06:00h	0-20, 20-50, 50-100, 100-170	03:30h	0-20, 20-50, 50-100, 100-170	13:00h	0-50, 50-100, 100-170	02:45h	0-20, 20-50, 50-80, 80-100, 100-170
P3	0-20, 20-50, 50-100, 100-200, 200-300	17:15h	0-20, 20-50, 50-100, 100-200, 200-300	20:20h	0-20, 20-50, 50-100, 100-200, 200-300	07:05h	N.A.	N.A	0-20, 20-50, 50-100, 100-200, 200-280
P4	0-20, 20-50, 50-100, 100-200, 200-300	17:40h	0-20, 20-50, 50-100, 100-200, 200-300	16:35h	0-20, 20-50, 50-100, 100-200, 200-300	11:20h	0-50, 50-100, 100-150, 150-200, 200-300	09:30h	0-20, 20-50, 50-100, 100-200, 200-300
P5	0-20, 20-50, 50-100, 100-150	15:15h	0-20, 20-50, 50-100, 100-150	16:35h	0-20, 20-50, 50-100, 100-150	07:50h	0-50, 50-100, 100-150	04:15h	0-20, 20-50, 50-80, 80-100, 100-125
P6	0-20, 20-50, 50-100, 100-200, 200-300	03:40h	0-20, 20-50, 50-100, 100-200, 200-300	21:05h	0-20, 20-50, 50-100, 100-200, 200-300	15:15h	0-50, 50-100, 100-150, 150-200, 200-300	17:30h	0-20, 20-50, 50-200, 200-600, 600-750
P7	0-20, 20-50, 50-100, 100-200, 200-300	13:45h	0-20, 20-50, 50-100, 100-200, 200-300	20:45h	0-20, 20-50, 50-100, 100-200, 200-300	18:20h	0-50, 50-100, 100-150, 150-200, 200-300	09:10h	0-20, 20-50, 50-100, 100-200, 200-300

Table S2. Organic and inorganic standing stock contribution of planktic foraminifera and pteropods.

	MARCH 2021				MAY 2021				JULY 2021				AUGUST 2019				DECEMBER 2019			
	INORGANIC ($\mu g\ CaCO_3\ m^{-3}$)		ORGANIC (μg protein m^{-3})		INORGANIC ($\mu g\ CaCO_3\ m^{-3}$)		ORGANIC (μg protein m^{-3})		INORGANIC ($\mu g\ CaCO_3\ m^{-3}$)		ORGANIC (μg protein m^{-3})		INORGANIC ($\mu g\ CaCO_3\ m^{-3}$)		ORGANIC (μg protein m^{-3})		INORGANIC ($\mu g\ CaCO_3\ m^{-3}$)		ORGANIC (μg protein m^{-3})	
P1	0.0		0.0		8.2		1.2		25.1		1.00		164.8		24.8		2.7		0.4	
F | P	0.0	0.0	0.0	0.0	0.4	7.8	0.0	1.2	19.6	5.5	0.01	1.0	13.7	151.1	0.01	24.8	0.1	2.6	0.0	0.4
P2	0.0		0.0		101.8		11.0		72.6		19.0		856.8		145.1		44.9		72.7	
F | P	0.0	0.0	0.0	0.0	0.1	101.6	0.0	11.0	5.8	66.8	0.01	19.0	4.4	852.4	0.0	145.1	1.6	43.3	0.0	72.7
P3	21.9		2.5		28.7		5.2		200.6		32.3		N.A.		N.A.		158.3		61.1	
F | P	0.00	21.9	0.0	2.5	0.0	28.7	0.0	5.2	5.3	195.3	0.01	32.3	-	-	-	-	0.0	158.3	0.0	61.1
P4	26.3		2.2		97.5		12.9		77.1		20.0		198.2		32.5		198.1		123.9	
F | P	0.00	26.3	0.0	2.2	0.00	97.5	0.0	12.9	3.3	73.9	0.0	20.0	4.2	194.0	0.01	32.5	0.00	198.1	0.0	123.9
P5	17.6		1.6		81.7		11.7		41.3		11.3		115.1		16.9		17.2		206.5	
F | P	0.00	17.6	0.0	1.6	1.6	80.2	0.0	11.7	12.6	28.7	0.01	11.3	15.1	100.1	0.02	16.9	0.01	17.2	0.0	206.5
P6	9.2		2.0		3.2		0.7		25.1		2.8		54.2		0.8		28.5		8.0	
F | P	0.00	9.2	0.0	2.0	0.3	2.8	0.0	0.7	19.4	5.7	0.01	2.8	49.3	4.9	0.06	0.8	0.8	27.7	0.00	8.0
P7	0.8		0.01		2.7		0.3		21.3		0.02		6.9		1.1		8.6		1.8	
F | P	0.00	0.8	0.00	0.01	0.5	2.2	0.0	0.3	21.3	0.00	0.02	0.0	6.2	0.7	0.01	0.1	0.03	8.5	0.01	1.8

Table S3. Organic and inorganic export production contribution of planktic foraminifera and pteropods.

	MARCH 2021				MAY 2021				JULY 2021				AUGUST 2019				DECEMBER 2019			
	INORGANIC ($mg\ CaCO_3\ m^{-2}d^{-1}$)		ORGANIC (mg protein $m^{-2}d^{-1}$)		INORGANIC ($mg\ CaCO_3\ m^{-2}d^{-1}$)		ORGANIC (mg protein $m^{-2}d^{-1}$)		INORGANIC ($mg\ CaCO_3\ m^{-2}d^{-1}$)		ORGANIC (mg protein $m^{-2}d^{-1}$)		INORGANIC ($mg\ CaCO_3\ m^{-2}d^{-1}$)		ORGANIC (mg protein $m^{-2}d^{-1}$)		INORGANIC ($mg\ CaCO_3\ m^{-2}d^{-1}$)		ORGANIC (mg protein $m^{-2}d^{-1}$)	
P1	0.0		0.0		5.3		0.8		9.1		0.4		24.2		3.7		0.02		0.0	
F | P	0.0	0.0	0.0	0.0	0.05	5.2	0.0	0.8	6.7	2.5	0.0	0.4	2.3	21.9	0.0	3.7	0.02	0.0	0.0	0.00
P2	0.0		0.0		70.6		6.3		28.8		4.4		552.7		94.0		44.9		7.5	
F | P	0.0	0.0	0.0	0.0	0.0	70.6	0.0	6.3	0	28.8	0.0	4.4	2.5	550.1	0.0	94.0	1.5	43.3	0.0	7.5
P3	15.0		1.7		22.1		3.2		82.4		12.4		N.A.		N.A.		158.3		27.4	
F | P	0.0	15.0	0.0	1.7	0.0	22.1	0.00	3.2	0.0	82.37	0.0	12.4	-	-	-	-	0.00	158.3	0.0	27.4
P4	14.5		1.0		79.3		10.4		31.2		4.6		105.5		17.6		198.1		34.2	
F | P	0.0	14.5	0.0	1.0	0.0	79.3	0.0	10.4	0.3	30.9	0.0	4.6	0.4	105.2	0.0	17.6	0.00	198.1	0.00	34.2
P5	7.9		0.8		4.4		0.6		29.6		3.9		73.0		11.9		17.2		3.0	
F | P	0.0	7.9	0.0	0.8	0.0	4.4	0.0	0.6	4.7	24.9	0.0	3.9	2.7	70.3	0.0	11.9	0.01	17.2	0.00	3.0
P6	11.1		1.2		0.80		0.1		12.0		0.6		8.5		0.5		28.5		4.8	
F | P	0.0	11.1	0.0	1.2	0.01	0.8	0.0	0.1	8.1	3.9	0.0	0.6	5.7	2.8	0.01	0.5	0.8	27.7	0.00	4.8
P7	0.1		0.0		2.1		0.3		4.7		0.0		0.4		0.0		8.6		1.5	
F | P	0.0	0.1	0.0	0.0	0.30	1.8	0.01	0.3	4.7	0.0	0.0	0.0	0.4	0.0	0.0	0.0	0.03	8.5	0.01	1.5

Table S4. Organic:inorganic ratio (%) of planktic foraminifers and pteropods at all stations and seasons.

		March		May		July		August		December	
		O:I foraminifers	**O:I pteropods**	**O:I foraminifers**	**O:I pteropods**	**O:I foraminifers**	**O:I pteropods**	**O:I foraminifers**	**O:I pteropods**	**O:I foraminifers**	**O:I pteropods**
Standing stock (0-100 m)	P1	0.00	0.00	0.18	14.66	0.06	18.16	0.09	16.44	0.16	17.31
	P2	0.00	0.00	0.10	10.84	0.12	28.44	0.07	17.03	0.10	17.26
	P3	0.00	11.48	0.00	18.23	0.13	16.55			0.10	17.28
	P4	0.00	8.39	0.00	13.27	0.15	27.08	0.16	16.77	0.00	17.29
	P5	0.00	8.85	0.11	14.63	0.11	39.43	0.12	16.85	0.13	17.30
	P6	0.00	21.23	0.12	25.35	0.08	49.43	0.12	16.02	0.12	34.58
	P7	0.00	1.74	0.06	14.77	0.11	0.00	0.14	16.19	0.12	17.31
	average	**0.00**	**7.38**	**0.08**	**15.96**	**0.11**	**25.58**	**0.12**	**16.55**	**0.10**	**19.76**
Export production (50-100 m)	P1	0.00	0.00	0.13	14.72	0.05	17.20	0.09	16.68	0.12	0.00
	P2	0.00	0.00	0.00	8.94	0.00	15.15	0.04	17.08	0.10	17.22
	P3	0.00	11.08	0.00	14.08	0.00	15.03			0.00	17.27
	P4	0.00	6.55	0.00	13.11	0.12	14.99	0.13	16.78	0.00	17.28
	P5	0.00	10.31	0.25	12.62	0.08	15.62	0.08	16.86	0.24	17.29
	P6	0.00	11.05	0.11	13.90	0.04	15.76	0.09	16.08	0.00	17.31
	P7	0.00	1.74	0.04	14.87	0.08	0.00	0.12	0.00	0.11	17.31
	average	**0.00**	**5.82**	**0.08**	**13.18**	**0.05**	**13.39**	**0.09**	**13.91**	**0.08**	**14.81**

Table S5. Foraminiferal absolute abundances (ind m^{-3}) and species distribution (%) in summer.

STATION	**DEPTH**	**Abundance foraminifera**	*N. pachyderma (%)*	*T. quinqueloba (%)*	*N. incompta (%)*	other (%)
P1	0-50	**5.97**	25.64	48.72	0.00	25.64
P1	50-100	**17.19**	50.00	13.46	16.03	20.51
P1	100-150	**15.61**	33.87	8.06	46.77	11.29
P1	150-200	**12.40**	81.45	6.45	1.61	10.48
P1	200-290	**5.24**	91.89	2.70	1.35	4.05
P2	0-50	**2.82**	100.00	0.00	0.00	0.00
P2	50-100	**2.89**	75.00	0.00	0.00	25.00
P2	100-150	**17.06**	94.39	1.87	0.00	3.74
P2	150-200					
P2	200-300					
P3	0-50					
P3	50-100					
P3	100-150					
P3	150-200					
P3	200-300					
P4	0-50	**9.71**	40.63	18.75	0.00	40.63
P4	50-100	**6.89**	100.00	0.00	0.00	0.00
P4	100-150	**29.52**	97.97	0.00	0.00	2.03
P4	150-200	**26.57**	96.00	0.89	1.78	1.33
P4	200-300	**7.88**	92.91	2.13	1.42	3.55
P5	0-50	**20.34**	93.43	2.92	2.19	1.46
P5	50-100	**21.32**	94.85	0.74	2.94	1.47
P5	100-150	**15.16**	100.00	0.00	0.00	0.00
P5	150-200	**0.00**				
P5	200-300					
P6	0-50	**76.37**	80.00	5.93	7.97	6.10
P6	50-100	**47.11**	80.31	8.81	4.40	6.48
P6	100-150	**46.65**	93.59	3.20	1.07	2.14
P6	150-200	**38.64**	90.70	0.00	0.00	9.30
P6	200-300	**2.99**	95.71	0.00	0.00	4.29
P7	0-50	**13.52**	93.33	1.33	0.00	5.33
P7	50-100	**7.09**	94.44	2.78	0.00	2.78
P7	100-150	**39.17**	97.21	1.86	0.00	0.93

P7	150-200	**28.21**	92.97	2.70	0.00	4.32
P7	200-300	**4.95**	88.35	11.65	0.00	0.00

	N. pachyderma	*T. quinqueloba*	*N. incompta*	other
Relative abundance (%)	**85.19**	**4.73**	**4.36**	**5.72**

Table S6. ANOVA results of the environmental parameters that significantly describe the distribution of foraminifers and pteropods.

	Parameters	*p value*
Foraminifers	Temperature	0.047620 *
	Nitrate	7.346e-06 ***
	Nitrite	0.007751 **
	Silicate	0.002304 **
Pteropods	Salinity	0.0024571 **
	Temperature	0.0001737 ***
	Nitrite	0.0005978 ***

1. Supplementary information

SEASONAL ABUNDANCES

1) MARCH 2021

The Atlantic shelf station is dominated by small veliger stages of pteropods, which are only present in low abundances (1.48 ind m^{-3}) at the deepest part of the water column (200–300 m) (figure 4).

At the polar shelf stations the highest abundances of pteropods are at subsurface or deep subsurface (at P2 100–200 m, with 22.3 ind m^{-3}) compared to lower abundances found at surface 0–20 m (av 2.6 ind m^{-3}, min 0 ind m^{-3}, max 6.9 ind m^{-3}) (figure 4). The pteropod community is mostly composed by small veliger larvae (av 67.2%, min 21.7%, max 100%), and veligers/young juveniles (av 32.5%, min 8.2%, max 78.3%). The average abundance of pteropods (0–300 m depth) is stable along these stations (av 5.2 ind m^{-3}, min 4.5 ind m^{-3}, max 6.8 ind m^{-3}) (figure 4).

At the slope station we recorded low abundances of calcifiers at the surface 0–20 m (0.6 ind m^{-3}), increasing at the subsurface (4.4 and 6.4 ind m^{-3} at 20–50 m and 50–100 m, respectively) and decreasing again with depth (0.7 and 0.3 ind m^{-3} at 100–200 and 200–300 m, respectively) (figure 3 and 4). This station is characterized by a low abundance of planktic foraminifera (0.1 ind m^{-3}) at 100–200 m, where small specimens dominate but medium sized specimens are also present (33%). The pteropod community is dominated by small veligers (av 74.8%, min 55%, max 100%), followed by veligers/young juveniles (av 25%, min 0%, max 45%).

At the basin station we find a low abundance of pteropods, decreasing with depth: from 1.7 sp m^{-3} at the surface 0–20 m to 0.35 ind m^{-3} at depth 200–300 m (figure 4). This station is dominated by small veligers (av 96.5%, min 82.4%, max 100%), accompanied with the presence of veligers/young juveniles at the depth 100 to 200 m, representing the 17.6% of the population. No foraminifera were found at this station at any depth (figure 3).

2) MAY 2021

At the Atlantic shelf station (P1), we find higher (compared to March) abundances of foraminifera, being stable from the subsurface towards the seabed (av 9.7 ind m^{-3}, min 0.6 ind m^{-3}, max 1.3 ind m^{-3}) (figure 3, 4 and 9). Most of the specimens found in the water column are classified as small (av 75.7%, min 45%, max 100%), followed by medium-sized specimens (av 19.3%, min 0%, max 35%) and large specimens (av 5%, min 0%, max 20%) (figure 3 and 4). The foraminiferal assemblages represent up to 46.9% of the total of the marine calcifiers. The highest abundance of pteropods (1.9 ind m^{-3}) at the station is found in the 50–100 m layer, and the lowest (0.2 ind m^{-3}) at the 200–300 m depth interval (figure 3 and 4). This season is characterized mainly by juveniles of *L. helicina* (av 83.8%, min 50%, max 100%) (figure 4).

The polar shelf stations are dominated by pteropods (av 91.5%, min 83.8%, max 99.1%) (figure 3, 4 and 9). Their abundances increase towards the subsurface or deep subsurface reaching maximum values of 49.6 ind m^{-3} in case of P2 at the 50–100 m depth interval (figure 3 and 4). This region is composed by veligers/young juveniles (av 61.3%, min 16.1%, max 100%), followed by small veligers (av 33.1%, min 28.3%, max 80.6%), adults (av 0.8%, min 0%, max 6.25%) and juveniles/young adults (av 0.15%, min 0%, max 3.2%) (figure 4). In contrast, planktic foraminifera have lower abundances than pteropods (av 8.5%, min 1.1%, max 46.9%) decreasing in abundance towards the deeper parts of the water column. In this case, small-medium specimens dominate the foraminiferal community (av 52.6%, min 0%, max 100%) nearly followed by small specimens (av 43.5%, min 0%, max 100%) (figure 3).

At the slope station the distribution of pteropods and foraminifera shows a close relative abundance (49.9% and 50.1% respectively) (figure 3, 4 and 9). The abundance of pteropods

decreases from the surface 0– 20 m (2.2 ind m^{-3}) to the deepest part of the water column 200–300 m (0.03 ind m^{-3}) (figure 4). The community is dominated by veligers/young juveniles (av 74.9%, min 50%, max 100%) (figure 4). Like pteropods, the foraminiferal distribution at the slope station also decreases from the surface (3 ind m^{-3}) to the deepest part (0.03 ind m^{-3}), and in this case dominated by small-medium sized specimens (av 61.4%, min 50%, max 100%) (figure 3).
At the basin station planktic foraminifera dominates (av 82%, min 28.6%, max 100%) (figure 3, 4 and 9). Their abundances decrease towards depth, from 0.38 ind m^{-3} to 0 sp m^{-3} and are dominated by small-medium sized specimens (av 65%, min 0%, max 100%), followed by large specimens (av 18.3%, min 0%, max 50%) (figure 3). Shelled pteropods are present scarcely at 50–100 m (0.7 ind m^{-3}) (figure 4).

3) JULY 2021

At the Atlantic shelf station, the absolute abundance increases towards the subsurface and decrease again with depth (figure 3 and 4). Most of the specimens of pteropods found in the water column are classified as juveniles (av 72.5%, min 59.0%, max 84.8%) (figure 3 and 4). This is the only season where juveniles were found at all depths, and adults (>500 μm) were observed occasionally (at 20–50 m and at 100–200 m). The foraminiferal assemblages represent up to 92.6% of the total of the marine calcifiers. The highest abundance of pteropods (3.4 ind m^{-3}) at the station is found at 20–50 m, and the lowest (0.1 ind m^{-3}) at 50–100 m depth (figure 4). In contrast to the size that dominated in previous seasons, the size distribution is clearly differentiated within depths. At the surface (0–20 m) all organisms observed (100%) were juveniles/young adults; at the subsurface (20–50 m) is characterized small veligers (69.0%); while below the subsurface (from 50 to 300 m) the fauna is characterized by adults (av 74,2%, min 50%, max 100%) (figure 4).
The polar shelf stations are mostly dominated by foraminifera (av 56.1%, min 48.7%, max 63.6%) (figure 3, 4 and 9). Their abundances increase towards the subsurface or deep subsurface reaching highest values of 21.6 ind m^{-3} at P5 (100–200 m) (figure 3). The foraminiferal community is dominated small-medium sized specimens (av 52.3%, min 0%, max 79.3%), followed by small specimens (av 46.4%, min 15.5%, max 100%) (figure 3). The relative abundance of pteropods (av 43.9%, min 36.4%, max 44.6%) decreases from the surface (0–20 m) to the subsurface (20–50 m). Their highest value (55.9 ind m^{-3}) is recorded at P3 (20–50 m) (figure 4). The pteropod community is dominated by veligers/young juveniles (av 78.0%, min 0%, max 100%) followed by juveniles (av 20.1%, min 0%, max 100%) (figure 4).
The slope station is dominated by foraminifera (88.1%) (figure 3, 4 and 9). The foraminiferal abundances increase from the surface (3.4 ind m^{-3}) to the subsurface 50–100 m (48.5 ind m^{-3}) (figure 3). Small-medium sized planktic foraminifera are most abundant (av 50.4%, min 37.6%, max 58.7%), closely followed by small specimens (av 47.0%, min 31.1%, max 62.4%) (figure 3). Like foraminifera, the abundances of pteropods also increase from the surface (1.1 ind m^{-3}) to the subsurface (5.7 ind m^{-3}) and is dominated by veligers/young juveniles (av 80.0%, min 56.3%, max 100%), followed by juveniles (av 13.2%, min 0%, max 43.8%) (figure 4).
The basin station is dominated by planktic foraminifera (av 99.7%, min 98.9%, max 100%), most of them being small (av 66.55%, min 54.4%, max 80.7%) (figure 3, 4 and 9). The abundances increase towards the subsurface (20–50 m), from 10.69 ind m^{-3} to 33.4 ind m^{-3} and decrease towards the deepest part 200–300 m. The (almost) negligible abundance of shelled pteropods (0.03 sp m^{-3}) (only juvenile stages), is only found at 100–200 m (figure 3 and 4).

4) AUGUST 2019

At the Atlantic shelf station, we observe the highest abundances of foraminifera and pteropods at the surface 0–50 m (23.03 ind m^{-3}) and which decreases with depth (figures 3 and 4). In the

upper 300 m foraminifera dominate (79%), while pteropods dominate (74%) at the surface (0–50 m) (figure 3, 4 and 9, and supplementary material table 4). The relative abundance of the foraminiferal community increases with depth (25.9–97.4 %) (supplementary material table 4) and is dominated by small-medium size specimens (42.9% at surface and 99.3% at depth) followed by small specimens (40.7% at surface to 0.7% depth) (figure 3).
At the polar shelf stations the distribution of foraminifera and pteropods increases from surface (0–50 m) to subsurface (50–100 m) (from 20 to 30 ind m^{-3}), except for P5 where the abundances increase at the sub-surface (150 m) to 82.3 ind m^{-3} (figure 3 and 4) This is the highest abundance recorded in the whole transect. This depth from this specific station is characterized by a high absolute (67.11 ind m^{-3}) and relative (81.6%) abundance of pteropods where the 92.8% are juveniles/young adults (figure 4).
The slope station is characterized by the highest abundance of calcifiers at surface 0–50 m (76.6 ind m^{-3}) with decreasing abundances with depth (figures 3 and 4). This station is highly dominated by planktic foraminifera (average (=av) 93.8%, minimum (=min) 73.1%, and maximum (=max) 99.7%), mainly from small-medium specimens (av 52.3%, min 39.5%, max 73.7%) (figure 3).
At the basin station the absolute abundance of foraminifera increases from surface to subsurface, where it reaches the highest absolute abundance (39.2 ind m^{-3} at 100–150 m) (figure 3, and supplementary material table 4), and a negligible presence of pteropods (figure 4). The station is characterized by planktic foraminifera (av 99.77%, min 99.0%, max 100%), specially dominated by small specimens (av 56.4%, min 33.1%, max 66.7%), increasing with depth (figure 3 and supplementary material table 4).

STANDING STOCKS

In March the total carbon standing stocks (0–28.52 µg m^{-3}) were highest at P4 and zero at P1 and P2 (figure 7 and figure 1-SM). In general, higher standing stocks were estimated at the shelf stations, from P3 to P5 (19.15–28.52 µg m^{-3}), compared to the slope and basin stations (11.18 and 0.85 µg m^{-3}, respectively) (figure 7 and table 1-SM). The total carbon standing stocks were driven by pteropods (100%), since no foraminifera were found in the upper 100 m of the water column (which is the depth range considered to estimate the standing stocks). The organic carbon contribution was low in the total carbon standing stock pool (av 9.08%, min 1.71%, max 17.51%), being lower along the basin station (1.71%) and higher at the shelf and slope stations (av 8.72% and 17.51%, respectively).

In May the total carbon standing stocks (2.99–112.77 µg m^{-3}) were highest at P2 and lowest at P7 (figure 7 and table 1-SM). In general, higher standing stocks were estimated at shelf stations (9.35–112.77 µg m^{-3}) compared to slope and basin stations (3.88 and 2.99 µg m^{-3}, respectively) (figure 7 and table 1-SM). The standing stocks of pteropods (2.48–112.65 µg m^{-3}) were higher than the ones from foraminifera (0–1.57 µg m^{-3}) (figure 7 and table 1-SM). On average pteropods drive the standing stocks (av 95.46%) being the highest contribution (av 98.86%) estimated at shelf stations. The organic carbon contribution is low in the total carbon standing stock pool (av 12.98%, min 9.77%, max 18.4%), being slightly higher at the slope station and lower at P2 and basin stations (9.77%, and 10.64 %, respectively). The organic contribution of shelled pteropods standing stock pool was higher (av 13.1%, min 9.77%, max 18.46%) than from foraminifera.

In July the total carbon standing stocks (21.34–232.91 µg m^{-3}) were highest at P3 and lowest at P7 (figure 7 and table 1-SM). In general, higher standing stocks were estimated at shelf stations (26.1–232.91 µg m^{-3}) compared to slope and basin stations (27.96 and 21.34 µg m^{-3} respectively) (figure 7 and table 1-SM). The standing stocks of pteropods (0–227.66 µg m^{-3})

were higher than the ones from foraminifera (3.26–19.64 µg m^{-3}) respectively (figure 7 and table 1-SM). On average pteropods drive the standing stock pool (59.92%), being the highest contribution estimated at shelf stations (av 77.77%). The organic carbon contribution is low in the total carbon standing stock pool (av 12.98%, min 0.11%, max 21.53%), being the highest along the shelf stations (av 19.19%). The organic contribution of shelled pteropods standing stock pool was significantly higher (av 13.07%, min 0.11%, max 21.5%) than for the foraminifera.

In August the total (inorganic and organic) carbon standing stocks (6.98–1001.93 µg m^{-3}) were the highest at P2 and lowest at P7 (figure 7 and table 1-SM). In general, higher standing stocks are found at shelf stations (132.00–1001.93 µg m^{-3}) compared to slope and basin stations (55.07 and 6.98 µg m^{-3}, respectively) (figure 7). The standing stocks of pteropods (0.79–997.53 µg m^{-3}) were higher than for the foraminifera (4.23–49.38 µg m^{-3}) (figure 7 and table 1-SM). On average pteropods drive the standing stocks (66.79%), being the highest contribution (av 94.77%) at shelf stations. The organic carbon contribution was low for the total carbon standing stock pool (av 6.46%, min 1.70%, max 14.49%), being higher along the shelf stations (12.79–14.49%) and lower in the slope and basin (1.53 and 1.70%, respectively). The organic contribution of shelled pteropod to standing stock pool was significantly higher (av 9.36%, min 1.43%, max 14.49%) than the one by foraminifera.

In December the total carbon standing stocks (3.12–1400.94 µg m^{-3}) were highest at P5 and lowest at P1 (figure 7, and table 1-SM). In general, higher standing stocks were calculated at the shelf stations (496.72–1400.94 µg m^{-3}), except for P1, compared to the slope and basin stations (32.68 and 13.16 µg m^{-3} respectively) (figure 7 and table 1-SM). The standing stocks of pteropods (3.00–1399.86 µg m^{-3}) were higher than from foraminifera (0–3.27 µg m^{-3}) (figure 7 and table 1-SM). On average pteropods drive the standing stocks (87.73%), being the highest contribution (av 89.9%) at shelf stations. The organic carbon contribution was low in the total carbon standing stock pool (av 14.9%, min 7.95%, max 24.59%), being higher along the slope station (24.59%) and lower at P3 (7.95%). The organic contribution of shelled pteropods is significantly higher (av 16.86%, min 13.45%, max 31.58%) than for the foraminifera.

EXPORT PRODUCTION

In March the total carbon export production (0–16.62 mg m^{-2} d^{-1}) was highest at P3 and lowest at P1 and P2 (figure 8 and supplementary material table 2). Highest export productions are estimated at the polar shelf stations, P3–P5, and P6 (8.66–16.62 mg m^{-2} d^{-1} and 12.34 mg m^{-2} d^{-1}, respectively) compared to the basin station (0.06 mg m^{-2} d^{-1}) (figure 8 and table 2-SM). Pteropods dominates the export production (100%). The organic carbon contribution is low in the total carbon export production pool along the transect during this season (av 7.43%, min 1.71%, max 9.97%).

In May the total carbon export production (0.91–89.63 mg m^{-2} d^{-1}) was the highest at P4 and lowest at P6 (figure 8 and table 2-SM). In general, highest export productions are estimated at the shelf stations (4.99–89.63 mg m^{-2} d^{-1}) compared to the slope and basin stations (0.91 and 2.41 mg m^{-2} d^{-1} respectively) (figure 8 and table 2-SM). Pteropods strongly dominates the export production (av 97.95%, min 87.47%, max 100%), being slightly higher at shelf stations (av 99.81%), compared to slope and basin stations (av 93.3%). The organic carbon contribution is lower than the total carbon export production pool (average 11.35%, min 8.21%, max 12.72%). The organic contribution of shelled pteropods to export production is significantly higher (average 11.30%, min 8.21%, max 12.72%) than from the foraminifera.

In July the total carbon export production (4.69–94.75 mg m^{-2} d^{-1}) was highest at P3 and lowest at P7 (figure 8 and table 2-SM). In general, higher export productions are estimated at the Polar shelf stations (33.45–94.75 mg m^{-2} d^{-1}) compared to the Atlantic shelf, slope, and basin stations (9.55, 12.62 and 4.69 mg m^{-2} d^{-1} respectively) (figure 8 and table 2-SM). Pteropods contribute largely to the export production (av 64.41%, min 0%, max 100%) being at the polar shelf stations the highest (96.25%). The organic carbon contribution is low in the total carbon export production pool (av 8.60%, min 0.085%, max 13.16%), being slightly higher along the shelf stations (4.44–13.15%) and slightly lower in the slope and basin stations (4.90 and 0.085%, respectively). The organic contribution of shelled pteropods to export production is significantly higher (average 8.39%, min 0%, max 13.16%) than from the foraminifera.

In August the total carbon export production (0.44–646.64 mg m^{-2} d^{-1}) was the highest at P2 and lowest at P7 (figure 8 and figure 2-SM). In general, higher export productions are estimated at shelf stations (27.81–646.64 mg m^{-2} d^{-1}) compared to slope and basin stations (8.96 and 0.44 mg m^{-2} d^{-1} respectively) (figure 8 and figure 2-SM). Pteropods dominates the export production (av 70.80%) contributing the highest along shelf stations (av 97.00%). The organic carbon contribution is lower than the total carbon export production pool (av 10.21%, min 0.12%, max 14.53%), being higher along the shelf stations (13.14–14.53%) and lower in the slope and basin stations (5.15 and 0.12%, respectively). The organic contribution of shelled pteropods to export production is significantly higher (av 10.12%, min 0%, max 14.53%) than from the foraminifera.

In December the total carbon export production (0.02–232.32 mg m^{-2} d^{-1}) is highest at P4 and lowest at P1 (figure 8 and table 2-SM). In general, highest export productions are estimated at shelf stations (20.21–232.32 mg m^{-2} d^{-1}), except of P1 (0.02 mg m^{-2} d^{-1}), compared to the slope and basin stations (33.28 and 10.03 mg m^{-2} d^{-1}, respectively) (figure 8 and table 2-SM). The inorganic export production from pteropods and foraminifera is on average 64.74 mg m^{-2} d^{-1} (0–198.1 mg m^{-2} d^{-1}) and 0.35 mg m^{-2} d^{-1} (0–1.59 mg m^{-2} d^{-1}), respectively (figure 8 and table 2-SM). Pteropods drive the export production (av 79.39%, min 0%, max 100%). The organic carbon contribution is low in the total carbon standing stock pool (av 12.53%, min 0.12%, max 14.74%), being the lowest at P1 and relatively constant along the rest of the stations (14.59±0.21%). The organic contribution of shelled pteropods to the export production pool is significantly higher (av 12.51%, min 0%, max 14.74%) than from the foraminifera.

Paper III

ISBN 978-82-8236-555-0